University of South Wales
2059684

DYNAMIC LOADING OF SOIL-CEMENT FOR FLEXIBLE PAVEMENT DESIGN

By

L.M. FENDUKLY B.Sc.

A thesis submitted in partial fulfilment of the requirements of the Council for National Academic Awards for the degree of Master of Philosophy

June 1991

The Polytechnic of Wales in collaboration with the University of Aston Birmingham

CERTIFICATION OF RESEARCH

This is to certify, except when specific reference to other investigation is made, that the work described in this thesis is the result of the investigation of the candidate.

L.M. FENDUKLY
(Candidate)

J. DAVIES
(Director of Studies)

P.S. COUPE
(Supervisor)

DECLARATION

This is to certify that neither this thesis, nor any part of it, has been presented, or is being currently submitted, in candidature for any degree at any other Academic Institution.

L. Fendukly

L.M. FENDUKLY
(Candidate)

LIST OF CONTENTS

		PAGE No.
CERTIFICATION OF RESEARCH		i
DECLARATION		ii
LIST OF CONTENTS		iii
LIST OF TABLES		vii
LIST OF FIGURES		viii
ACKNOWLEDGEMENTS		xiii
ABSTRACT		xiv
NOTATION		xv
CHAPTER 1	Introduction	1
CHAPTER 2	Literature Review	5
2.1.	Introduction	5
2.2.	Properties of soil-cement	6
2.2.1.	Soil type	7
2.2.2.	Cement content	10
2.2.3.	Moisture content and dry density	12
2.2.4.	Curing conditions	14
2.3.	Pavement design	14
2.3.1.	Traffic effects	16
2.3.2.	Environmental effects	19

2.3.3.	Layer thickness	21
2.3.4.	Design criteria	22
2.3.5.	Fatigue life	24
2.4.	Dynamic testing methods	25
2.4.1.	Dynamic uniaxial unconfined compression test	25
2.4.2.	Dynamic flexure test	29
2.4.3.	Dynamic tension test	31
2.4.4.	Dynamic tension-compression test	36
2.5.	Testing apparatus and monitoring equipment	40
2.5.1.	Specimen deformation measurement	40
2.5.2.	Apparatus for static and dynamic tension and tension-compression tests	47
CHAPTER 3	Preliminary Work	49
3.1.	Introduction	49
3.2.	Materials selection	49
3.3.	Soil classification tests	50
3.4.	Specimen preparation	51
3.5.	Equipment calibrations and trial tests	53
CHAPTER 4	Development of Equipment and Experimental Procedures	56
4.1.	Introduction	56
4.2.	Specimen's geometry	56
4.2.1.	Cylindrical specimens	56
4.2.2.	Beam specimens	58
4.2.3.	Other types of specimens	59

	4.3.	Testing Equipment	60
	4.3.1.	Static loading equipment	60
	4.3.2.	Dynamic loading equipment	60
	4.4.	Measuring and recording systems	62
	4.5.	Testing procedures	63
	4.5.1.	Static and dynamic compression test procedures	63
	4.5.2.	Static and dynamic flexure test procedures	64
CHAPTER 5		Experimental Results and Analysis	77
	5.1.	Introduction	77
	5.2.	Unconfined static compression test	77
	5.2.1.	Unconfined compressive strength, cement content and curing time relationships	77
	5.2.2.	Stiffness-cement content and curing time relationships	86
	5.3.	Unconfined dynamic compression test results	101
	5.4.	Static and dynamic flexure test results	120
	5.5.	Static and dynamic tension and tension-compression tests	124
CHAPTER 6		Numerical Analysis of a Layered System	125
	6.1.	Introduction	125
	6.2.	Layered system of linearly elastic materials	126
	6.3.	Finite element procedures	126
	6.4.	The finite element program	127
	6.5.	Numerical modeling of the problem	129
	6.6.	Finite element analysis	130

6.6.1. Book example model - model 1 130

6.6.1.1. Description of the control model 130

6.6.1.2. Type of elements used 131

6.6.1.3. Boundary conditions 131

6.6.1.4. Loading 133

6.6.1.5. Results and discussion 133

6.6.2. Three-layer carriageway model - model 2 138

6.6.2.1. Description of the model 138

6.6.2.2. Type of elements used 138

6.6.2.3. Boundary conditions 139

6.6.2.4. Loading and materials properties 139

6.6.2.5. Results and discussion 142

6.6.3. Four-layer carriageway model - model 3 146

6.6.3.1. Description of the model 146

6.6.3.2. Results and discussion 148

6.6.4. General conclusion 148

CHAPTER 7 Summary and Conclusion 150

REFERENCES 158

LIST OF TABLES

		PAGE No.
Table 2.1.	Required quantities of cement for adequate hardening of several soils	11
Table 2.2.	Values of (Fmax/Ti) and (Nf) as suggested by the Fatigue Failure Criteria	35
Table 3.1.	Chemical analysis of Portland cement	50
Table 5.1.	The UCS-curing time relationships for various cement contents in static compression tests	78
Table 5.2.	Coefficients A and B and the sum of errors squared for various cement contents	81
Table 5.3.	Stress-Strain relationships for various cement content after 7 days curing time	87
Table 5.4.	Modulus of Elasticity for various cement contents and curing times	97
Table 5.5.	Dynamic compression test results for 7-day curing time.	102
Table 5.6.	Dynamic compression test results for 14-day curing time	103
Table 5.7.	Dynamic compression test results for 28-day curing time	104
Table 5.8.	Coefficient J for various cement contents and curing times	113
Table 5.9.	Coefficient K for various cement contents and curing times	114
Table 5.10.	Sum of errors squared for various cement contents and curing times	114
Table 5.11.	Dynamic flexure test results for 6% and 10% cement contents at 28-day curing time	122
Table 6.1.	Model 2 - PAFEC output showing maximum vertical UY and horizontal UX displacements at element nodes	143

LIST OF FIGURES

PAGE No.

Fig.2.1. The grain-size distribution curve range of soils suitable for cement stabilization 9

Fig.2.2. Typical soil ranges
(a) in triangle-diagram form;
(b) in the Casagrande plasticity diagram 9

Fig.2.3. Typical compaction curves 13

Fig.2.4.a. The effect of cement addition on the compaction characteristics 13

Fig.2.4.b. Difference between the Proctor curve of untreated soil and soil cement 13

Fig.2.5. Friction grip system 34

Fig.2.6. Fatigue performance related to uniaxial tensile strength 34

Fig.2.7. Variation of Tensile Strength with Number of Stress Applications for a Given Fmax 35

Fig.2.8. Jig for cyclic uniaxial tension 38

Fig.2.9. Typical stress-strain and strain-time curves recorded during uniaxial tension-compression cycling (1 bar = 100kPa) 38

Fig.2.10. Experimental results and S-N curve for Westerly granite under cyclic uniaxial tension-compression (compression peak constant-tension peak varied from test to test). Comparison with S-N curve for uniaxial tension 38

Fig.2.11. Tension and compression zones of pavement layer under a moving wheel load 39

Fig.2.12. Deformations of the cylindrical specimen
a) in compression
b) in tension 41

Fig.2.12. c) Deformations of the beam specimen 41

Fig.2.13.a. Protective steel platens suitable to fit a NX Hoek triaxial cell 44

Fig.2.13.b. Test specimen mounted with resistance wire (diameter of specimen 54mm) 44

Fig.2.14.a. The effects of tilting: (a) non-parallel end before test, electrolevel axes horizontal: (b) tilting caused in early stage of test σ1 positive, σ2 negative for similar triangles experiencing small rotations, with angles in radians 46

Fig.2.14.b. Construction of electrolevel gauges 46

Fig.3.1. Grain size distribution curve for Abergavenny Red Marl 54

Fig.3.2. Dry density/moisture content relationship of the Red Marl 54

Fig.3.3. Type of mixers used during the investigation 55

Fig.3.4. Controlled environment curing chamber 55

Fig.4.1. BS mould and accessories for preparation of 100 x 50mm diameter cylindrical specimen 65

Fig.4.2. Frame and jacking system of specimen 65

Fig.4.3. Parallel plates capping rig for tensile test specimen 65

Fig.4.4. Mould for preparation of 76 x 76 x 286mm long prismatic specimen and compaction accessories. 66

Fig.4.5. Four-point loading flexure test 67

Fig.4.6. BS mould and accessories for 100 x 100mm & 150 x 100mm diameter cylindrical specimens 68

Fig.4.7. Mould and accessories for preparation of tensile test specimen to ensure uniform stress distribution in the middle portion 68

Fig.4.8. Instron testing machine model 1251 for static and dynamic loading, with displacement, load and strain control facilities 69

Fig.4.9. Dynamic compression loading on cylindrical specimen 70

Fig.4.10. Dynamic tension-compression loading on cylindrical specimen 71

Fig.4.11. MTS-850 dynamic test system with anti creep circuit and UV strain recorder 72

Fig.4.12. Uniaxial tension-compression loading on prismatic specimen in the MTS-850 loading system 72

Fig.4.13. Transducer assembly for dynamic tension - compression test on prismatic specimen 73

Fig.4.14. Modified design for transducer assembly system for dynamic tests on all types of specimens 74

Fig.4.15. Detail of transducer fixings 75

Fig.4.16. Detail of transducer pedestal 76

Fig.5.1. UCS-Curing Time Relationship for Various Cement Contents 79

Fig.5.2. A Coefficient-Cement Content Relationship 82

Fig.5.3. B Coefficient-Cement Content Relationship 83

Fig.5.4. UCS-Cement Content Relationship for Various Curing Periods 85

Fig.5.5. Stress-Strain Relationship for 7-Day Curing Time 88

Fig.5.6. Stress-Strain Relationship for 14-Day Curing Time 89

Fig.5.7. Stress-Strain Relationship for 28-Day Curing Time 90

Fig.5.8. Stress-Strain Relationship for 56-Day Curing Time 91

Fig.5.9. Stress-Strain Relationship for 6% Cement Content 92

Fig.5.10. Stress-Strain Relationship for 10% Cement Content 93

Fig.5.11. Stress-Strain Relationship for 14% Cement Content 94

Fig.5.12. Stress-Strain Relationship for 18% Cement Content 95

Fig.5.13. Stress-Strain Relationship for 22% Cement Content 96

Fig.5.14. Elastic Modulus-Curing Time Relationship for Various Cement Contents 99

Fig.5.15. Elastic Modulus-Cement Contents Relationship for Various Curing Periods 100

Fig.5.16. Dynamic Compression Tests for 7-Day Curing Time 105

Fig.5.17. Dynamic Compression Tests for 14-Day Curing Time 106

Fig.5.18. Dynamic Compression Tests for 28-Day Curing Time 107

Fig.5.19. Dynamic Compression Tests for 6% Cement Content 108

Fig.5.20. Dynamic Compression Tests for 10% Cement Content 109

Fig.5.21. Dynamic Compression Tests for 14% Cement Content 110

Fig.5.22. Dynamic Compression Tests for 18% Cement Content 111

Fig.5.23. Dynamic Compression Tests for 22% Cement Content 112

Fig.5.24. Typical stress-strain graph for dynamic compression test 116

Fig.5.25. Resilient Modulus - Log_{10}(Cycle No.) 10% CC 28CT & 3.56N/mm² Stress 117

Fig.5.26. Resilient Modulus - Log_{10}(Cycle No.) 10% CC 28CT & 3.31N/mm² Stress 118

Fig.5.27. Dynamic Flexure Tests for 28-Day Curing Time 123

Fig.6.1. Model 1 - Book example pavement section 132

Fig.6.2. Model 1 - Mesh refinement and boundary conditions 132

Fig.6.3. Model 1 - Enlarged section showing the pressure load and the number of nodes, plotted using PIGS 134

Fig.6.4. Model 1 - Displacement in the vertical UY and the horizontal UX directions 135

Fig.6.5. Model 1 - Enlarged corner section showing stress contours 136

Fig.6.6. Model 2 - Three-layer carriageway section 140

Fig.6.7. Model 2 - PIGS plot showing mesh refinement and number of nodes with maximum displacement 141

Fig.6.8. Model 2 - PIGS plot showing vertical UY and horizontal UX surface displacements along the carriageway 144

Fig.6.9. Model 2 - PIGS plot showing the stresses along the centre line under the LHS wheel load 145

Fig.6.10. Model 3 - Four-layer carriageway section 145

ACKNOWLEDGEMENTS

The Candidate wishes to express his gratitude and sincere thanks to Dr J. Davies, his Director of Studies, and Mr B.S. Bhogal, his Supervisor, for their constant suggestions, help and encouragement.

The Candidate is grateful to Prof. P.S. Coupe, his Head of Department and Supervisor, for the use of departmental facilities and for his help and encouragement with the final preparation of this thesis.

He is also grateful to the technical staff of the Department of Civil Engineering and Building for their valuable help in performing the experimental work.

A special word of thanks to my wife Hilda for typing this thesis patiently, and for her continued support, interest and encouragement during this study.

ABSTRACT

Stabilised soil-cement has been used in road pavements for considerable time. Certain design criteria concerning the properties of the material have been established. However, there is little knowledge of the material's behaviour under dynamic loading conditions simulating traffic loads. The aim of this research was to develop an understanding of the response of soil-cement to dynamic loading representing traffic stresses in compression, flexure, tension and tension-compression.

Studies on the material have shown that a large number of factors affect the soil-cement properties. To obtain consistent results and to reduce the variables, pulverised Red Marl was used as the soil in this research. All specimens were prepared to constant density and moisture content, and cured at constant temperature and relative humidity. Variables such as cement content and curing time have been selected to study their effects on the static and fatigue characteristics of the soil-cement.

Regression analyses were carried out on all results. Generalised relationships for parameters such as the unconfined compressive strength, stress-strain characteristics, Elastic and Dynamic Moduli have been developed for a wide range of cement contents and curing times as input variables for pavemant design. Fatigue relationships in the form of number of load cycles to failure related to applied stress, based on experimental results, have also been developed for use as input for soil-cement pavement design.

The static and dynamic flexure test results show a substantial drop in strength due to the fatigue effect in flexure. This is caused by the development of tension cracks at the underside of the beam specimen.

The techniques of deformation measurement have been investigated, and a transducer system of high accuracy LVDT's developed. This system can meet most of the testing requirements such as reliability, accuracy at high frequency, ease of preparation and assembling.

The finite element method was used to analyse three models of pavement structures. The Program for Automatic Finite Element Calculations (PAFEC) was used to predict the response of the layered pavement system and to quantify the traffic-induced displacements and stresses.

NOTATION

a	distance between the line of fracture and the nearest support, measured along the centre line of the bottom surface of the beam.
a	constant = 4
a	radius of load contact area
a	$h^{1.5}/(2.1h-1)$ where, h = slab thickness
A	coefficient of the best polynomial and increases with the increase of cement content
A1	exponent 0.3 for granular and 0.315 for fine-grained soil-cements
A2	exponent 40 for granular and 20 for fine-grained soil-cements
b	average width of specimen = 76.2mm
b	0.025 for granular soil-cement and 0.05 for fine grained soil-cement
B	slope coefficient which also increases with cement content
C, CC	cement content (%) by weight
C	constant 10.4 for granular and 10 for fine-grained soil-cements
CBR	California bearing ratio
CT	curing time (days)
d	average depth of the specimen = 76.2mm
E	static Young's modulus
E1,E2..	Young's modulus values
F	equivalent load applications
F	stress factor
FEA	Finite Element Analysis
Fmax	maximum stress factor

Fmax/Ti	function of maximum stress level
f(h)	$(2.1h-1)^2/ h^{1.5}$
h	pavement thickness (in)
h1,h2..	layer depths
Hz	frequency (cycle/sec)
J	an ordinate coefficient of the best polynomial
K	70C for granular soils and 10C for fine grained soils
K	modulus of subgrade reaction (pci)
K	slope coefficient
Kc	material constant
k1	0.20 to 0.6
k2	0.25 to 0.7
l	span length = 228.6mm
L	load
Ls	standard load
LVDT	linear variable differential transducer
MR	resilient modulus
MRc	compressive resilient modulus
MRe	estimated modulus of rupture (also known as the bending tensile strength)
n	1 + 0.18C, C is cement content
n	80-150 for granular soils and 40-80 for fine grain soils
N	allowable number of load repetitions
N,Nf	number of load cycles to failure
P	maximum applied load (N)
P	wheel load (kips)

P	pressure load
PAFEC	Program for Automatic Finite Element Calculations
PIGS	PAFEC Interactive Graphic Suite
R	Modulus of Rupture (N/mm^2)
S	flexural stress level
Ti	initial tensile strength
T'	decreases from initial value Ti to new value
UCS	unconfined compressive strength (N/mm^2)
(UCS)D	unconfined compressive strength at an age of D days
(UCS)Do	unconfined compressive strength at an age of Do days
UX	displacement in the horizontal direction
UY	displacement in the vertical direction
$\mu, \mu 1, \mu 2..$	Poisson's ratios
ϵi	initial maximum flexural strain
σ	applied stress
σb	biaxial stress
σc	compressive stress applied
σi	initial bending stress
$\sigma Tmax$	maximum applied tensile stress
$\sigma(UCS)$	unconfined compressive strength
σx	horizontal direct stress
σy	vertical direct stress
$\sigma 1$	major principal stress
$\sigma 1-\sigma 3$	deviator stress
$\sigma 3$	minor principal stress (confining pressure)
τxy	shear stress

CHAPTER 1

Introduction

Stabilised soil-cement is a hardened material formed by curing a mechanically compacted mixture of pulverised soil, Portland cement and water. The material has found wide applications in the construction of roads internationally since the first soil-cement road was constructed in Johnsonville, South Carolina, USA in 1935. It has also been used in other civil engineering constructions such as earth dams and foundation material for large structures. However, its main application is in the sub-base and/or roadbase of flexible pavements.

Many surveys have been made to study the performance of stabilised soil-cement bases in pavement structures, e.g. Reid (1948), Zube (1969) and Corps of Engineers (1956). These surveys have shown that the condition of the pavements varies from excellent to poor, some of which required extensive maintenance even at an early stage after construction.

Some studies of the structural failure of the soil-cement roadbase caused by repeated traffic loads, which includes fatigue failure, have also been reported by the Highway Research Board (1955, 1961, 1962) and Mitchell and Freitag

(1959). These findings confirmed that failure occurred due to development of cracks in fatigue without any apparent permanent deformation in pavements. Pretorius (1970) reports loss in road carrying capacity of the soil-cement roadbase due to infiltration of water through fatigue cracks. Hence, it is essential to design the soil-cement pavement to withstand the dynamic action of traffic loads with longer fatigue life.

In many areas around the world there has been a rapid increase in traffic loads and volume which has led to the gradual realisation of the inadequacy of the present design methods. These design methods are based on empirical input of pavement performance under moderate traffic loads and volumes. It is also becoming apparent that there are limitations in using design input related to material characteristics based on static loading test techniques, such as the unconfined compression and California Bearing Ratio (CBR) tests.

Developments of analytical design criteria for soil-cement pavements, to withstand fatigue effects caused by repeated traffic loads, have been suggested by some investigators in recent years. There are limitations to the work carried out so far because of the large number of factors involved in generating appropriate design input. Also there is

evidence of limited work carried out so far on the tensile properties of soil-cement under both static and dynamic loading conditions. The lack of information on tensile properties is due to the difficulties in carrying out tensile tests on low strength brittle materials.

The main aim of this research was to investigate the behaviour of soil-cement subject to dynamic loading under stresses in compression, flexure, tension and tension-compression. Variables, such as cement content and curing time prior to testing, have been selected to study their effects on the resilience and fatigue characteristics of soil-cement specimens under dynamic loading. In order to generate consistent data and study the effect of different variables on material characteristics, only one type of homogeneous soil, pulverised Red Marl, and ordinary Portland cement have been selected for experimental work.

The purpose of the experimental work was to establish relationships for soil-cement pavements under the action of dynamic loading. This has been carried out by:

a) utilising the results for each test to identify parameters for material characteristics.
b) establishing appropriate fatigue relationships in the form of a number of cycles to failure related to applied stress.

Some generalised relationships based on experimental results have been developed for use as computer input for soil-cement pavement analysis.

An important part of this investigation is related to the development of methods and techniques for carrying out dynamic loading tests and, at the same time, monitoring and recording the data necessary to establish the parameters for material characteristics.

CHAPTER 2

Literature Review

2.1. Introduction

The original concept of stabilising soil with cement is attributed to the trials by H.E. Brooke-Bradley on Salisbury Plain, (England, UK) in 1917. But the first substantial soil-cement road was constructed in Johnsonville, (South Carolina, USA) in 1935. Soon after that, stabilised soil-cement was used in pavements all over the world. A wealth of empirical information has been accumulated on aspects contributing to the successful performance of stabilised soil-cement pavements. In many areas however, where rapid increase in heavy traffic was noticeable, it was gradually realised that these empirical methods suffered some drawbacks. Failure due to extensive cracking of pavements, which was not accompanied by any apparent permanent deformation, led to the recognition by Hveem (1955) that resilient deformation under transient heavy loadings was of major importance. This was largely supported by the results of the American Association of State Highway Officials (AASHO) road test, Highway Research Board (1962). It was assumed that these resilient deformations were essentially elastic in nature. Following this concept, evaluation of resilient deformation under

moving load is logical. Consequently, this has given tremendous momentum towards the development of dynamic tests.

This Chapter contains literature reviews relevant to the following areas:

a) material properties.
b) pavement design and design requirements.
c) the work carried out in the development of the dynamic tests on soil-cement and other road construction materials.
d) the deployment of the test results in finding the material parameters which should provide bases for the analytical design of flexible pavements.

2.2. Properties of soil-cement

The soil-cement process was developed from the technology of soil mechanics to provide a means of increasing the shear strength of soil. Concrete is normally made from batched coarse and fine aggregates and cement, with the cement particles surrounding the granular soil and bridging its particles.

The physical properties of stabilised soil-cement mixtures

are influenced by many factors. Those which have major effects on the soil-cement mixture's characteristics can be grouped in the following:

1) Soil type.
2) Cement content.
3) Moisture content and dry density.
4) Curing conditions.

2.2.1. Soil type

This refers primarily to the particle size distribution, liquid and Atterberg limits and the chemical and mineral composition of the soil. The grading of the soil used determines the amount of stabiliser required. Well graded soil requires less stabiliser, while providing adequate structural capacity and protection against frost action. It is uneconomical to stabilise soils having liquid limits greater than 45 and plasticity indices over 20. Soil should be low in organic matter and mica for successful stabilisation since these constituents tend to reduce the strength of soil-cement (Ministry of Transport (1969)).

Kezdi (1979), presented a number of illustrations to assist in sampling soil for determining material characteristics. Typical grain size distribution curves

for a wide range of soil types are presented in Figure 2.1, and shown in a triangle-diagram form in Figure 2.2.a. The cohesive soils involved (types Nos. 3-5) are shown in the Casagrande diagram (Figure 2.2.b). If the characteristics of the soil under test are in the required range, then the next step is to determine the amount of cement to be added. It was concluded that soil types Nos. 2-6 can be cement stabilised.

The Red Marl which is chosen for the present research was related to Kezdi's diagrams. The grain size distribution, the liquid limit of 37% and the plasticity index of 18% (listed in Section 3.3) for the Red Marl indicate it is in the lean clay region. This indicates the suitability of the Red Marl for stabilisation with cement.

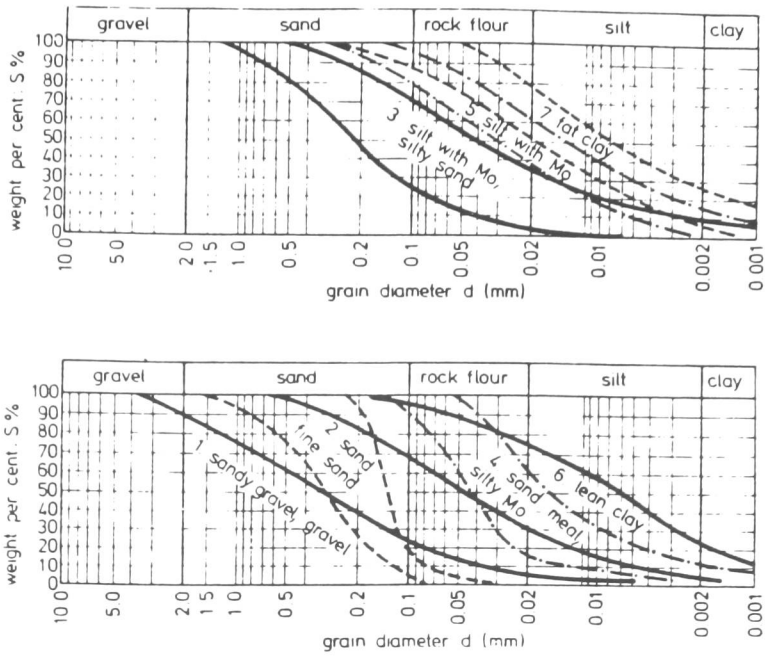

*Key-Mo is coarse silt or rock flour.

Fig.2.1. The grain-size distribution curve of soils suitable for cement stabilization.

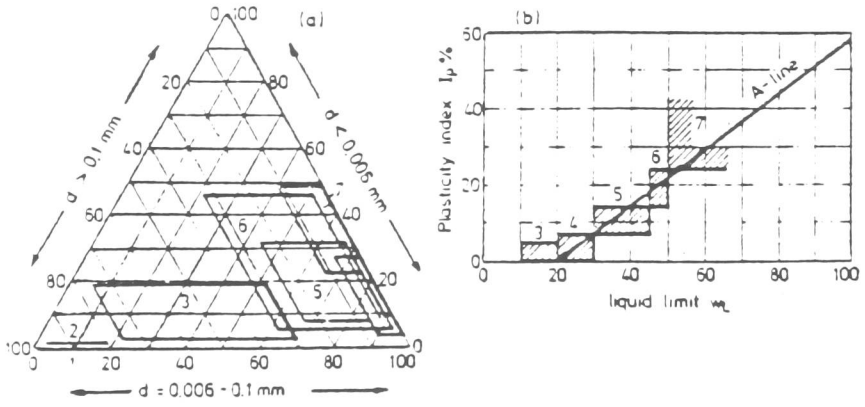

Fig.2.2. Typical soil ranges (a) in triangle-diagram form; (b) in the Casagrande plasticity diagram.

2.2.2. Cement content

Ordinary Portland cement is normally used to stabilise soils. Soils have been stabilised successfully with a cement content as low as 4%, but as much as 20-25% may be required; high percentages of stabiliser however would be uneconomical.

In Britain the minimum cement content required is usually determined by measuring the unconfined compressive strengths. A minimum strength of 2.76MN/m² at 7 days is required on cylindrical specimens, having a height/ diameter ratio of 2:1, cured under humidity conditions. A minimum strength of 3.45MN/m² is required for cubical specimens by the Ministry of Transport (1969). The minimum cement content required to stabilise the Red Marl chosen in this investigation is approximately 8%, to achieve the minimum compression strength specified.

In the United States the desired cement content is normally selected depending on the type of soil under consideration; see Highway Research Board (1962). The cement content required increases with increasing silt and clay in the soil. Cement contents for different soil classes are shown in Table 2.1. This is based on the statistical evaluation of experimental results involving

almost 2500 different soil types carried out by the American Portland Cement Association. In relating the Red Marl to Table 2.1, the cement content required will be in the range 8-15% (i.e. soil class A-5 to A-6). In the experimental work on Red Marl a wide range of cement contents was used for research purposes.

*Soil class	Soil type	Approximate cement content required (% of dry soil mass)
A-1	Sand + Gravel	3 - 8
A-2		5 - 9
A-3		6 - 11
A-4	Silt	7 - 12
A-5		8 - 14
A-6	Clay	9 - 15
A-7		10 - 16
	Organic Soils	

* Soil class in the (AASHO) soil classification system.

Table 2.1. Required quantities of cement for adequate hardening of several soils

2.2.3. Moisture content and dry density

Maximum dry density and the optimum moisture content are the most important factors with respect to the compaction of soil-cement. Atkins (1980) presented typical water content-dry density curves for several types of soil, shown in Figure 2.3. It should be noted that, at optimum water content, the maximum dry density of the gravel-sand mixture, is significantly higher than that of the heavy clay. The addition of stabiliser to the soil will also affect its maximum dry density; see Kezdi (1979) in Figures 2.4.a&b. To highlight this, the maximum dry density increases more for sand than for heavy clay after the addition of cement stabiliser. The Red Marl has a dry density of 1850kg/m^3 at an optimum moisture content of 15%; upon relating these values to Figure 2.3, it can be seen that the curve will lie just above the Till (d).

A more recent research by William et al (1987) on the tensile fracture of cement stabilised soil concluded that the cement content appeared to be the primary controlling factor for toughness, with compaction effort being the second most important factor. The cement content apparently controls the stress to failure with the strain to failure being relatively constant.

(a) Gravel–sand mixture
(b) Well-graded sand
(c) Uniform sand
(d) Till
(e) Heavy clay

Fig.2.3. Typical compaction curves.

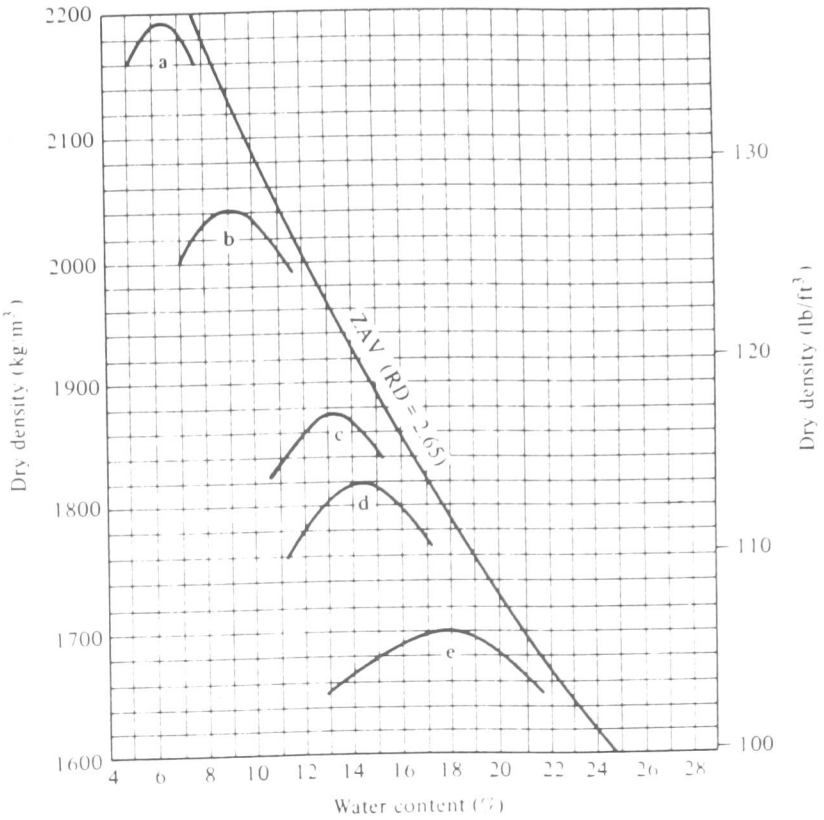

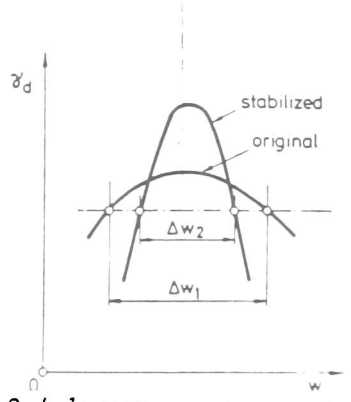

Fig.2.4.b. Difference between the Proctor curves of untreated soil and soil cement

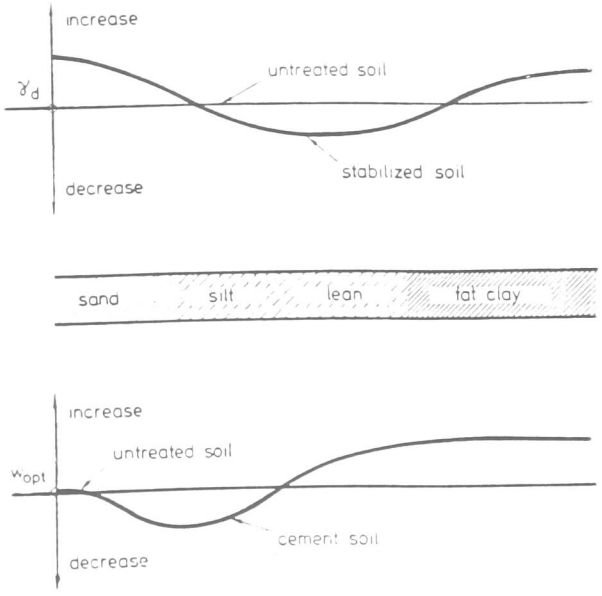

Fig.2.4.a. The effect of cement addition on the compaction characteristics

2.2.4. Curing conditions

The relationship between the strength of compacted soil-cement specimens and the time of curing can be expressed as a straight line on a semi-logarithmic or logarithmic plot, depending on the soil type. For this reason the criterion for the strength of soil-cement must specify the number of curing days. As a result of this, curing times of 7, 14 and 28 days were investigated for the dynamic and static tests in compression. The 56-day test was investigated by the static unconfined compression test only.

The temperature and time under which curing takes place have a considerable effect on the stabilised soil. In this investigation the temperature under which the specimens are cured, will be constant at 25°C, as specified by BS 1924 (1975). This will relate to an approximate pavement layer temperature when sealed by the wearing course.

2.3. Pavement design

Methods for design are classified in three groups: empirical, semi-empirical and analytical or theoretical methods. Empirical and semi-empirical design methods for pavements are satisfactory as long as the materials and

conditions of loading for which they are developed do not change. However traffic volumes and maximum axle load are increasing. Furthermore the introduction of new materials may be inhibited if it is not possible to assess with any precision the thickness and conditions under which they should be used. The extension of semi-empirical design methods into regions of new loading and new materials can be achieved only by carrying out expensive and time consuming full-scale pavement experiments.

Analytical design methods do not suffer from these drawbacks, because the design of flexible pavements is related to the design of structures; the composition and thicknesses of the layers are selected so that the stresses, strains and deformations produced by traffic loading do not exceed the capabilities of any of the materials in the pavement.

The theoretical approach provides a more reliable base for extrapolation beyond the boundaries of previous observations. However, the use of elastic theory for pavement design is still limited and little use has been made of the theory in connection with pavements containing stabilised sections.

There are a number of analytical design theories which started as early as the 1940's, such as Burmister's two-

layer method and Palmer and Barber's approximate displacement equation. In these methods layer thickness is selected so that the displacement under the wheel is limited to an arbitrary quantity of 0.2in (5mm) displacement as suggested by Burmister (1945). Burmister extended his analysis to three layers but did not analyse the stresses.

The three layer system by Jones (1962), presented extensive tabulation of the stresses at the layer interfaces, on the axis of the circle. Some solutions for a four layer system, subjected to uniform vertical loading over a circular area, have been obtained by Verstraeten (1967). The present position is that sufficient information on the deformation and fatigue properties of materials is not sufficient to permit the use of a purely theoretical approach to pavement design.

For this thesis, a literature review and examination was made on factors which affect pavement design, material characteristics, pavement stress conditions, laboratory tests, and finally pavement response.

2.3.1. Traffic effects

The structural damage of flexible pavements is caused

mainly by traffic. Sebaaly (1988) investigated traffic effects and developed accurate prediction models for better methods of pavement design. Traffic effects result in deformation and cracking. Weights and frequencies of axle loads are major factors in determining the pavement design thicknesses. Axle configurations also influence pavement design, together with tyre pressure which controls the load contact area and affects the wearing course. Wheel spacing and impact effects may cause considerable damage if associated with irregular surfaces and high speed vehicles.

General design analysis involves:

1) prediction of frequencies of daily traffic in both directions.
2) projection of future traffic intensities.
3) determination of the probable axle load distributions.
4) computation of fatigue factors.

The structural damage to the pavement is caused almost entirely by commercial traffic, private cars causing little damage. Normal traffic on conventional roads is mixed in composition; the damaging effects of different axle loads are assessed by the AASHO Road test (1962) to give equivalent factors for flexible pavement design. The concept of equivalent load means that one application of a

load L is equivalent in terms of pavement damage to F applications of a standard load Ls, where

$$F = (L/Ls)^a$$

The value of the power a, found by most investigators, is about 4 and the standard load Ls most generally used is 80KN.

Axle loads and their frequencies cause two forms of damage to the pavement. The first form of damage is permanent deformation which accumulates with wheel load and has an allowable limit of 25mm by the British Standard in HMSO (1977). Alternatively the deformation must be limited to 20mm under a 2m straight edge. The other form of damage is fatigue cracking, where cracks develop well before the maximum allowable deformation is reached. The crack development will reduce the load carrying capacity of the pavement and allow water to penetrate through to the subgrade and expose both the pavement and subgrade to frost attack.

The fatigue factor is important to compute the life of the flexible pavement; however each material in the pavement has a different fatigue life. Tests have been carried out to predict the fatigue life of bituminous materials, soils and soil-cement. An example from a research report prepared by the American Portland Cement Association (1979), on the allowable number of load repetitions N on a

soil-cement pavement of a certain thickness has been given in the form:

$$N = \left[\frac{(1.77K)^{A1}}{C/f(h)} \right]^{A2} \cdot \left[\frac{a^{\frac{1}{2}}}{P} \right]^{A2}$$

where,

N = allowable number of load repetitions

K = modulus of subgrade reaction (pci)

A1 = exponent 0.3 for granular and 0.315 for fine-grained soil-cements

A2 = exponent 40 for granular and 20 for fine-grained soil-cements

C = constant 10.4 for granular and 10 for fine-grained soil-cements

$f(h) = (2.1h-1)^2 / h^{1.5}$

h = pavement thickness (in)

a = radius of load contact area (in)

P = wheel load (kips).

2.3.2. Environmental effects

Environmental effects are important in flexible pavement design. The two main factors are temperature and moisture changes. Temperature has a strong influence on the stiffness and behaviour of bituminous materials. Increasing temperature decreases the stiffness and this results in more load being transferred to the lower parts

of the pavement structure. Decreasing temperature increases the stiffness and high stresses develop in the bituminous layer with cracks developing at the under side of the layer and propagating to the surface.

The effect of softening of the roadbase due to thawing of the frozen soil results in a reduction of the load-carrying capacity of the pavement.

Lister (1972) showed that 30% of the total stress in a roadbase may be caused by temperature and 70% by the wheel load. Cement-treated base temperature stresses can be reduced by using a thick cover of crusher-run or a more expensive bituminous surfacing as a thermal insulator. Bonnot's (1972) theoretical calculations showed that only a small drop in temperature is sufficient to cause thermal cracking in an uncracked cement-treated layer.

At design stage the extreme temperatures have to be accounted for, as the different stiffnesses of the materials should be incorporated as input parameters. To reduce frost attack the layers most affected by frost should be kept as deep as possible where temperatures do not drop to freezing. The subbase layer may be constructed of impervious or granular non-frost-susceptible material to cut off sources of moisture.

2.3.3. Layer thickness

Treated materials should be constructed as a thick layer, because the load-bearing ability increases substantially when the thickness is increased. This requirement has been looked into by Nussbaum and Larsen (1965). They found that the load-bearing capacity (measured in terms of deflection) of a 100mm cement-treated layer is about 1.5 times that of a 100mm granular layer and if the layer thickness is increased to 250mm, the load capacity increases to 3.3 times that of a granular layer of the same thickness. This means that the structural equivalency of the material is not fixed but increases with thickness.

Increasing the base thickness has its limitations because of construction problems. If in-situ mixing is used, it becomes very difficult to handle the material of a layer thicker than 150mm on the roadway; this problem may be overcome by central mixing and paver laying. Also the compaction of a layer thicker than 150mm might pose a problem. This difficulty could be overcome by careful use of a powerful vibrating roller. However some work needs to be done on the problem of achieving the required density in a thick soil-cement layer.

In determining layer thicknesses for a pavement, a balanced structural layout in which all layers or

components of the structure are stressed or strained just within their allowable limits should be achieved. Otte (1978) emphasised that if a design is not balanced, excessive stress and/or strain will occur in one or more of the layers. This may result in unacceptable performance of the road and possibly in premature failure. To provide an optimum economical design, all the layers in the structure must be utilised to their design load-bearing capacity.

2.3.4. Design criteria

When pavement design used to be merely a matter of materials' evaluation, the design criterion was either a minimum CBR or a minimum unconfined compressive strength. With the introduction of a more fundamental approach to the structural design of pavements (using elastic theory) it became necessary to obtain design criteria for the various materials. Whiffin and Lister (1962) compared the calculated tensile stress to the tensile (flexural) strength of a soil-cement beam and recommended use of the tensile stress as the design criterion. They also reported on the tensile strain "corresponding to the onset of hair cracking", that is, at failure of the beam. They also prepared a theoretical discussion on how elastic theory can be applied to cement-treated materials and considered

horizontal tensile stress at the bottom of the cement-treated layer as a most important factor and used it as the design criterion.

Lister (1972) argued that failure in cement-bound materials is related more closely to a strain criterion than to one of simple stresses; however he used stresses throughout his paper. A certain part of the confusion, as to whether stress or strain should be used as the criterion, originates from the lack of understanding of the stress-strain and fracture properties of cement-treated materials under biaxial loading conditions. Generally stress design values have been obtained under uniaxial loading conditions.

The Griffith failure provided a crack theory indicating the stress state likely to cause fatigue failure in soil-cement. Abboud (1973) studied the failure of cement-treated materials under relatively high confining stresses. He stated that the existence of the tensile zones (hair cracks) in the hardened material, together with the knowledge that failure may be related to stress concentrations around these cracks, suggests that the Mohr-Coulomb failure criteria may not be the best tool for failure prediction in these materials. Raad (1976) observed that the Griffith failure criterion applies very well to low tensile stress ranges, while the modified

Griffith criterion is more applicable to higher stress levels. From this work the failure of cement-treated materials under biaxial loading conditions can be represented by:

$$\sigma 1 = \sigma(UCS) + 5\sigma 3$$

where, $\sigma 1$ = the major principal stress

$\sigma 3$ = the minor principal stress

$\sigma(UCS)$ = the unconfined compressive strength

In spite of Raad's development, uniaxial tensile strain is still used as the design criterion.

2.3.5. Fatigue life

A literature study by Otte (1978) on the static failure of concrete indicated that failure usually starts when the applied stress (σ) has reached about 35% of the strength (σb), that is at $(\sigma/\sigma b)=0.35$. The failure starts with microcracking and a loss of bond at the interface between the aggregate and the matrix of fine material and cement. These microcracks propagate under load until the sample collapses. From this it can be concluded that the material would be able to withstand an unlimited number of load repetitions while the stress ratio ($\sigma/\sigma b$) remains below 0.35 because the applied stress is too low to start the development of microcracking.

Research performed by nine researchers and reviewed by Otte(1978) indicates that concrete and cement-treated materials will withstand about one million load repetitions before failing in fatigue if the applied stress (σ) is about 50% of the strength (σb), that is $\sigma/\sigma b=0.5$. This relationship was also assumed by the Portland Cement Association (1973) when they developed their pavement design procedures.

2.4. Dynamic testing methods

2.4.1. Dynamic uniaxial unconfined compression test

The popularity of this test is due to its simplicity, as it requires a minimum of specimen preparation. Raad, Monismith and Mitchell (1977), carried out a study on the fatigue behaviour of soil-cement pavement material subjected to dynamic load tests. They found that the confining pressures ($\sigma 3$) in soil-cement bases are generally small because such base materials support traffic loads in flexure and the overburden pressure is low.

The U.S. Army Engineers Waterway Station has conducted a number of investigations (1967, 1969, 1972, 1974) on the dynamic behaviour of stabilised soils, mainly clayey in

nature, under dynamic compressive stresses. Some of their principal findings which have influenced pavement design procedures are listed below:

1. Comparison of the behaviour of soil-cement and lime stabilised soil under dynamic compressive stresses indicates that although the strengths of some soils, as measured by CBR tests prior to treatment and after a specified curing period, are the same, their behaviour under dynamic loading may differ. Thus it can be concluded that CBR values are misleading for empirical design.
2. The Unconfined Compressive Strength (UCS) in (psi) appears to be a suitable correlating parameter for different material properties such as:

a) cement content which may be approximated by:

$$(UCS) = nC$$

where,

n = 80-150 for granular soils and 40-80 for fine grain soils

C = cement content (%) by weight.

b) curing time which can be expressed by:

$$(UCS)D = (UCS)Do + k \log_{10} D/Do$$

where,

(UCS)D = unconfined compressive strength at an age of D days

(UCS)Do = unconfined compressive strength at an age of Do days

k = 70C for granular soils and 10C for fine grained soils

C = cement content (%) by weight.

c) stresses which can be expressed by the compressive Resilient Modulus (MRc):

$$MRc = Kc\ (\sigma 1-\sigma 3)^{-k1}\ .\ (\sigma 3)^{k2}\ .\ (UCS)^{n}$$

where,

$(\sigma 1-\sigma 3)$ = deviator stress

$\sigma 3$ = confining pressure

Kc = material constant

k1 = 0.20 to 0.6

k2 = 0.25 to 0.7

n = 1 + 0.18C

C = cement content (%) by weight.

Lotfi and Witczak (1985) conducted a study on the dynamic characteristics of typical materials used by Maryland State Highway Administration (MSHA). Two broad materials' categories were tested in this study, dense-graded aggregate (DGA) and stabilised soil-cement. The (DGA) includes (LS) as an upper gradation material and (MS) as a lower one. The soils, as specified by the American

Association of State Highway Officials (AASHO), include types A-2 (sand), A-3 (silty sand) and A-2-4 (sandy silt). Material type, gradation, cement content, density level and curing period were used to investigate their influence on the Resilient Modulus (MR) response.

The tests were carried out on a compression machine in static and dynamic unconfined compression and the objective of their study was to determine the Resilient Modulus of several materials. Correlations between (MR), the unconfined compressive strength (UCS) and the static Young's Modulus (E) were determined. Comprehensive laboratory analysis for the evaluation of Resilient Modulus response was carried out for five different types of materials, two of which were dense-graded aggregates. Lotfi and Witczak also concluded that:

1. The Resilient Modulus for different materials can be expressed by:

Material	Regression Equation
DGA-LS	MR = 1.445 + 1.023 C
DGA-MS	MR = -0.785 + 0.763 C
Soil A-2	MR = -0.379 + 0.235 C
Soil A-3	MR = -1.477 + 0.241 C
Soil A-2-4	MR = -0.948 + 0.222 C

for cement contents (C) from 1.5 to 6.0%.

2. The Resilient Modulus at 28 days is higher than that at 7 days by a factor ranging from 1.25 to 1.55. A linear regression relationship between the modulus at 28 and 7 days could be represented by the equation:

$$MR28 = 0.1887 + 1.093\ MR7$$

3. The Resilient Modulus is related to the static Young's Modulus (E) by:

(DGA) $MR = 0.185 + 4.41\ E$

(Soils) $MR = 0.303 + 2.07\ E$

4. The Resilient Modulus is related to the unconfined compression strength by:

(DGA) $\log_{10} MR = -0.141 + 0.000529\ (UCS)$

(Soils) $\log_{10} MR = 0.659 + 0.001135\ (UCS)$

2.4.2. Dynamic flexure test

The traffic load applied on the pavement causes compression at the upper layer and tension at the underside. This condition can be simulated by the flexure test in the laboratory.

Ahlberg and McVinnie (1962) conducted the first study on the fatigue behaviour of lime-flyash-aggregate mixtures, using beam specimens tested in dynamic flexure. They concluded that the number of cycles to fracture in flexure

tests depends on σTmax/MRe, where σTmax is the maximum applied tensile stress and MRe is the estimated Modulus of Rupture (also known as the Bending Tensile Strength). The Equation

$$\sigma Tmax / MRe = 1.0 - 0.0798 \log_{10} N$$

was established to predict the number of load cycles (N) to cause fatigue failure.

The U.S. Army Engineers Waterway Station (1967, 1969, 1972, 1974) concluded that the fatigue behaviour of stabilised soil-cement can be expressed by:

$$S = a N^{-b}$$

where,

S = the flexural stress level,

a = $h^{1.5}/(2.1h-1)$

h = slab thickness

b = 0.025 for granular soil-cement and 0.050 for fine grained soil-cement

N = the number of load cycles to failure.

It was also shown that the stiffness and strength characteristics in flexure and compression are different e.g. the Resilient Modulus is greater in flexure than that in compression.

Pretorius (1970), carried out flexural fatigue tests on a stabilised granular soil-cement. The beam specimens were tested under third point loading with a frequency of 2Hz. Strains were measured at the top and bottom surface of the beams and the results were presented in terms of either initial maximum flexural strain ϵi, and/or initial bending stress σi, versus the number of load repetitions (N). Straight line approximations of the results gave the following equations:

$$\log_{10} N = 9.110 - 0.05780\ \epsilon i$$

$$\log_{10} N = 7.481 - 0.01618\ \sigma i$$

Bending tensile strains remained fairly constant over a large portion of the fatigue life after which the rate of change increased at an increasing rate until failure.

2.4.3. Dynamic tension test

Tensile strength is an important engineering property of brittle materials, such as concrete, most rocks and soil cement. Ironically it remains one of the least well-defined material properties. This results from lack of experimental techniques that are both practical and reliable and rigorous enough from a continuum mechanics viewpoint.

There has been only a limited amount of published work to

establish the fatigue behaviour of soil-cement materials under uniaxial tensile fatigue. An important finding was established when Bofinger (1965) conducted the first dynamic uniaxial tensile test. His work has shown that fatigue effect in tension is a lot higher than that in compression. This can be attributed to high stress levels caused by the applied tensile stresses.

Kolias (1975), and Kolias and Williams (1978), carried out dynamic loading tests in direct uniaxial tension, using a relatively soft friction grip system (Figure 2.5), on fine grain soil-cement prismatic specimens. The number of cycles for each stress level has been averaged out and plotted against stress level (Figure 2.6). The stress level is then defined as a percentage of the uni-axial tensile strength. In the case where the test was discontinued before failure occurred, the number of cycles up to this point is considered and then a conservative estimate of the fatigue life of the specimen is made.

Raad, Monismith and Mitchell (1977), carried out a study on the fatigue behaviour of soil-cement specimens subjected to dynamic load in direct uniaxial tension. The material used in their investigation was clayey gravel and tests were conducted for curing periods of 4 and 10 weeks. It was found that tensile fatigue failure takes place when the tensile strength of the material decreases from

initial value Ti to a value T' equal to the maximum value of the stress factor F i.e. Fmax. The decrease in strength with repetitions of stress applications is illustrated in Figure 2.7 where:

$$a = (\log_{10} Ti - \log_{10} T') / \log_{10} Nf$$

$$a = (\log_{10} Ti - \log_{10} Fmax / \log_{10} Nf$$

$$a = \log_{10} [1 / (Fmax/Ti)] / \log_{10} Nf$$

where,

Nf = number of load cycles to failure

Fmax/Ti = function of maximum stress level.

Table 2.2 shows a comparison of the function of maximum stress level Fmax/Ti with number of load cycles of failure Nf for curing periods of 4 and 10 weeks.

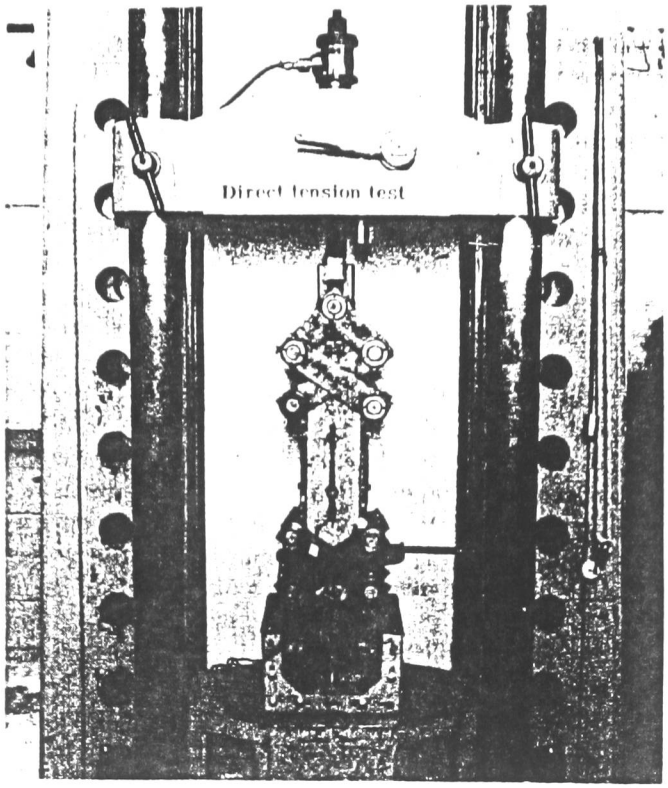

Fig.2.5. Friction grip system.

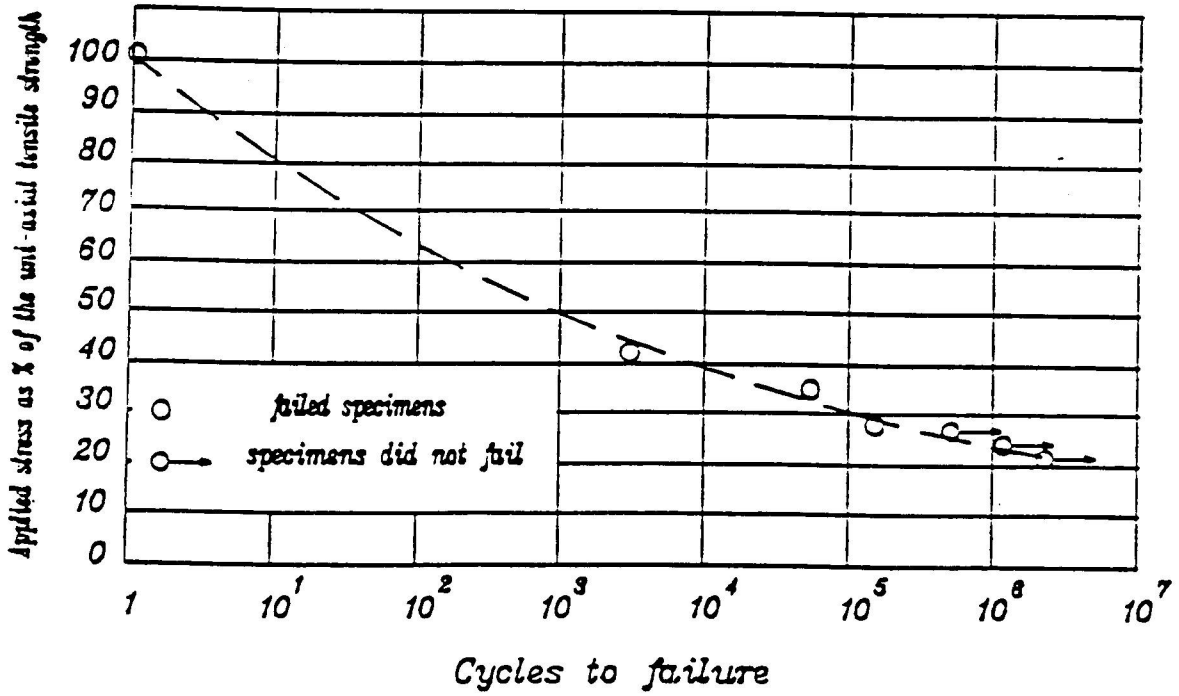

Fig.2.6. Fatigue performance related to uniaxial tensile strength.

Table 2.2. Values of (F_{max}/T_i) and (N_f) as Suggested by the Fatigue Failure Criteria

N_f	F_{max}/T_i (4 weeks)	F_{max}/T_i (10 weeks)
10^{35}	0.20	0.47
10^{7}	0.55	0.71
10^{6}	0.58	0.73
10^{5}	0.62	0.75
10^{4}	0.67	0.78
10^{2}	0.78	0.84
1	1.00	1.00

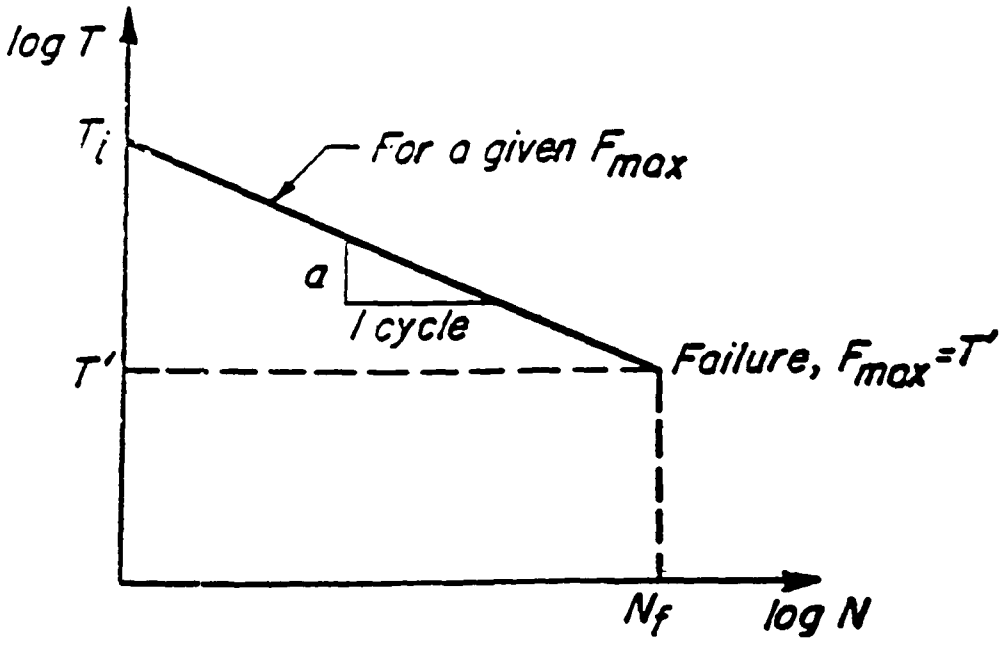

Fig.2.7. Variation of Tensile Strength with Number of Stress Applications for a Given F_{max}.

2.4.4. Dynamic tension-compression test

Haimson (1978), conducted a series of dynamic loading tests including dynamic uniaxial tension-compression tests on rocks. This work was intended to improve the design of rock structures, assist in earthquake prediction and control, and advance rock breaking methods. The tests carried out by Haimson involved the use of a purpose made jig, shown in Figure 2.8. Typical stress-strain and strain-time curves recorded during the test are shown in Figure 2.9. The slopes of the stress-strain curves indicate that the dynamic modulus differs in tension and compression. The stress-Number of cycles to failure (S-N) curves for the dynamic tension and tension-compression tests are shown in Figure 2.10. Haimson concluded that the dynamic tension-compression loading regime appears to be the most fatigue-inducing loading mode. In view of these findings particular care has to be exercised at the design stage if structures are expected to be subjected to tension-compression loads.

Figure 2.11, illustrates a wheel exerting load on a pavement. Directly beneath the wheel, the top layer undergoes a state of compression, leaving the bottom layer in a state of tension. Opposite stresses occur either side of the wheel load. As the wheel moves, the region which

was under compression changes to tension and that under tension changes to compression. This indicates that the tension-compression dynamic test is more realistic than the flexure test in reproducing the effects of traffic loads.

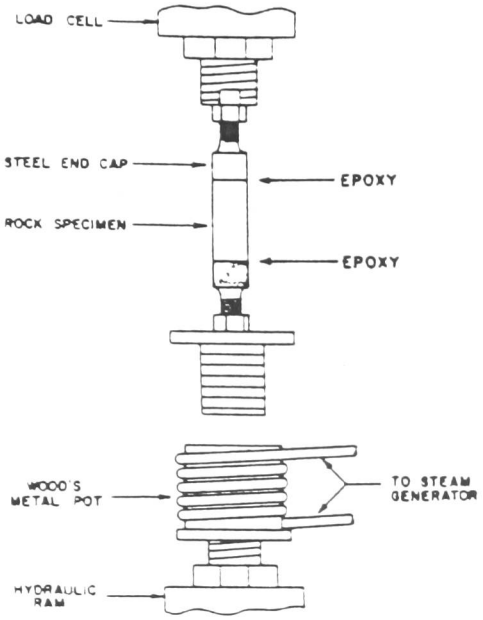

Fig.2.8. *Jig for cyclic uniaxial tension.*

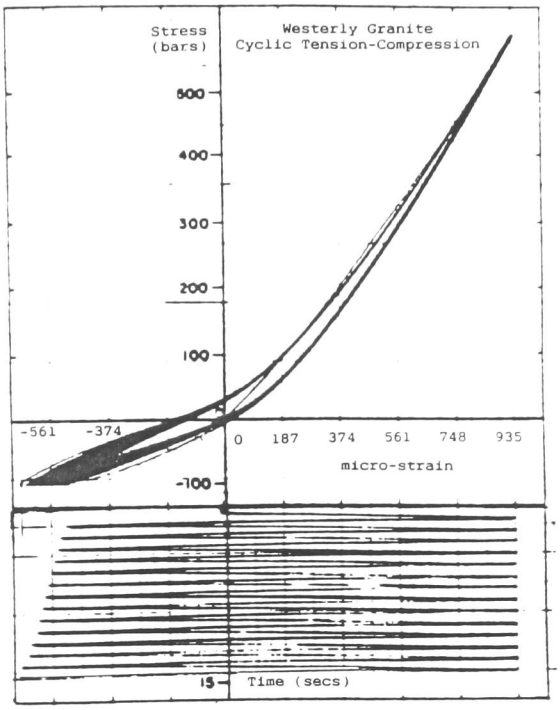

Fig.2.9. *Typical stress-strain and strain-time curves recorded during uniaxial tension-compression cycling (1 bar = 100 kPa).*

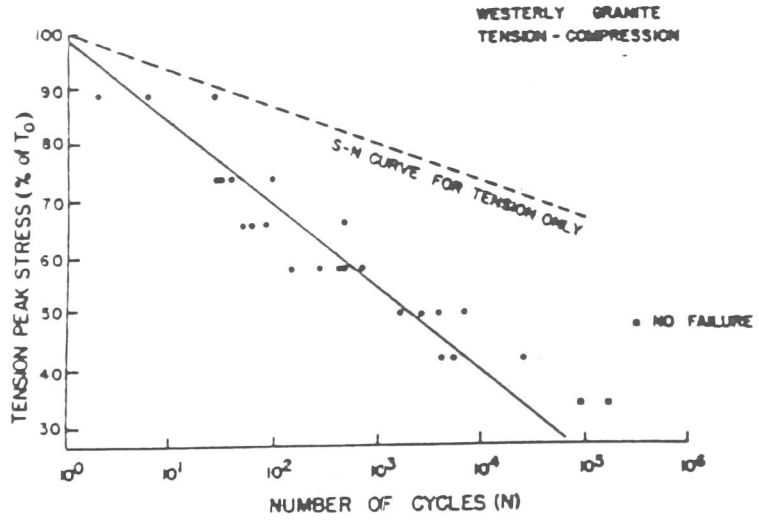

Fig.2.10. *Experimental results and S-N curve for Westerly granite under cyclic uniaxial tension-compression (compression peak constant-tension peak varied from test to test). Comparison with S-N curve for uniaxial tension.*

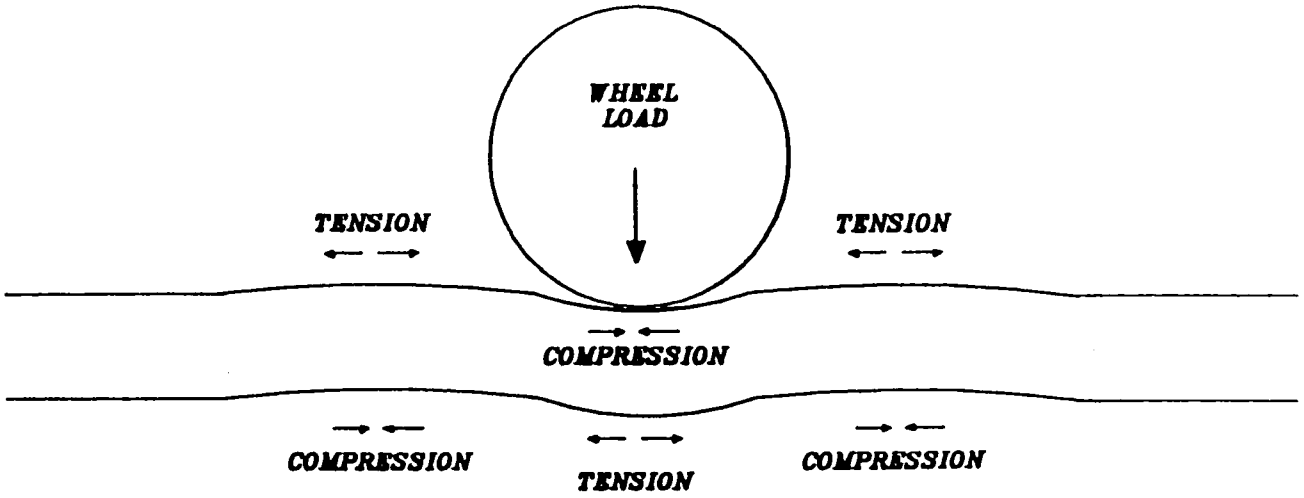

Fig. 2.11. Tension and compression zones of pavement layer under a moving wheel load

2.5. Testing apparatus and monitoring equipment

Before commencing the experimental programme, the suitability of equipment used by other establishments was investigated.

2.5.1. Specimen deformation measurement

The amount of deformation of soil-cement is considered to be similar to that of concrete and rocks, but much less than that of unstabilised soils. The resulting strains are small and accurate measuring devices are required. These devices should be capable of measuring 0.01% and 0.001% strains in the axial and lateral directions respectively.

When considering cylindrical specimens in dynamic tension or compression, measurement of axial and lateral deformations is necessary to determine the Resilient (Dynamic) Modulus and Poisson's ratio. These are essential input parameters for pavement analysis. Under axial loading in both compression and tension the lateral deformation is smaller than the axial deformation. This is illustrated in Figures 2.12.a&b.

For a beam specimen in a flexure test, measurement of the bending deformation in the axial direction and the lateral

deformation at the underside of the beam are needed to determine the soil parameters. This is illustrated in Figure 2.12.c.

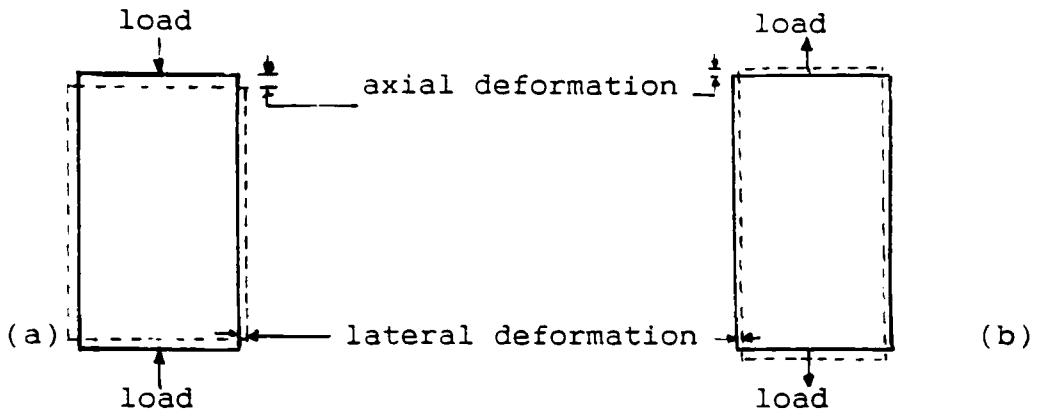

Fig.2.12. Deformations of the cylindrical specimen.
a) in compression b) in tension.

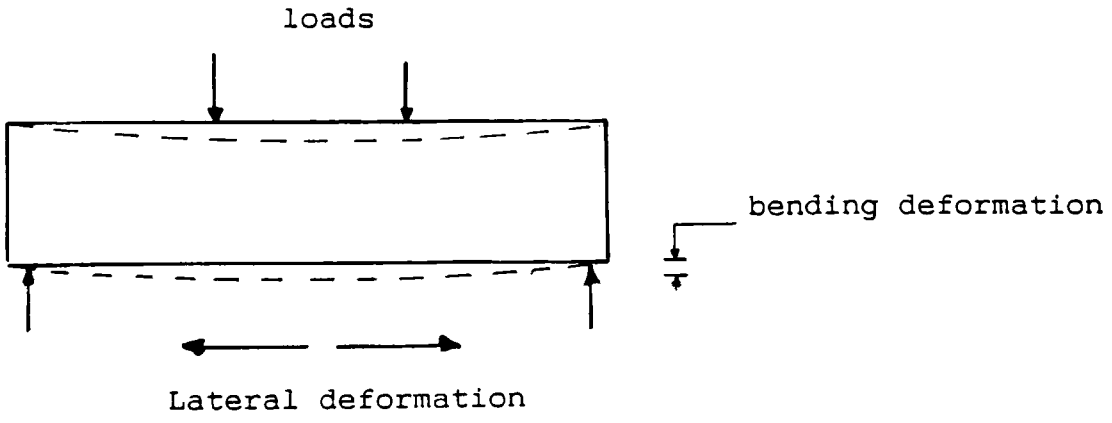

Fig.2.12.c. Deformations of the beam specimen.

Shah (1982), Raiss-Saadi (1985) and Kalantary (1986) used dial gauges to measure axial and lateral deformations. Dial gauges were also used during the early stages of this research but for static loading only.

Strain gauges have been used by Bhogal (1980 to 1983), to measure axial and lateral deformations of soil-cement specimens, by attaching them to the surface using adhesive. A disadvantage of this method is that the measurement of deformations may be affected by the strength of the adhesive. However, a new type of adhesive, which remains flexible during the early stages of its hardening time, is now available. Other disadvantages of strain gauges are:

a) strain gauge preparation prior to testing takes a long time; this limits the number of tests that can be carried out in a limited time schedule.

b) the cost of strain gauges for a large number of tests is high.

The use of specially manufactured wire to measure deformations was also considered. These wires have a perfectly constant cross-sectional area and are free from impurities. They are wound round the cylindrical specimen (Figure 2.13) and, as the load is applied, the wire

stretches causing a reduction in the cross-sectional area. This in turn alters the current flow, which can be measured and translated to give the lateral deformation. The method was proved to be very satisfactory by Attinger et al (1983) and Howarth (1984) (1985), where rock specimens were tested under dynamic compression. The main advantage of this method is that the deformation is measured integrally and not point wise. Hence it can be used on specimens with porous, rough or damp surfaces. The disadvantages are:

a) only cylindrical specimens under compression loads can be used.

b) the specimen's diameter reduces under tensile load. This causes slackness in the wire, leading to loss of contact with the specimen's surface. This can be overcome by stretching the wire initially to eliminate any slackness during testing. This means that the initial wire tension has to be constant for every specimen tested to give the same initial wire resistance, and this may prove difficult to carry out.

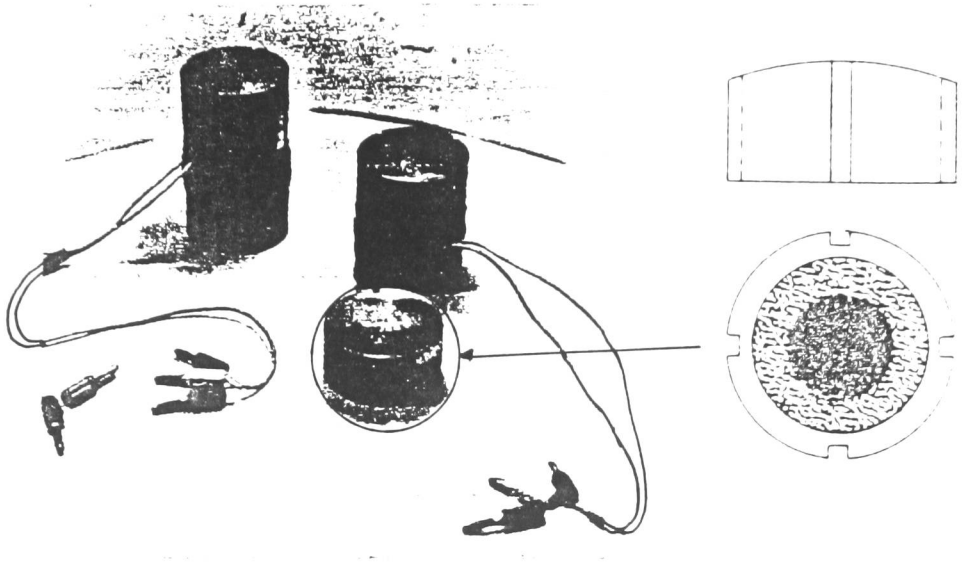

Fig.2.13.a. Protective steel platens suitable to fit a NX Hoek triaxial cell

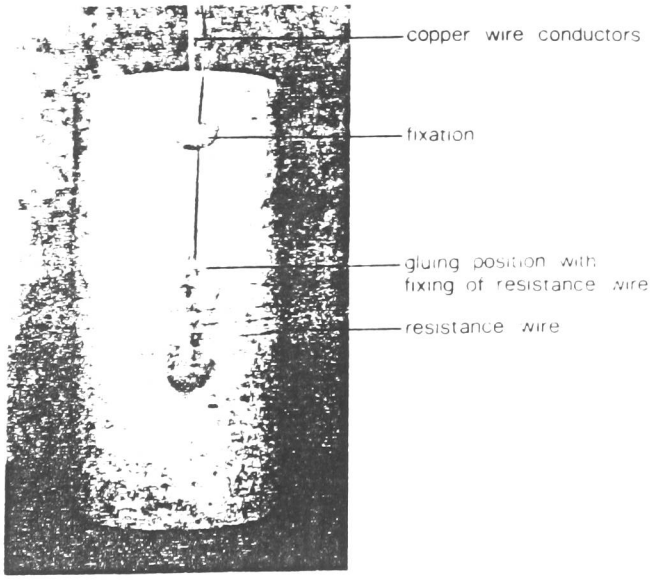

Fig.2.13.b. Test specimen mounted with resistance wire (diameter of specimen 54mm)

The use of electrolevel transducers for strain measurement was also investigated. See Figure 2.14. It was proven by Jardine et al (1985) that in weak rocks, the transducers are a reliable means of calculating stiffness at strains as low as 0.001%. These transducers however are not capable of measuring strains under high frequency dynamic loading. This is due to deformation resulting from movement of the liquid electrolyte inside the glass capsule.

Laser transducers were also considered for measurement of axial and lateral deformations, but the approximate cost of one thousand Pounds each was well over the allowed budget for this research. Another disadvantage of laser transducers is that they are bulkier in size than LVDT's.

It was finally decided that the best method for measuring axial and lateral deformations of the soil-cement specimens was by high accuracy LVDT's.

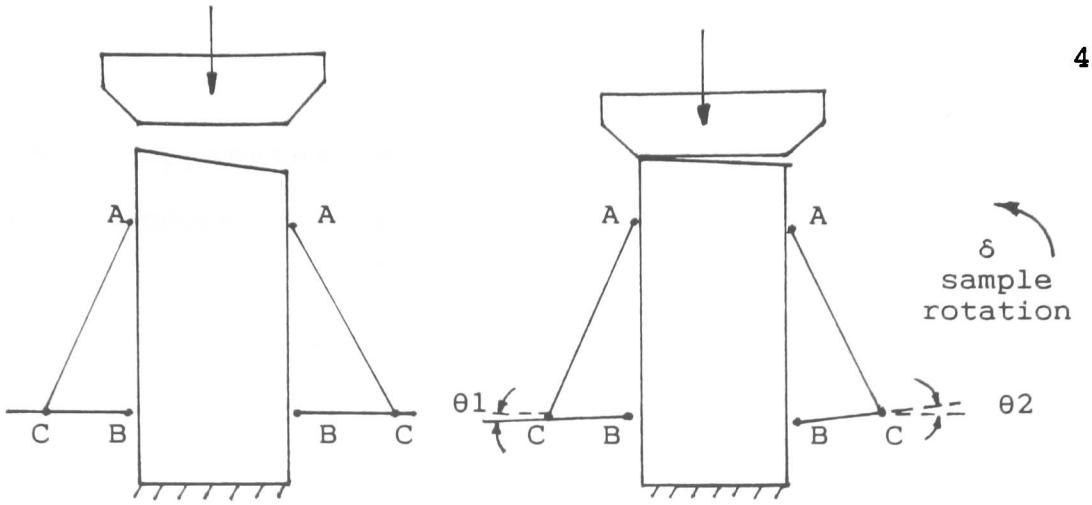

Fig.2.14.a. The effects of tilting: caused in early stage of test θ1 positive, θ2 negative for similar triangles experiencing small rotations, with angles in radians

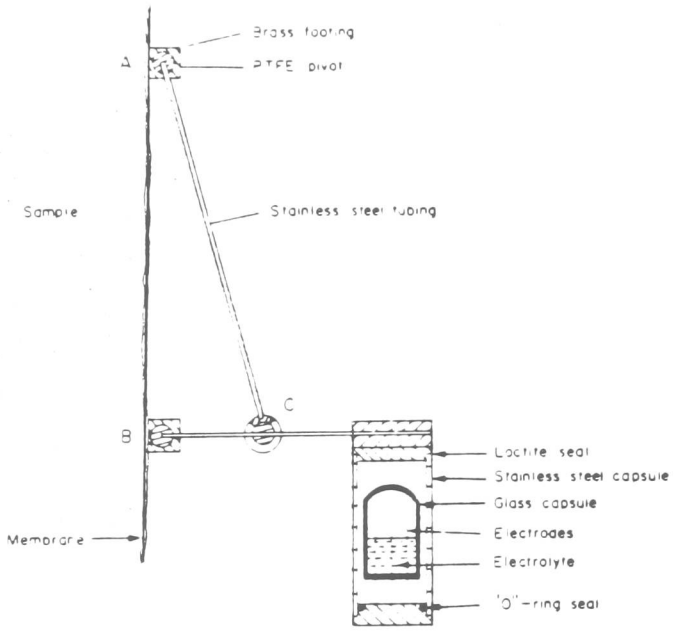

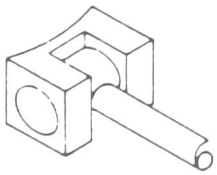

Hinges A and B

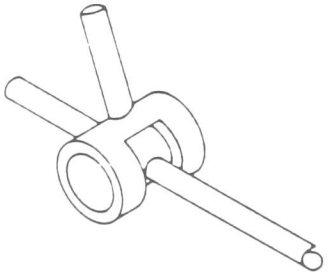

Hinge C

Fig.2.14.b. Construction of electrolevel gauges

2.5.2. Apparatus for static and dynamic tension and tension-compression tests

The apparatus developed for the dynamic tension and the tension-compression tests required careful design due to the following factors:

1. The tensile loading apparatus should be capable of eliminating eccentricity in the line of action of the applied tensile loads, which might develop during an experiment, and cause premature failure due to bending.

2. Soil-cement being of low strength and brittle was difficult to hold without damaging it. Scissor jaws were used by Kolias (1975), and Kolias and Williams (1978) in testing soil-cement specimens in direct tension; however this apparatus was not suitable for dynamic tension-compression tests.

Epoxy has been used when testing specimens of bitumen, soft rock and other materials. However the time required for the epoxy to set causes moisture losses which affect the strength of the specimen. In recent years epoxy technology has been advancing such that it can now reach its ultimate strength in a relatively short time and have a higher stiffness than the soil-cement.

3. The tensile strength of all brittle materials is a lot less than the compression strength. Soil cement is a brittle material and the load to cause failure in tension is approximately 10% of that in compression. Dynamic loading requires apparatus with a sensitive load cell to perform this type of test. The Instron 1251 and the MTS-850 testing machines are capable of producing high frequencies and monitoring the data output, and were used in the test program.

The detailed description of the apparatus used for these tests is given in Chapter four.

CHAPTER 3

Preliminary Work

3.1. Introduction

This Chapter covers the experimental work carried out during the early stages of this research and is concerned with the selection of materials, soil classification tests, specimen preparation, equipment calibration and establishing testing procedures.

3.2. Materials selection

It was decided that the soil selected for experimental work should be similar to materials encountered in the field for soil-cement stabilisation. It should also be suitable for laboratory investigation by being a homogeneous material, when pulverised, thus ensuring maximum consistency in test results. Based on these considerations, the soil chosen for this study is Red Marl from Abergavenny, South Wales, which is found in the old red sandstone originating from the Devonian age. The Red Marl is a silty clay representing a typical subgrade material in a pavement structure.

The stabiliser used is Ordinary Portland Cement

manufactured by Blue Circle cement company, supplied in sealed containers. The chemical analysis of this product, tabulated in Table 3.1, is furnished by the company as average values over the period during which samples were taken.

Loss on ignition	0.64%
Insoluble residue	0.82%
Soluble silica SiO_2	20.76%
Alumina Al_2O_3	5.25%
Ferric oxide Fe_2O_3	2.01%
Calcium oxide CaO	64.39%
Magnesia MgO	2.72%
Sulphuric anhydride SO_3	2.84%
Alkali equivalent (expressed as Na_2O)	0.57%

Table 3.1 Chemical analysis of Portland cement

3.3. Soil classification tests

The Red Marl was air dried, mechanically pulverised to a maximum 2mm diameter clod size, and well mixed before carrying out any tests. The routine classification tests (according to B.S. 1377:1975) gave the following values:

Liquid Limit (%) 37

Plastic Limit (%) 19

Plastic Index (%) 18

Specific Gravity 2.71

Particle Size Distribution: sand 9%,
silt 28% and
clay 63%, (Figure 3.1)

The organic matter is negligible.

The soil suitability was assessed by the criteria used for stabilised road pavements: for example the liquid limit at 37% is less than 45% and the plastic limit at 19% is less than the 20% limit specified for economical stabilisation by the Transport and Road Research Laboratory (1969). The Proctor Compaction test was carried out to determine the dry density/moisture content relationship of the soil using a 2.5kg rammer according to B.S. 1377:1975: Test 12. This test is often referred to as standard BS compaction, the heavy compaction used for airfield construction. The optimum moisture content and the maximum dry density were found to be 15% and 1.85 Mg/m^3 respectively (Figure 3.2).

3.4. Specimen preparation

The pulverised soil was oven dried then cooled, before the addition of the stabiliser and the water, to eliminate any moisture variations. The soil-cement mixture was dry-mixed

and a predetermined amount of distilled water was added and mixed thoroughly using an electric mixer (Figure 3.3), for exactly 11 minutes. The mixing time was developed during the research to give a homogeneous and consistent mix. The procedure for mixing was consistent for all the specimens prepared. The moisture content of the mix was adjusted to give a constant value of 15% just prior to moulding.

The cylindrical specimens were prepared according to BS 1924:1975: Test 10, and the prismatic specimens according to ASTM D 1632-63. To minimise friction all specimens were prepared by two-end static compaction in an oil lined mould. Sufficient mixture was placed in the mould so that the two rams did not reach the end of their travel when the full compaction pressure was applied by means of a hydraulic press. After compaction the end plugs on the specimen were removed and the specimen extruded carefully. It was immediately wrapped in a polyethylene sheet, which adhered to its damp surface, and then in aluminium foil to ensure constant temperature distribution around the specimen; it was finally placed in a plastic container to prevent moisture changes. The specimen and contents were then stored inside a controlled environment curing chamber (Figure 3.4), at 25°C and constant relative humidity of not less than 98%.

3.5. Equipment calibrations and trial tests

Each load cell was calibrated using a number of already calibrated proving rings. The 50KN load cell was calibrated in compression and tension; it was used on the Instron testing machine for the static and dynamic compression tests. The calibration results were plotted graphically and found to be linear. The 20KN load cell was calibrated, but found to have a non-linear relationship up to the first 10% of its load capacity. It was, therefore, considered unsuitable for flexure and tensile tests which require greater accuracy for small loads.

The rate of displacement or the ram movement against time was calibrated for the Instron 1251 testing machine, for a wide range of displacement rates and found to be uniform. The same procedure was adopted for the TRRL MTS-850 testing machine for dynamic tension-compression tests.

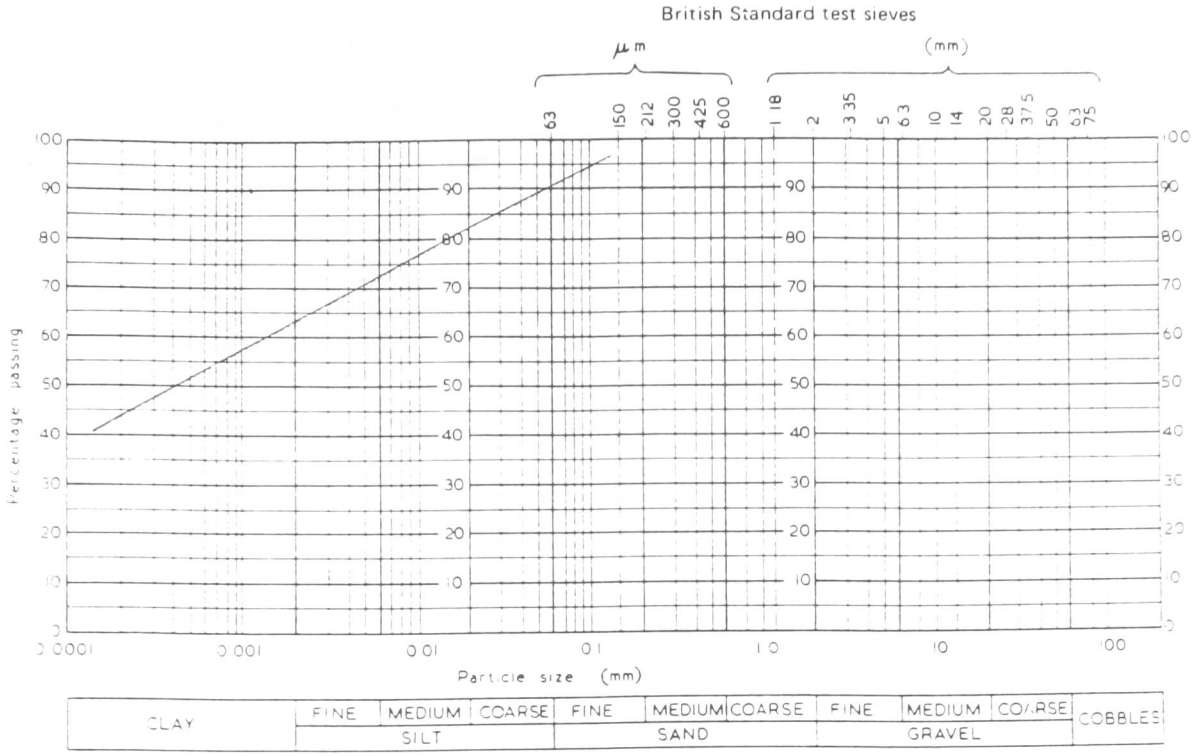

Fig.3.1. Grain size distribution curve for Abergavenny Red Marl

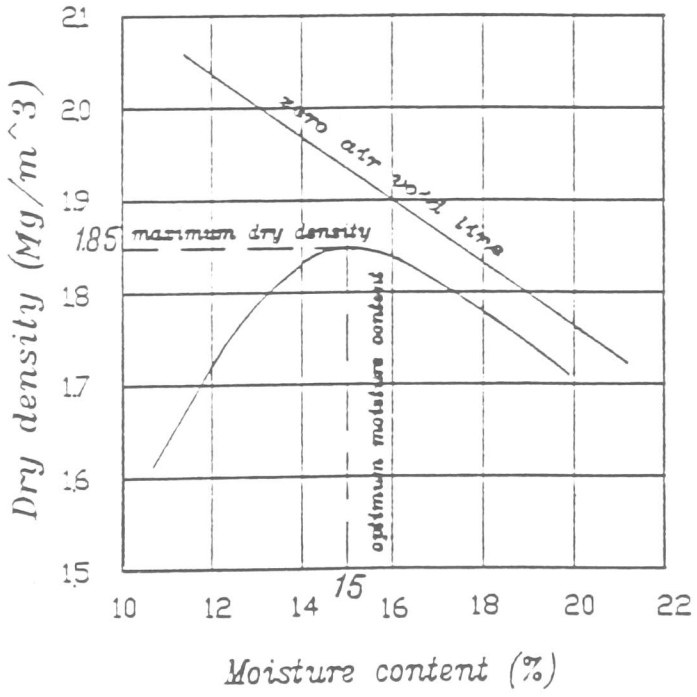

Fig.3.2. Dry density/moisture content relationship of the soil

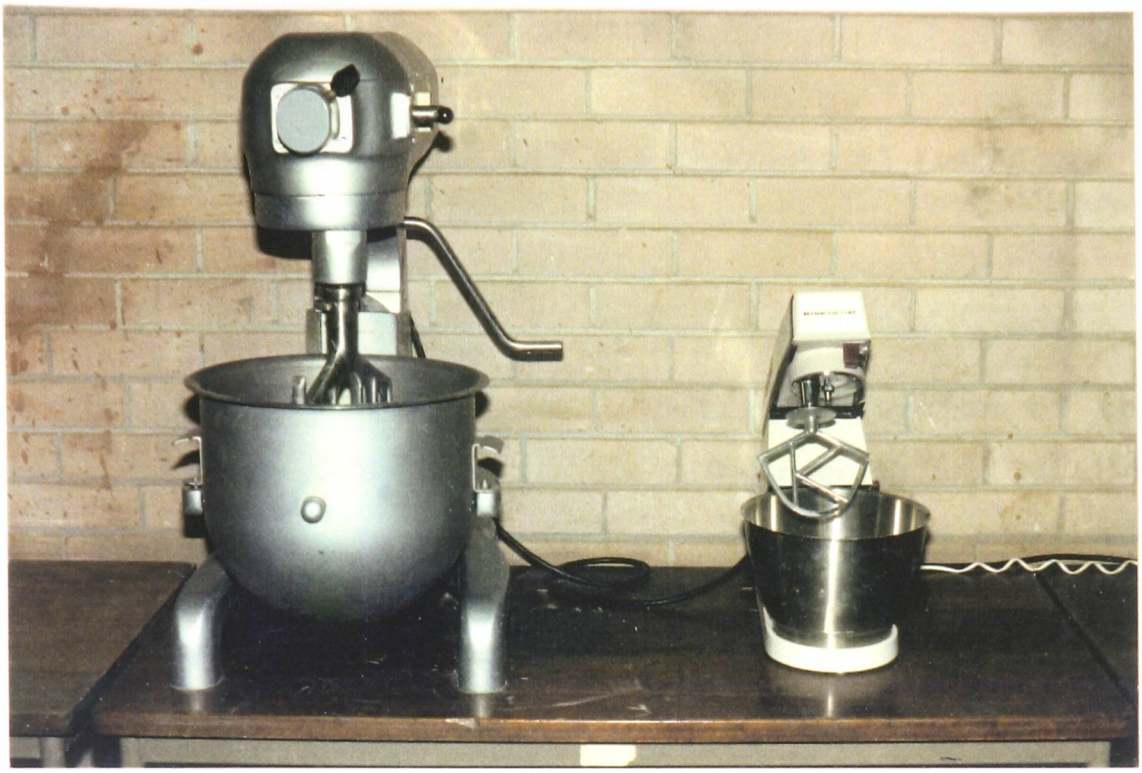

Fig.3.3. Type of mixers used during the investigation

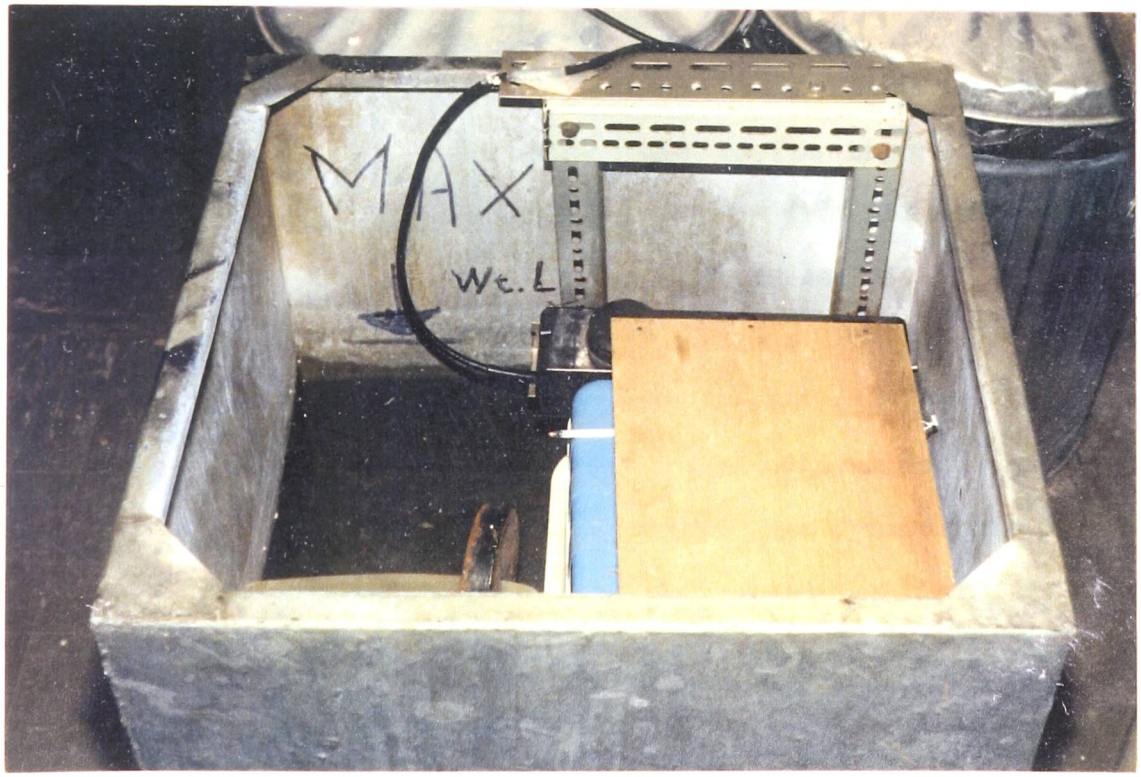

Fig.3.4. Controlled environment curing chamber

CHAPTER 4

Development of Equipment and Experimental Procedures

4.1. Introduction

This Chapter deals with a full description of the equipment available in the Civil Engineering and Building Department at The Polytechnic of Wales, and the additional equipment developed and used throughout the research.

4.2. Specimen's geometry

4.2.1. Cylindrical specimens

The cylindrical mould used in this investigation is specified in B.S. 1924:1975: Test 10 for the determination of unconfined compressive strength for fine and medium grain stabilised soils. The mould consists of: a tapered steel body of internal dimensions 100 x 50mm mean diameter; two steel plugs and displacing collars; an ejection plunger (Figure 4.1). The cylindrical specimens were used to investigate the static and dynamic properties of the soil-cement in uniaxial compression. Similar specimens were also used in static and dynamic tension and tension-compression tests. The end caps, seatings, all other fixing parts of the Instron load cell, and the ram

have been developed to accommodate such tests.

The clay-water-cement mixture was compacted in three equal layers, with an equal number of tamps uniformly applied to each layer. The top plug was placed and the displacing collars removed. After the mould was placed in the static compaction frame shown in Figure 4.2, pressure was applied until the plugs were fully pushed into the mould. This pressure was sustained for five minutes, this period of time being adequate, for this type of soil, to allow compressed air trapped between the soil particles to dissipate. The end plugs were then removed and the ejection plunger was pushed from the slightly smaller end, extruding the specimen. The specimen was weighed to the nearest 0.1g and the dimensions measured to the nearest 0.01mm. It was then stored away in the curing chamber (Figure 3.4) under controlled conditions.

For the tension and tension-compression tests, the end caps are glued to the specimen, using the rig manufactured and shown in Figure 4.3, to ensure they are perfectly parallel.

When carrying out the compression test, it is essential to reduce the friction between the specimen and the end caps. This contact area was treated with Silicone grease

polished with graphite powder, creating a smooth surface. This reduced the amount of friction between the specimen and the caps and allowed it to remain cylindrical when expanding laterally under axial compression.

4.2.2. Beam specimens

The mould (Figure 4.4) was manufactured specially for this project according to ASTM D1632-63 standard test method for flexural strength of soil-cement. It has internal dimensions (specimen size) of 76.2 x 76.2 x 285.8mm long (3 x 3 x 11.25in). This mould size was chosen because most flexure tests carried out on soil-cement material have used this mould size. This makes comparison with other results easier and, more importantly, the size of the specimen ensures specimen failure in flexure. This is because a smaller size beam may fail in shear rather than in flexure due to the small distances between the supports and the points of loading.

The mould is so designed that the specimen will be moulded with its longitudinal axis in a horizontal position. The sides of the mould were tightly fitted and held firmly to prevent spreading or warping. Two top and bottom machined steel plates were fitted to the mould with 0.13mm clearances on all sides. The mould can be dismantled completely to release the beam specimen. The four-point

loading system is shown in Figure 4.5. It is designed with four semi-circular loading points which may be rotated through small angles in any direction.

The soil-water-cement mixture was prepared and compacted in three equal layers as for the cylindrical specimens, with an equal number of tamps applied to each layer. The top plate was placed on the specimen surface and the mould moved to the compaction rig (Figure 4.4). A pressure was then gradually applied to the specimen by a hydraulic jack, until the gap between the cover plates and the mould's sides closed; this pressure was sustained for five minutes and then released. The specimen was then removed, by dismantling the mould, and wrapped with polyethylene sheet and an outer sheet of aluminium foil. With beam specimens more care was needed in handling and storing as they easily break.

4.2.3. Other types of specimens

Another cylindrical mould (B.S. 1924:1975), shown in Figure 4.6, was available for medium to coarse soil specimens. The specimen's height can be altered by using different lengths of end plugs producing specimens of 100x 100mm diameter and 150x100mm diameter. These specimens are suitable for dynamic compression or split tension tests.

A new shape of mould, shown in Figure 4.7, was developed in the Department of Civil Engineering and Building at The Polytechnic of Wales specifically for tensile testing of soil-cement. It was designed to ensure uniform stress distribution in the middle portion.

4.3. Testing Equipment

4.3.1. Static loading equipment

Static unconfined compression tests were performed according to B.S. 1924:1975; flexure tests were performed according to ASTM 1635-65, using the Instron machine, model 1251 (Figure 4.8). The tests were carried out in static mode with displacement control at 0.017mm/sec for the unconfined compression test and 0.02mm/sec for the flexure test.

4.3.2. Dynamic loading equipment

Dynamic unconfined compression and flexure tests were performed on the Instron 1251 machine. The mechanically operated crosshead is automatically clamped when the machine is switched to the dynamic displacement mode. The machine has the capability of a wide range of load control and load repetitions from 0.001 to 1000Hz. The load may be applied in a variety of waveforms including sinusoidal,

ramp, triangular or square waves.

The built in transducer simulates the ram movement; hence the specimen's deformation can be monitored fairly accurately. In dynamic testing the machine was set up loading sinusoidally from almost zero load to a load level less than that which would cause failure in static mode. The frequency of 5Hz was chosen to simulate traffic loading. The number of load repetitions was monitored on a cycle counter.

The automatic chart recorder was used to monitor maximum and minimum load applied, deformation and time. The oscilloscope provided on the Instron console was used to indicate the waveform, frequency and the load applied.

As a future recommendation the Instron 1251 can be linked to an external computer, through its console, recording all the data output. This will allow longer period dynamic tests to be carried out and an output of a comprehensive set of results.

Figures 4.5, 4.9 and 4.10 show the flexure, compression, and tension-compression tests in progress on the Instron.

The MTS-850 Structural Test System in Figures 4.11 and 4.12 is another testing machine similar in features to the Instron; this was used for fatigue tests on bituminous materials for the Transport and Road Research Laboratory and for carrying out preliminary dynamic tension and tension-compression tests on prismatic specimens. It is equipped with anti creep circuitry and an Ultra Violet (UV) strain recorder.

4.4. Measuring and recording systems

One of the difficulties experienced in this study was the measurement of deformations. The soil-cement materials are far stiffer and more brittle in character than compacted soils. The amount of measurable deformation under dynamic load is of the order of 0.01% strain axially and 0.001% strain laterally.

The techniques of deformation measurement have been discussed in Chapter two. The transducer assembly system, developed and shown in Figures 4.14, 4.15 and 4.16, was manufactured at The Polytechnic of Wales. The system consists of four LVDT's (manufactured by Sangamo) capable of measuring deformation around (±1mm) which is highly accurate. Another LVDT of higher accuracy (±0.25mm) was attached to the side of the specimens for measuring the lateral deformation. The design of this system was an

extension of the transducer assembly system designed by TRRL, shown in Figure 4.13, which has been successfully used for similar tests. The testing rig shown in Figure 4.14 can be used for cylindrical and beam specimens of soil-cement.

4.5. Testing procedures

4.5.1. Static and dynamic compression test procedures

Many unconfined compression tests were carried out during the early stages of the experimental work; the results produced from these tests are not documented in this thesis. They were carried out mainly to establish the best experimental techniques and mixing, moulding and curing procedures for the soil-cement specimens.

All specimens were cured in the curing chamber prior to testing, at a maintained temperature of 25°C. Establishing a proper curing technique is essential because part of this study concerns the effects of curing time on soil-cement stabilisation.

The cylindrical specimens were prepared in batches of ten. Fifteen batches in all were prepared with cement contents of 6, 10, 14, 18 and 22% and curing periods of 7, 14 and

28 days. Two specimens from each batch were tested statically on the Instron 1251 machine to find the unconfined compressive strength of the particular mix.

The dynamic tests were also performed on the Instron 1251 machine. Various percentages of the load at failure in the static test were applied dynamically in load control mode at a frequency of 5Hz. The number of load repetitions to failure was recorded. Where failure had not occurred by 100,000 cycles the cyclic loading was stopped. The residual and total lateral deformations occurring during the test were monitored and recorded by the Instron chart recorder.

4.5.2. Static and dynamic flexure test procedures

A large number of prismatic specimens was prepared for the static and dynamic flexure tests. Problems were encountered when failure of the 20KN load cell was detected. The load cell was sent away to the manufacturers but was damaged beyond repair and could not be replaced in that financial year. At this point a decision was made to terminate the experimental work and concentrate on the analytical and computational works.

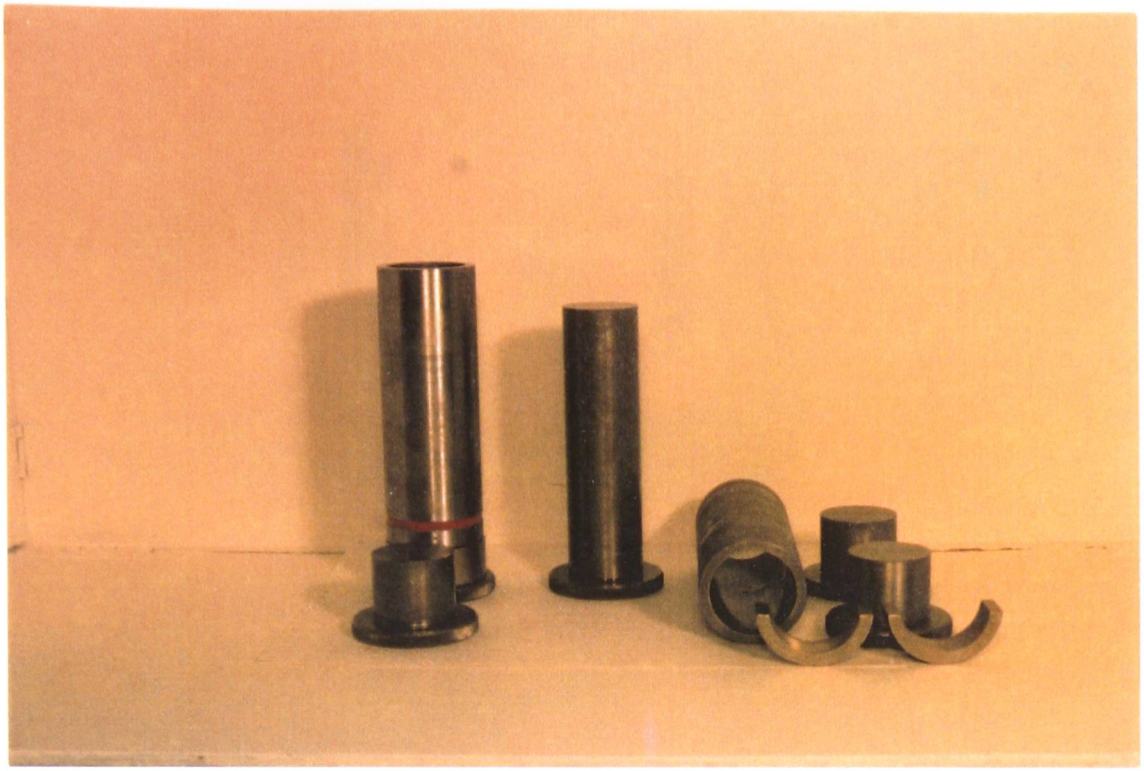

Fig.4.1. BS mould and accessories for preparation of 100 x 50mm diameter cylindrical specimen.

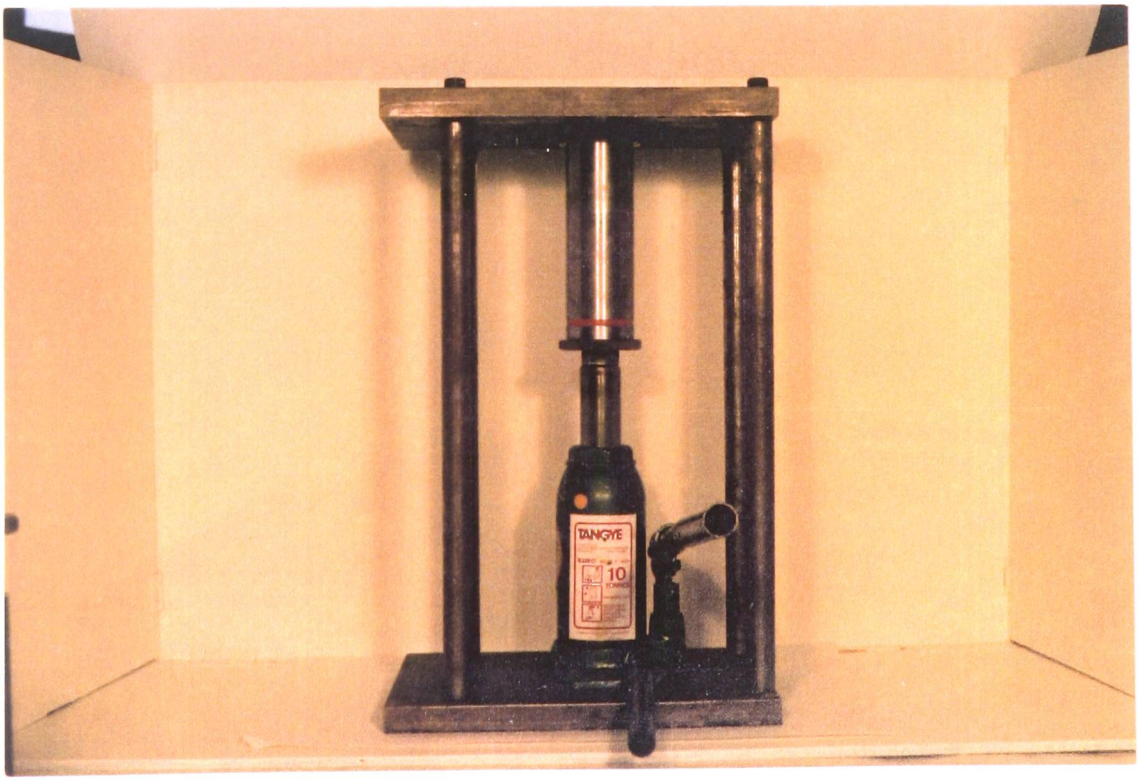

Fig.4.2. Frame and jacking system of specimen.

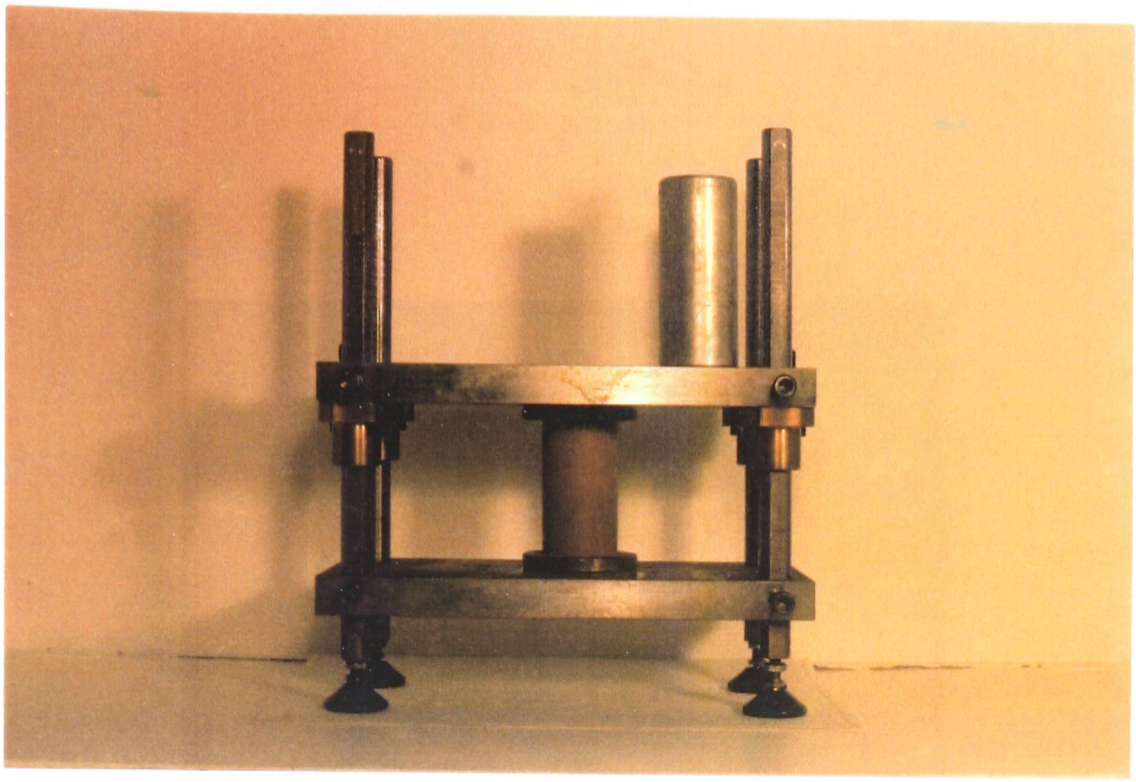

Fig.4.3. Parallel plates capping rig for tensile test specimen.

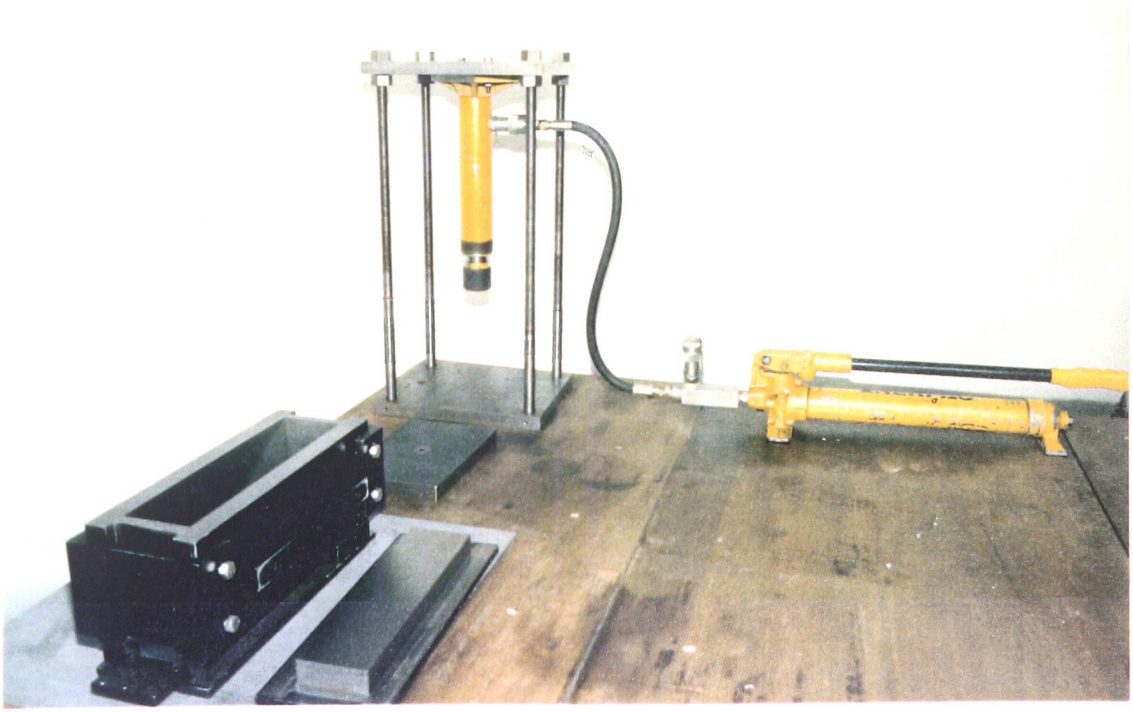

Fig.4.4. Mould for preparation of 76 x 76 x 286mm long prismatic specimen and compaction accessories.

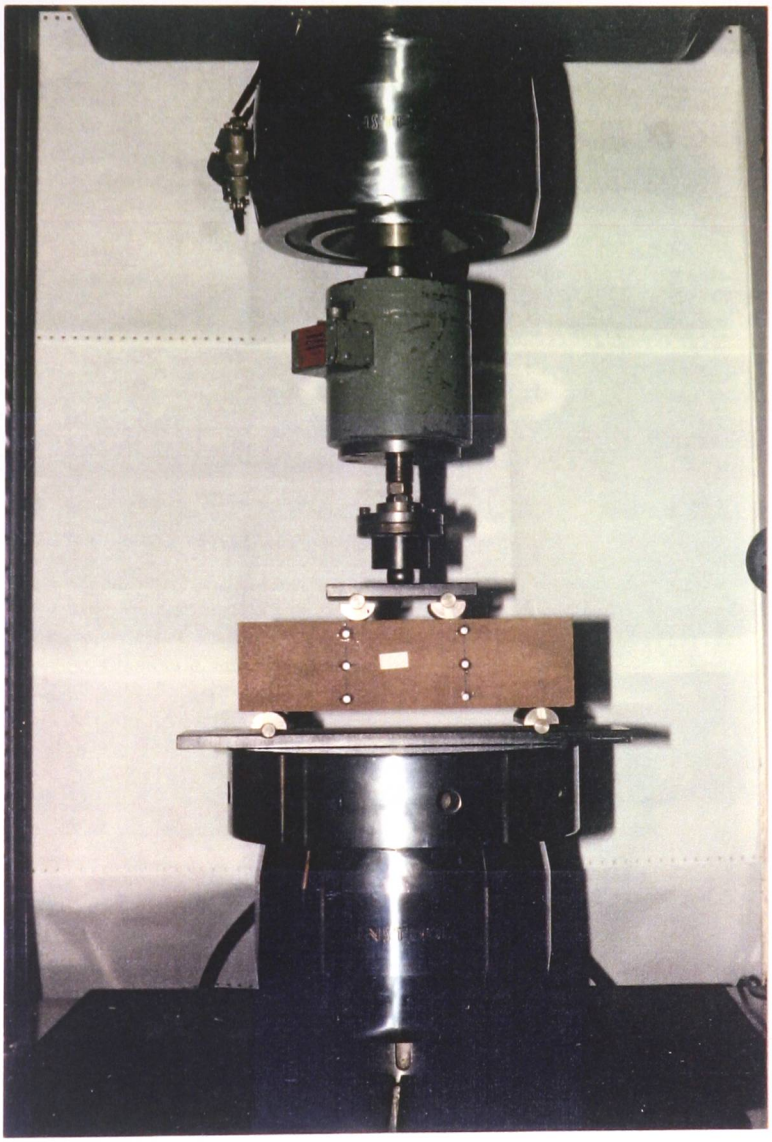

Fig.4.5. Four-point loading flexure test.

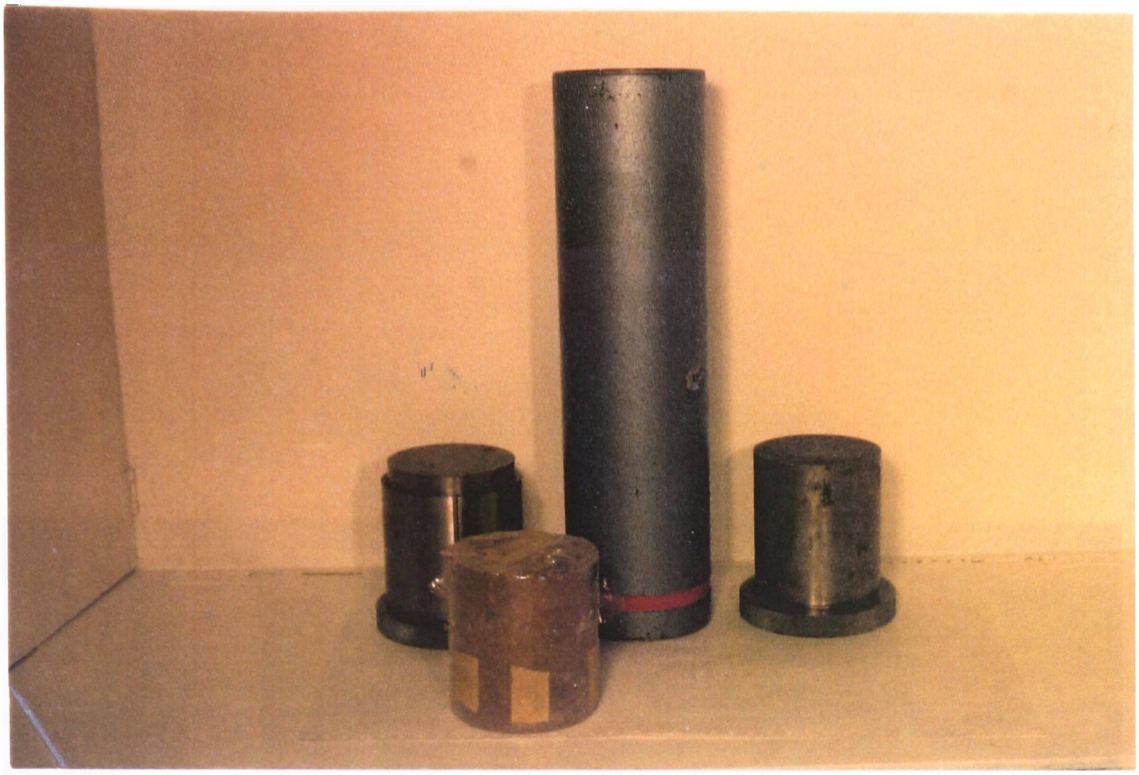

Fig.4.6. BS mould and accessories for 100 x 100mm & 150 x 100mm diameter cylindrical specimens.

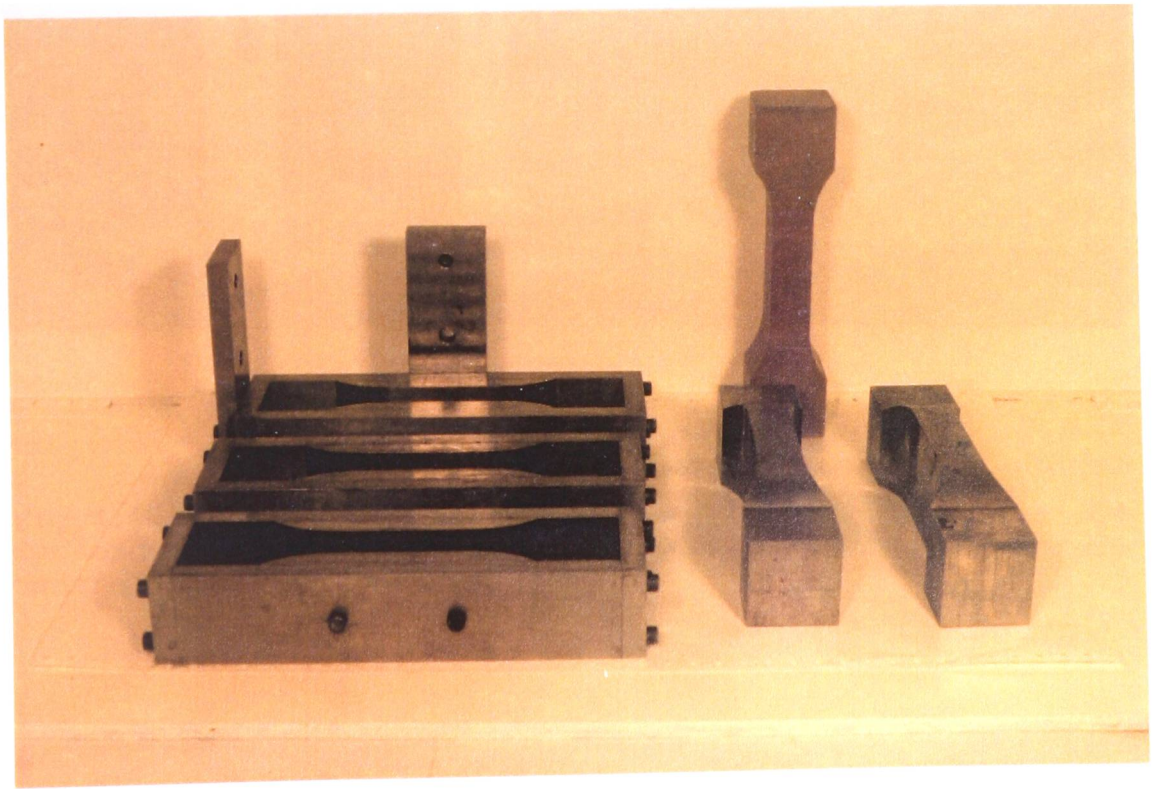

Fig.4.7. Mould and accessories for preparation of tensile test specimen to ensure uniform stress distribution in the middle portion.

Fig.4.8. Instron testing machine model 1251 for static and dynamic loading, with displacement, load and strain control facilities.

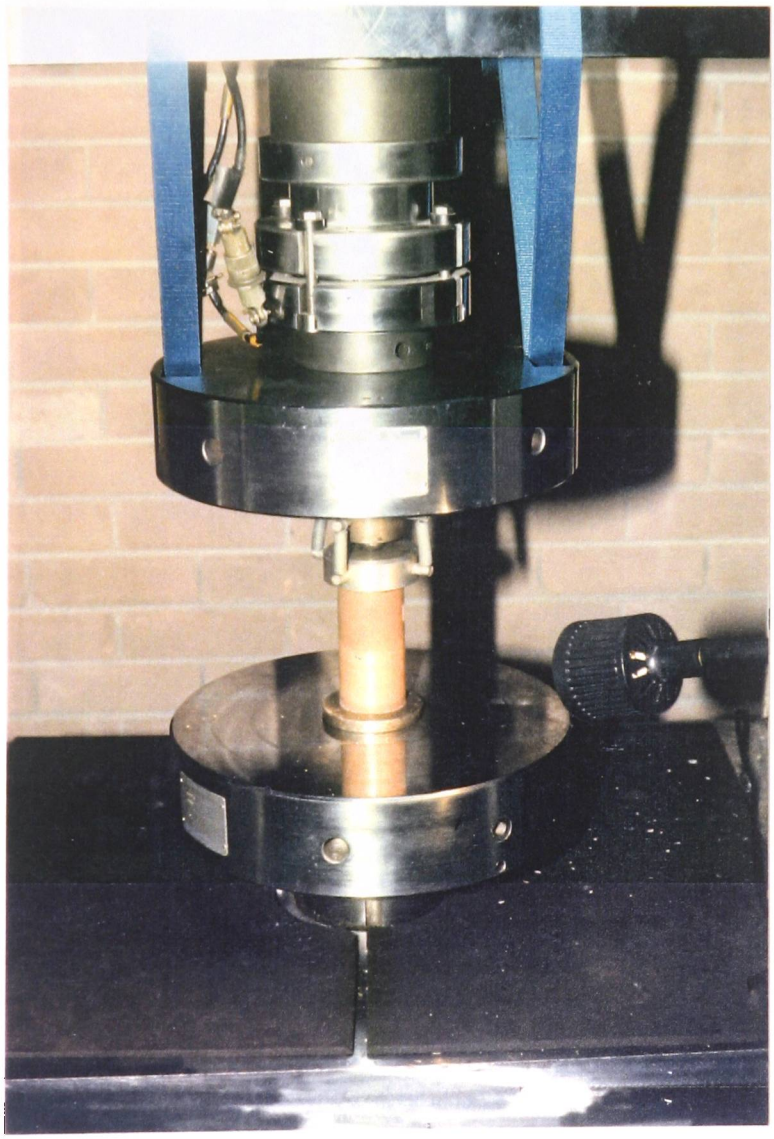

Fig.4.9. Dynamic compression loading on cylindrical specimen.

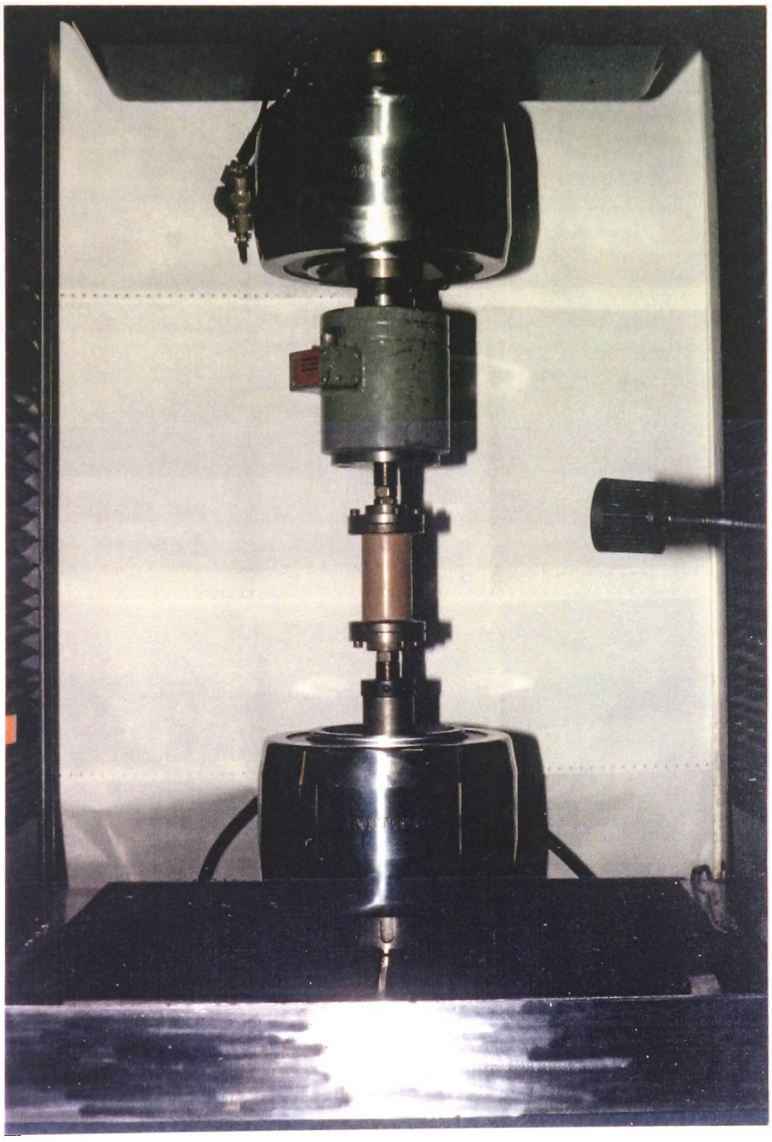

Fig.4.10. Dynamic tension-compression loading on cylindrical specimen.

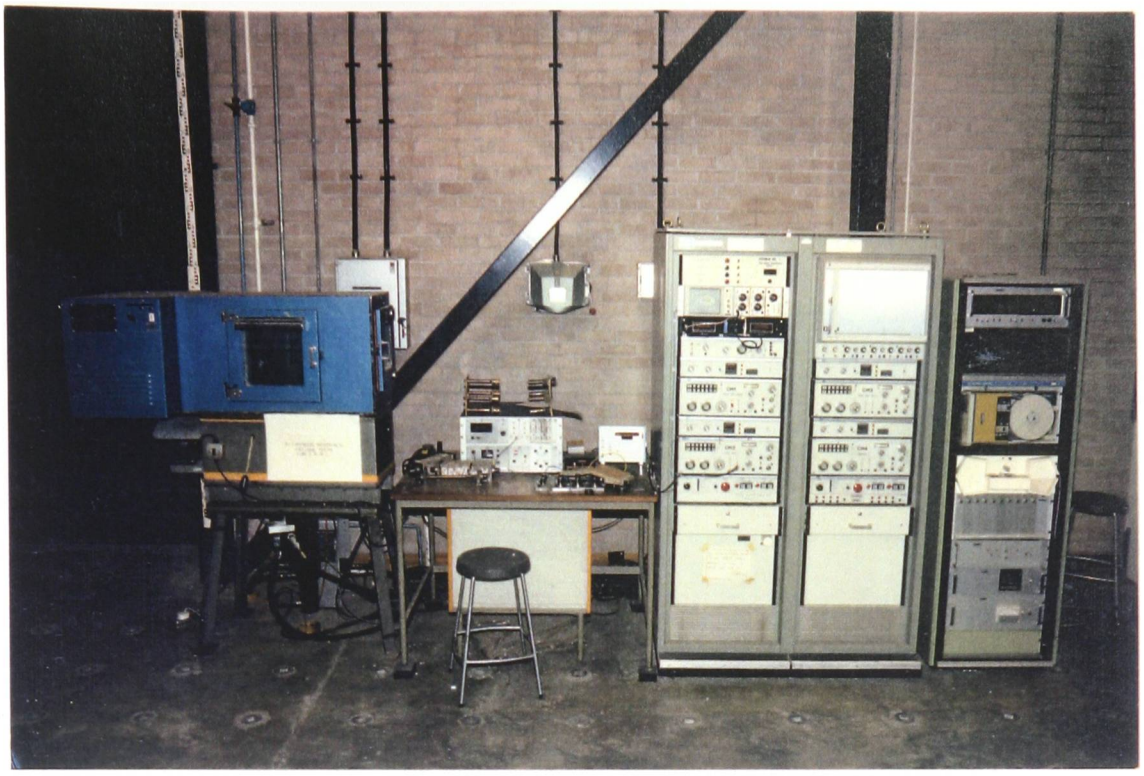

Fig.4.11. MTS-850 dynamic test system with anti creep circuit and UV strain recorder.

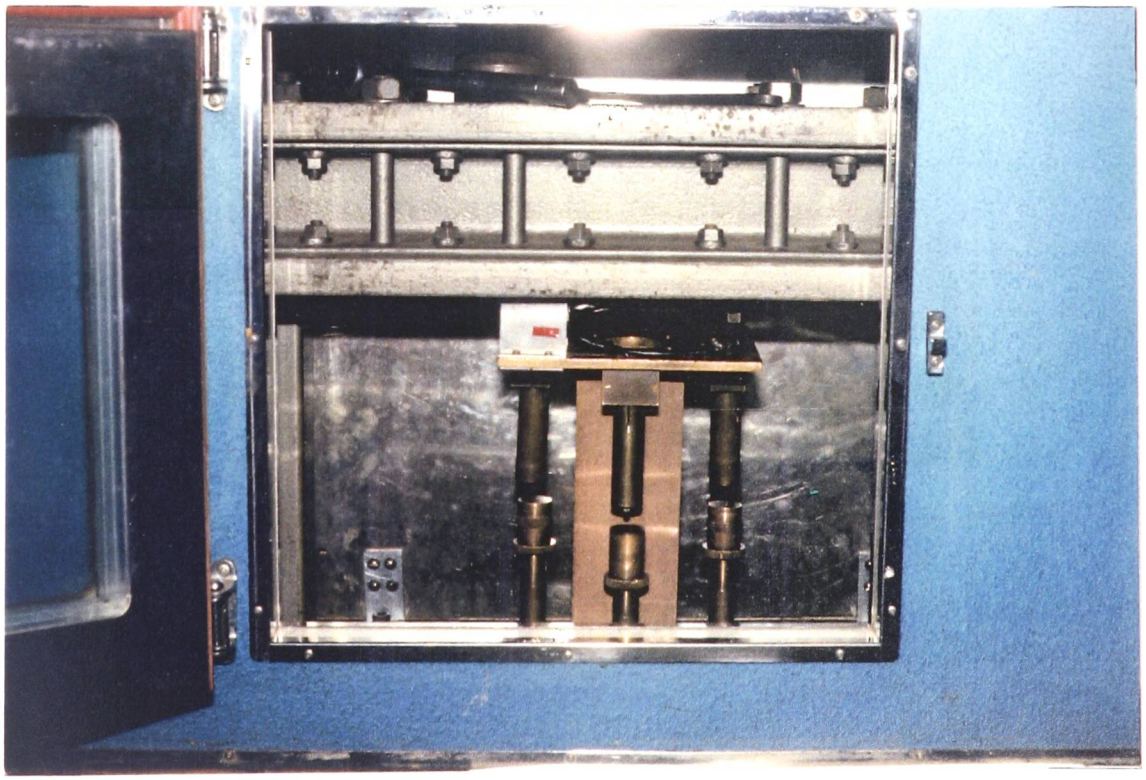

Fig.4.12. Uniaxial tension-compression loading on prismatic specimen in the MTS-850 loading system.

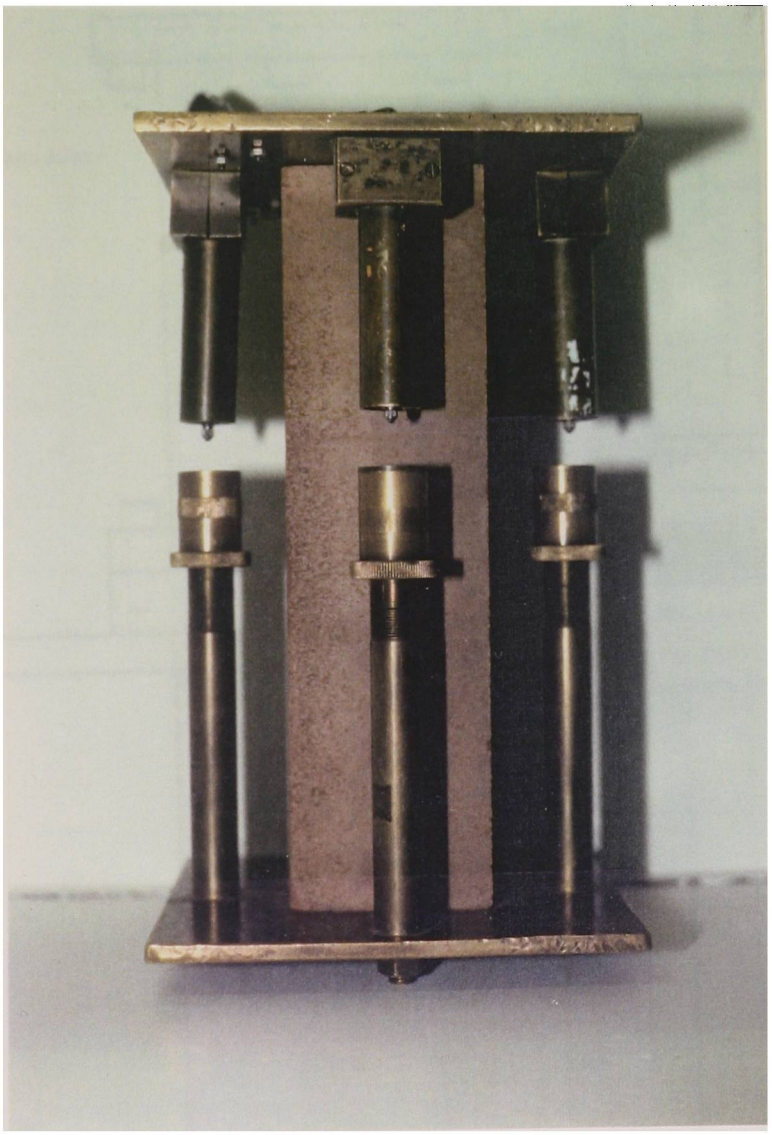

Fig.4.13. Transducer assembly for dynamic tension-compression test on prismatic specimen.

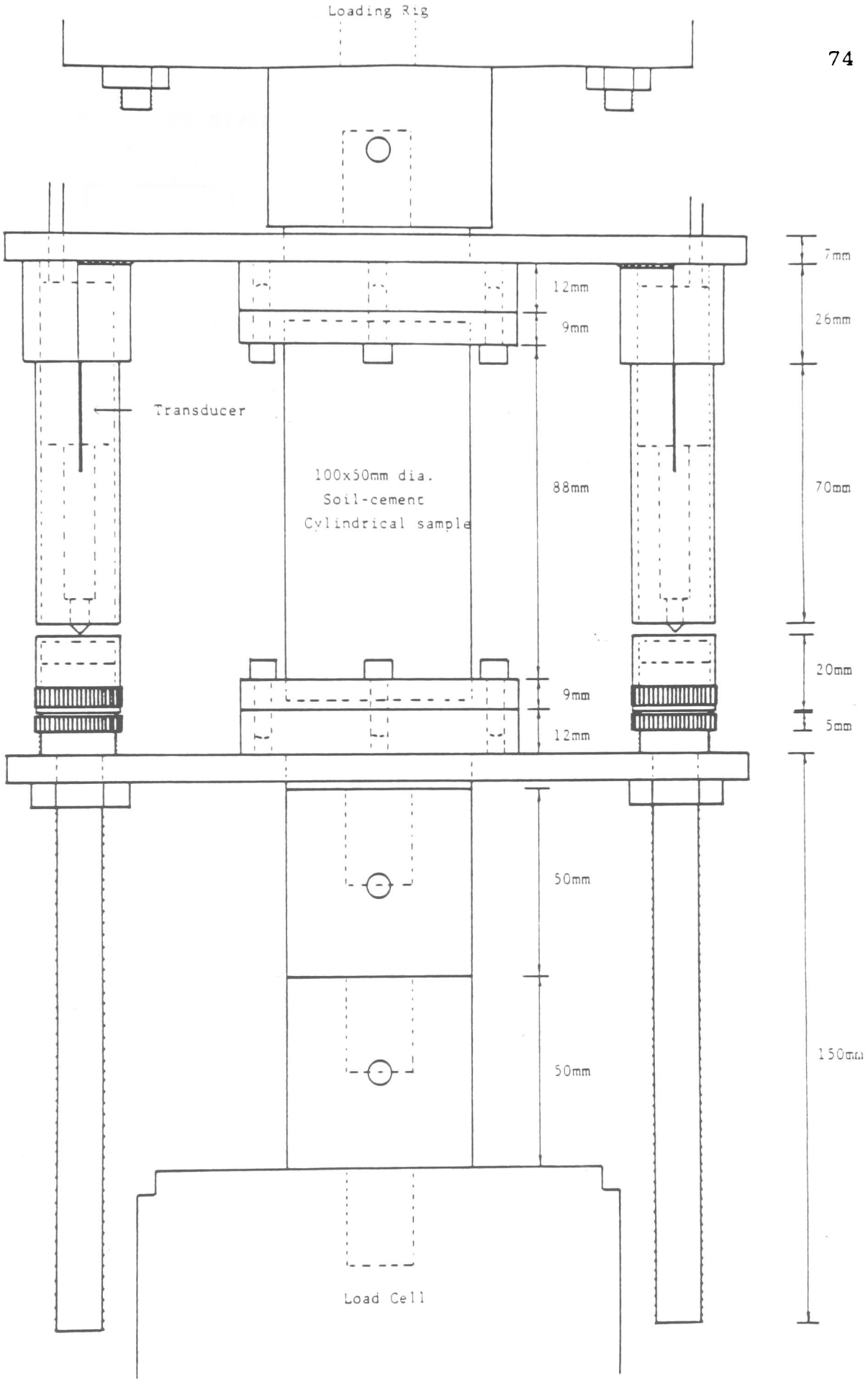

Fig.4.14. Modified design for transducer assembly system for dynamic tests on all types of specimens.

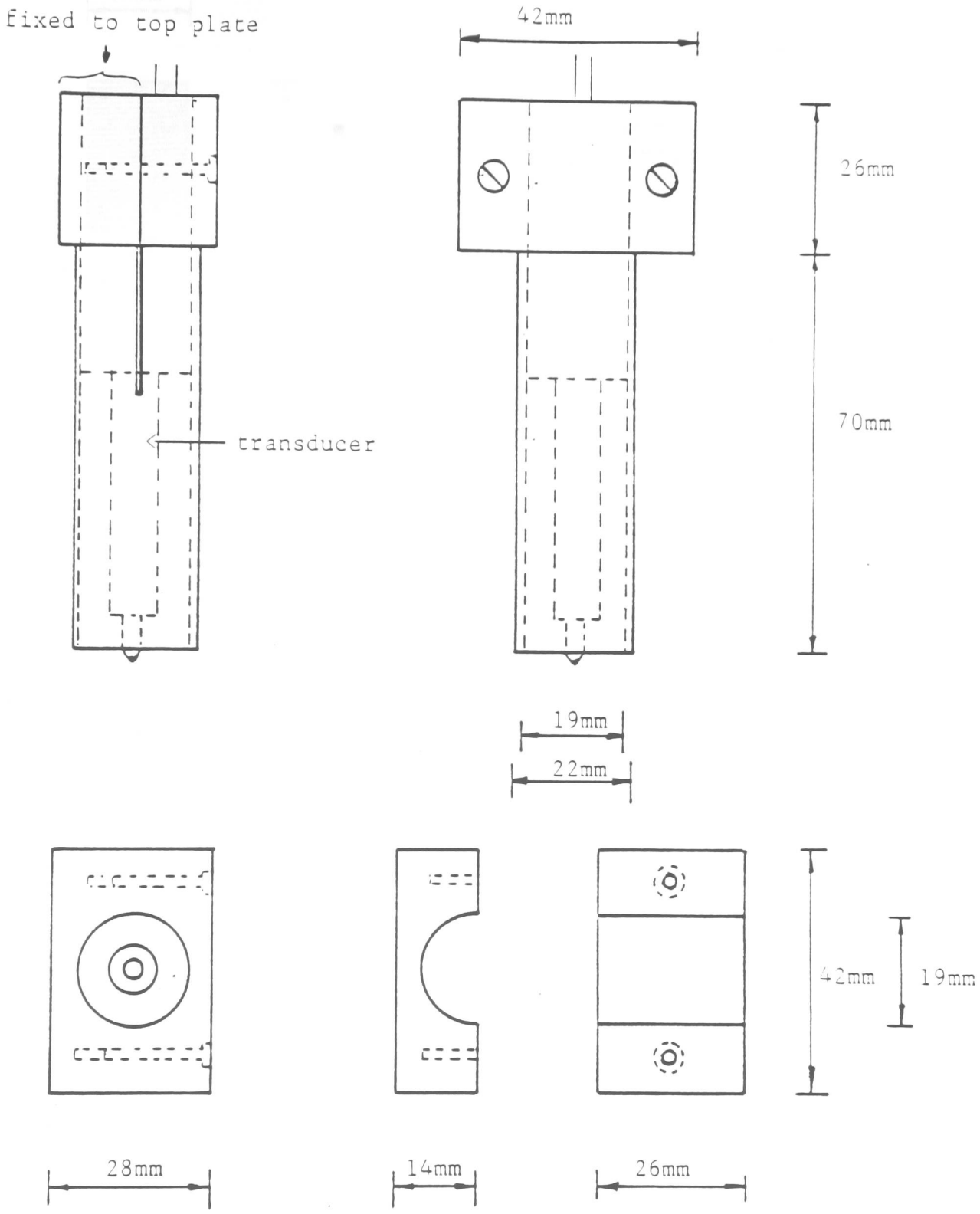

Fig.4.15. Detail of transducer fixings.

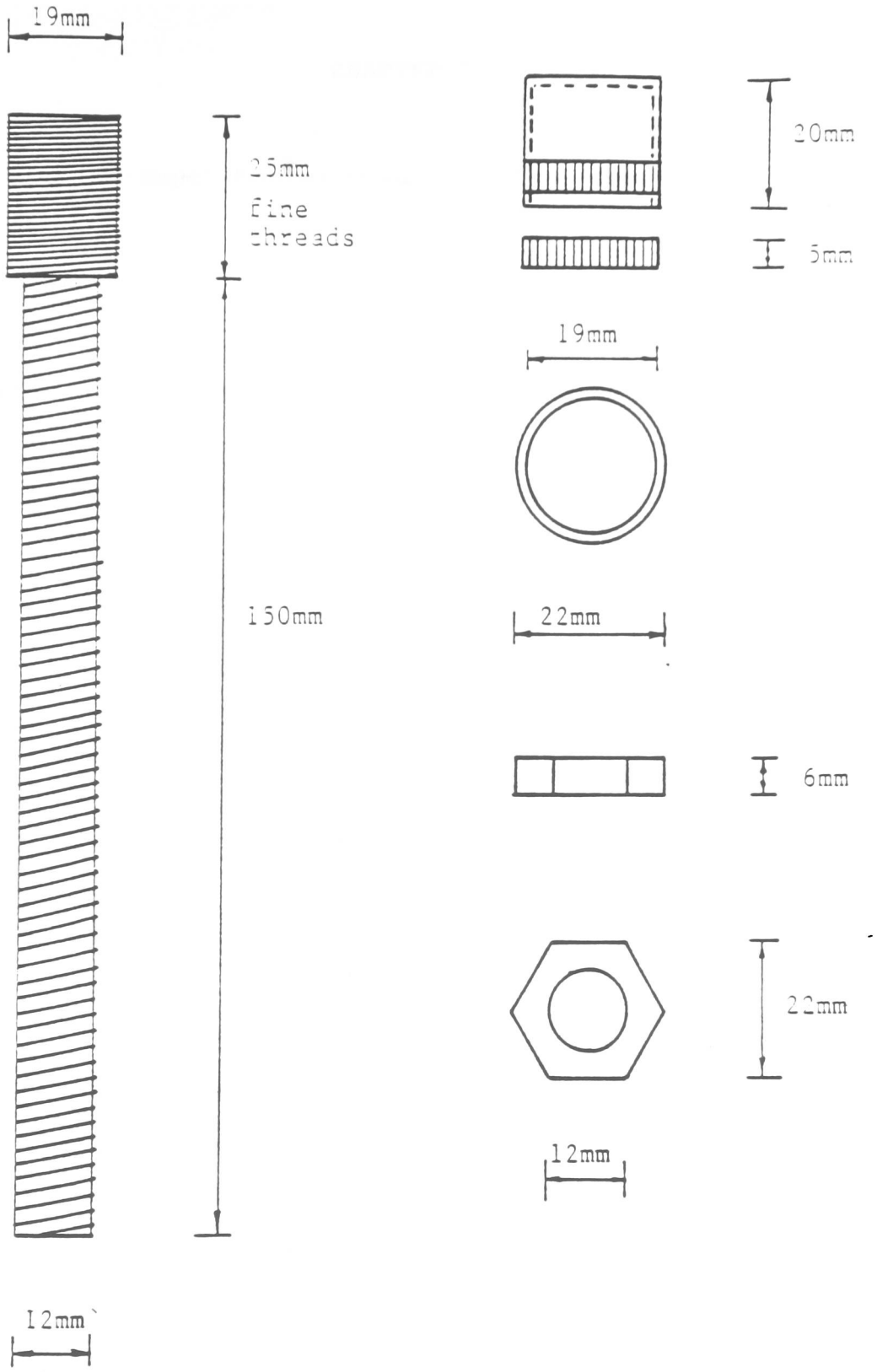

Fig.4.16. Detail of transducer pedestal.

CHAPTER 5

Experimental Results and Analysis

5.1. Introduction

Using the procedures described in the previous Chapters, static and dynamic tests were carried out on soil-cement specimens, in compression and flexure. A large amount of test data was accumulated, but due to a shortage of space only typical results are presented in this thesis. Discussions of results are also included in this Chapter.

5.2. Unconfined static compression test

5.2.1. Unconfined compressive strength, cement content and curing time relationships

The variation of the unconfined compressive strength (UCS) with curing time for several soil-cement mixtures is tabulated in Table 5.1, and plotted in Figure 5.1.

The unconfined compressive strength generally increases with increase in cement content and curing time. For example the least cement content used in this research is 6%. This has increased the UCS of the soil during the first week by over 8 times under the same compaction

Cement content	UCS (N/mm^2) for various curing periods			
	7 day	14 day	28 day	56 day
0%	.31	.31	.31	.31
6%	2.49	2.90	3.30	3.44
10%	3.45	3.87	4.20	5.04
14%	4.54	5.44	5.65	6.82
18%	5.70	6.52	7.48	8.66
22%	7.64	8.14	8.96	10.64
(mean UCS value)	4.76	5.37	5.92	6.92

Table 5.1. The UCS-curing time relationship for various cement contents in static compression tests

effort, and the 22% cement content has increased the UCS during the first week by over 24 times. The rate of increase of UCS with curing time is constant and of higher magnitude at higher cement contents. This results from the increase in Tricalcium Silicate (C_3S) at higher cement contents. By allowing the curing time to increase, higher strength values resulted for a given cement content. The 56, 28 and the 14-day mean UCS values are 1.45, 1.24 and 1.13 times the 7-day mean UCS value respectively over the

Fig.5.1. UCS–Curing Time Relationship

for Various Cement Contents

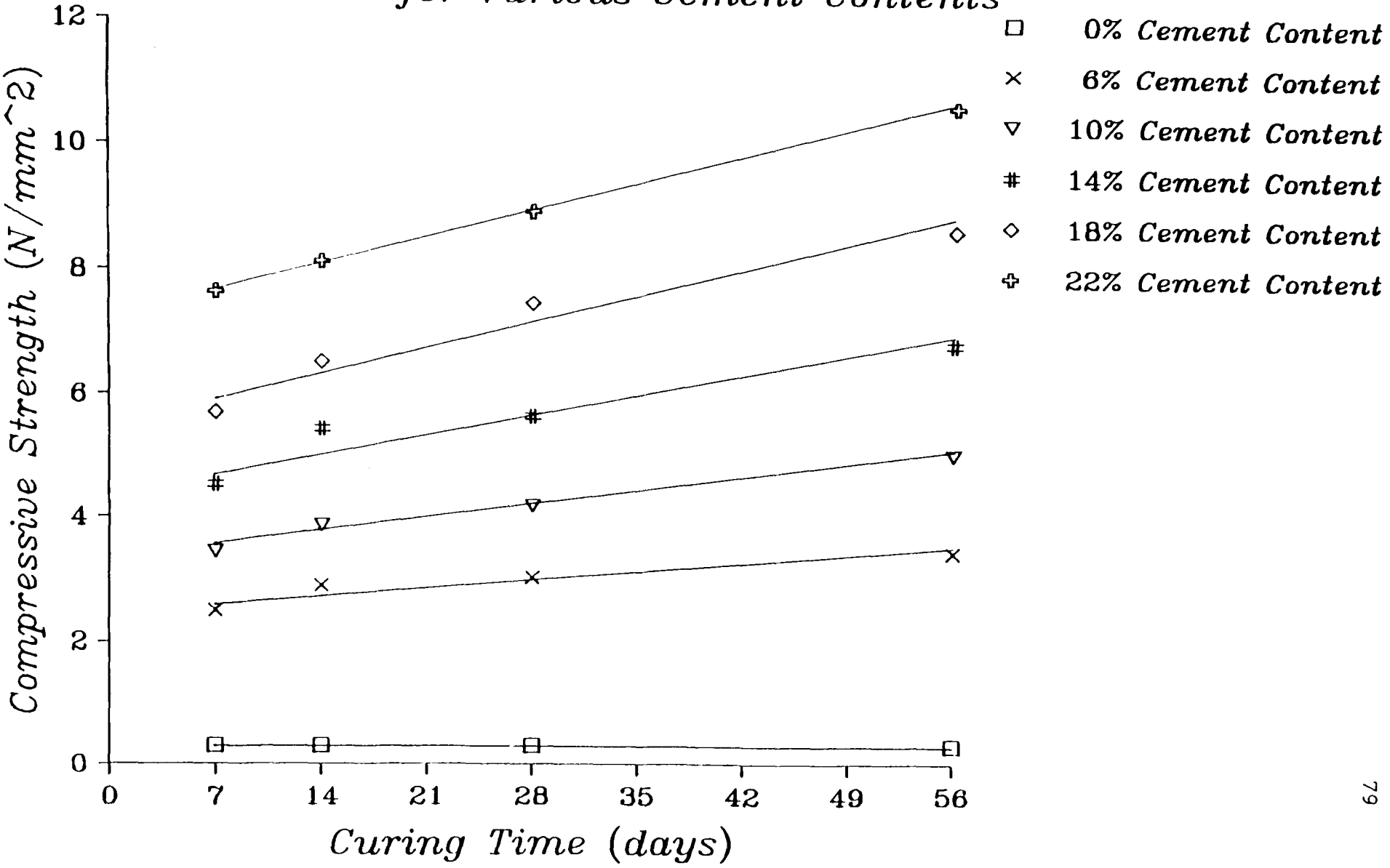

range of cement contents from 6% to 22%. This increase in UCS with time results from the continuation of cement hydration in the soil-cement mix. This increase in strength due to increase in cement content and/or curing time results in improved frictional characteristics of the soil.

Regression analyses were performed using the VAX main frame computer (plotter package), to determine the relationship between the unconfined compressive strength and curing time for various cement contents. This can be expressed as:

$$(UCS) = A + B\,(CT) \quad \ldots\ldots\ldots\ldots\ldots\ldots 5.1$$

where,

UCS = unconfined compressive strength (N/mm^2).

CT = curing time (days).

A = coefficient of the best polynomial and increases with the increase of cement content.

B = slope coefficient which also increases with cement content.

Values of the coefficient A are plotted against cement contents in Figure 5.2. A linear best fit line is plotted reflecting constant increase of the unconfined compressive strength for increase in cement content.

Values of the coefficient B are plotted against cement contents in Figure 5.3. As can be seen, a linear relationship holds up to 18% cement content and then levels out. Further investigation is necessary to explain this phenomenon at high cement contents.

Coefficients A and B and the sum of errors squared, determined from the regression analyses, are tabulated in Table 5.2 below. The sum of errors squared is a measure of the accuracy.

Cement content	A coefficient	B coefficient	Sum of errors squared
0%	.31	0	0
6%	2.49	0.017	0.03007
10%	3.29	0.031	0.01523
14%	4.45	0.043	0.22206
18%	5.57	0.057	0.20486
22%	7.23	0.060	0.00299

Table 5.2. Coefficients A and B and the sum of errors squared for various cement contents

Fig.5.2. A Coefffficient–Cement Content Relationship

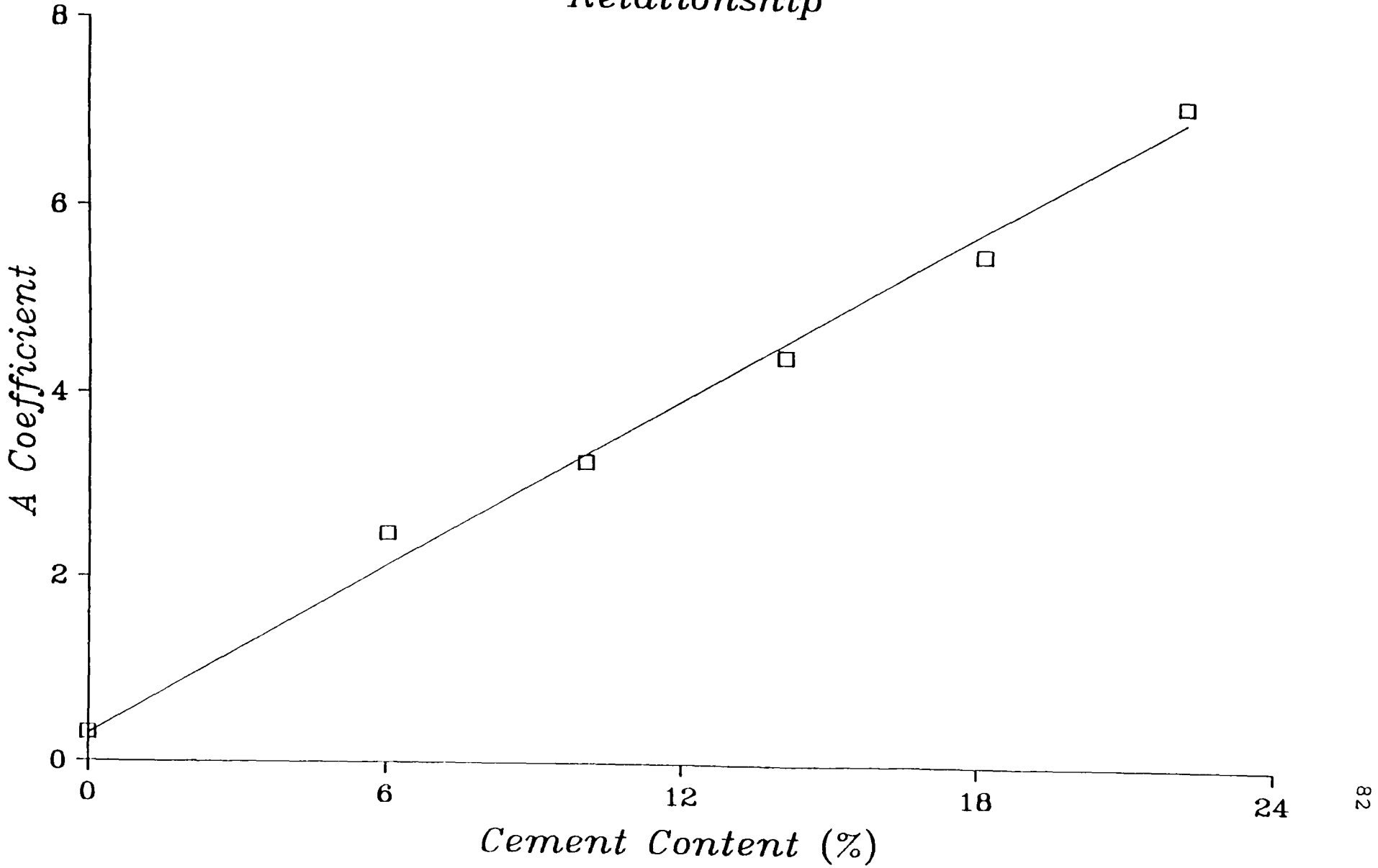

Fig.5.3. B Coefficient–Cement Content Relationship

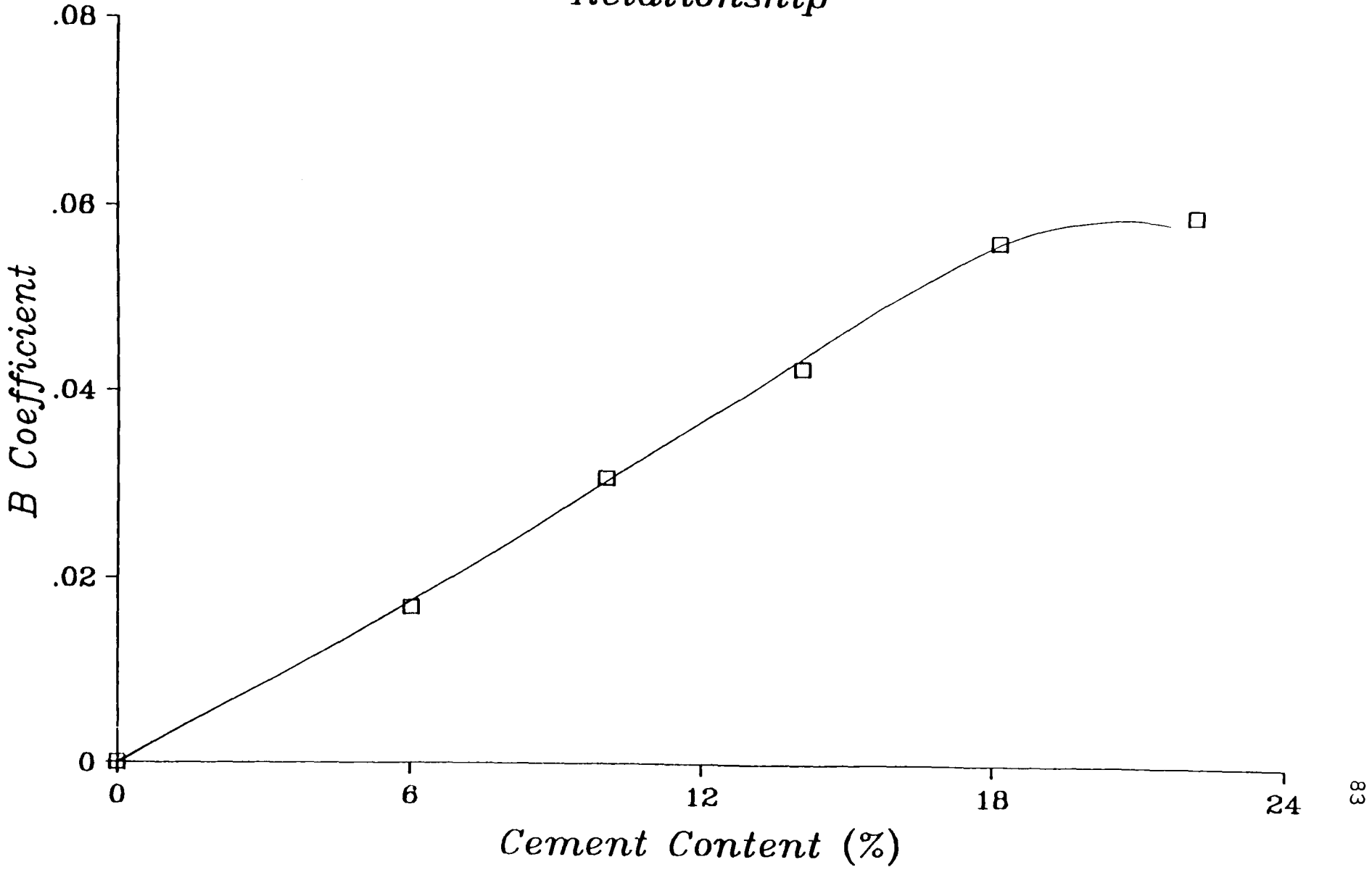

From Figures 5.2 and 5.3 it can be shown that for the linear part of the strength-time relationship,

$$(UCS) = A + B\,(CT). \quad \ldots\ldots\ldots\ldots\ldots\ldots\ldots\ldots 5.1\text{ bis}$$

where,

$$A = 0.29 + 0.31\,(CC) \quad \ldots\ldots\ldots\ldots\ldots\ldots\ldots\ldots 5.2$$

and,

$$B = 0 + 0.0031\,(CC) \quad (\text{for } CC \leq 18\%) \quad \ldots\ldots\ldots 5.3$$

By substituting Equations 5.2 and 5.3 in Equation 5.1 we have:

$$(UCS) = 0.29 + [0.31\,(CC)] + [0.0031\,(CC)(CT)] \quad \ldots\ldots 5.4$$

and,

$$(CC) = [(UCS) - 0.29] \,/\, [0.31 + 0.0031\,(CT)] \quad \ldots\ldots 5.5$$

Equation 5.5 is a useful tool for the design of a soil-cement mix e.g. the Ministry of Transport specifications stipulate a minimum 7-day (CT) compressive strength for a roadbase of 2.76 MN/m^2 (UCS). Applying Equation 5.5 to the Red Marl used in this investigation, the minimum cement content can be found as follows:

$$(CC) = [2.76 - 0.29] \,/\, [0.31 + (0.0031 \times 7)] = 7.446\%$$

Likewise, Equation 5.1 can be used to estimate the minimum time required for stabilisation to take place before traffic is allowed to use a new soil-cement road.

The UCS-cement content relationship for various curing periods is shown in Figure 5.4.

Fig.5.4. UCS–Cement Content Relationship

for Various Curing Periods

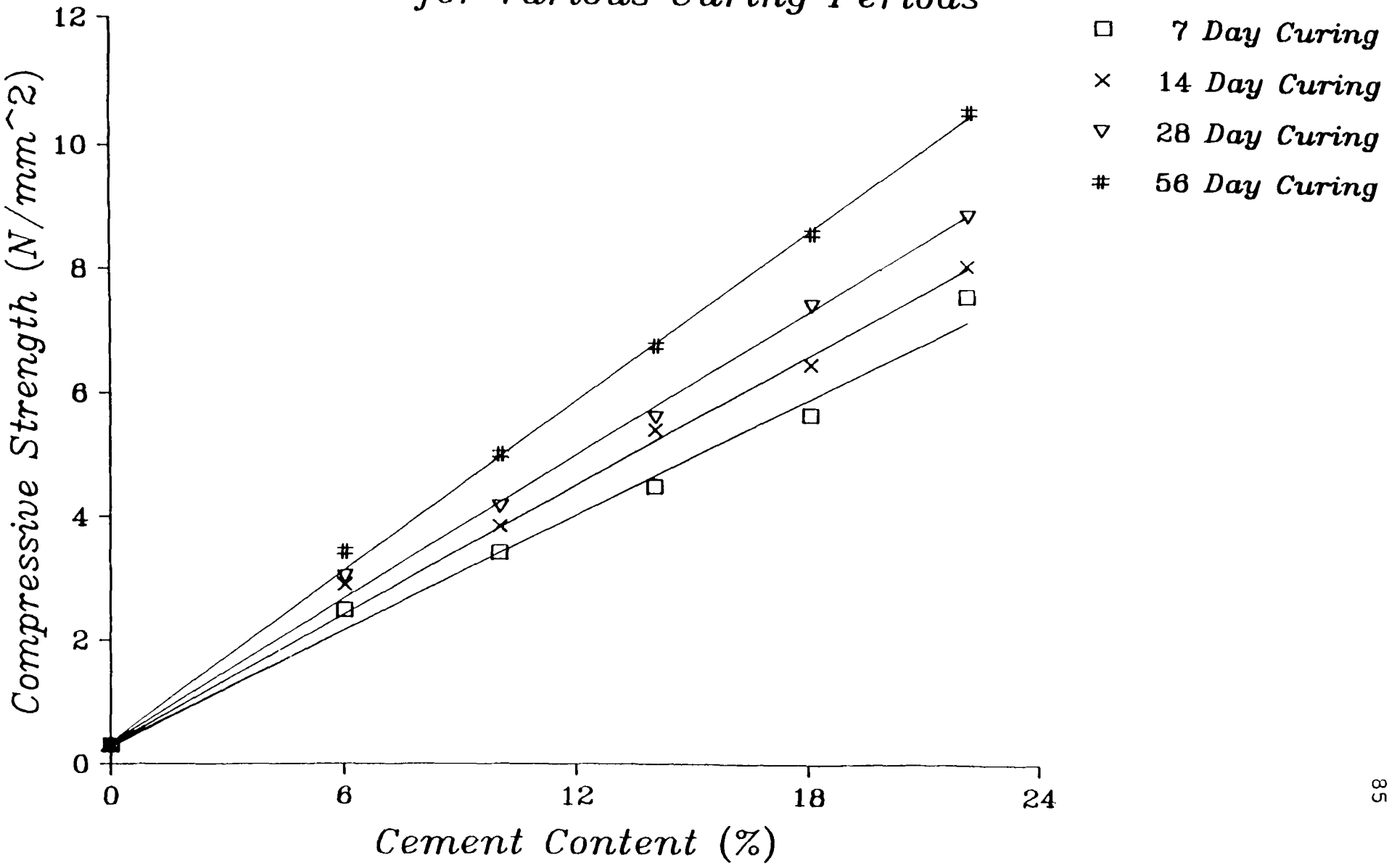

5.2.2. Stiffness-cement content and curing time relationships

Stress-strain output from the static compression tests was analysed in order to generate input parameters for soil-cement pavement analysis. A typical set of results from the unconfined static compression tests for 7-day curing only are given in Table 5.3. The stress-strain relationships are presented in Figures 5.5, 5.6, 5.7 and 5.8 for cement contents of 6%, 10%, 14%, 18% and 22% and 7, 14, 28 and 56 day curing times. These data are also presented in Figures 5.9, 5.10, 5.11, 5.12 and 5.13 to highlight the effect of curing times for each value of cement content.

Strain	Stress (N/mm^2) for cement contents of				
	6%	10%	14%	18%	22%
0.00	0.00	0.00	0.00	0.00	0.00
0.000625	0.36	0.10	0.20	0.05	0.05
0.00125	0.87	0.36	0.36	0.26	0.20
0.001875	1.37	0.82	0.66	0.87	1.02
0.0025	1.73	1.53	1.07	1.83	2.44
0.003125	1.99	2.19	1.58	2.90	3.87
0.00375	2.19	2.60	2.09	3.82	5.09
0.004375	2.29	2.90	2.65	4.48	6.06
0.005	2.39	3.11	3.16	4.99	6.67
0.005625	2.47	3.26	3.61	5.29	7.18
0.00625	2.49	3.36	3.92	5.55	7.48
0.006875		3.41	4.12	5.65	7.59
0.0075		3.44	4.38	5.70	7.64
0.008125			4.48		
0.00875			4.53		
0.009375					

Table 5.3. Stress-Strain relationships for various cement contents after 7 days curing time.

Fig.5.5. Stress–Strain Relationship

for 7 Day Curing Time

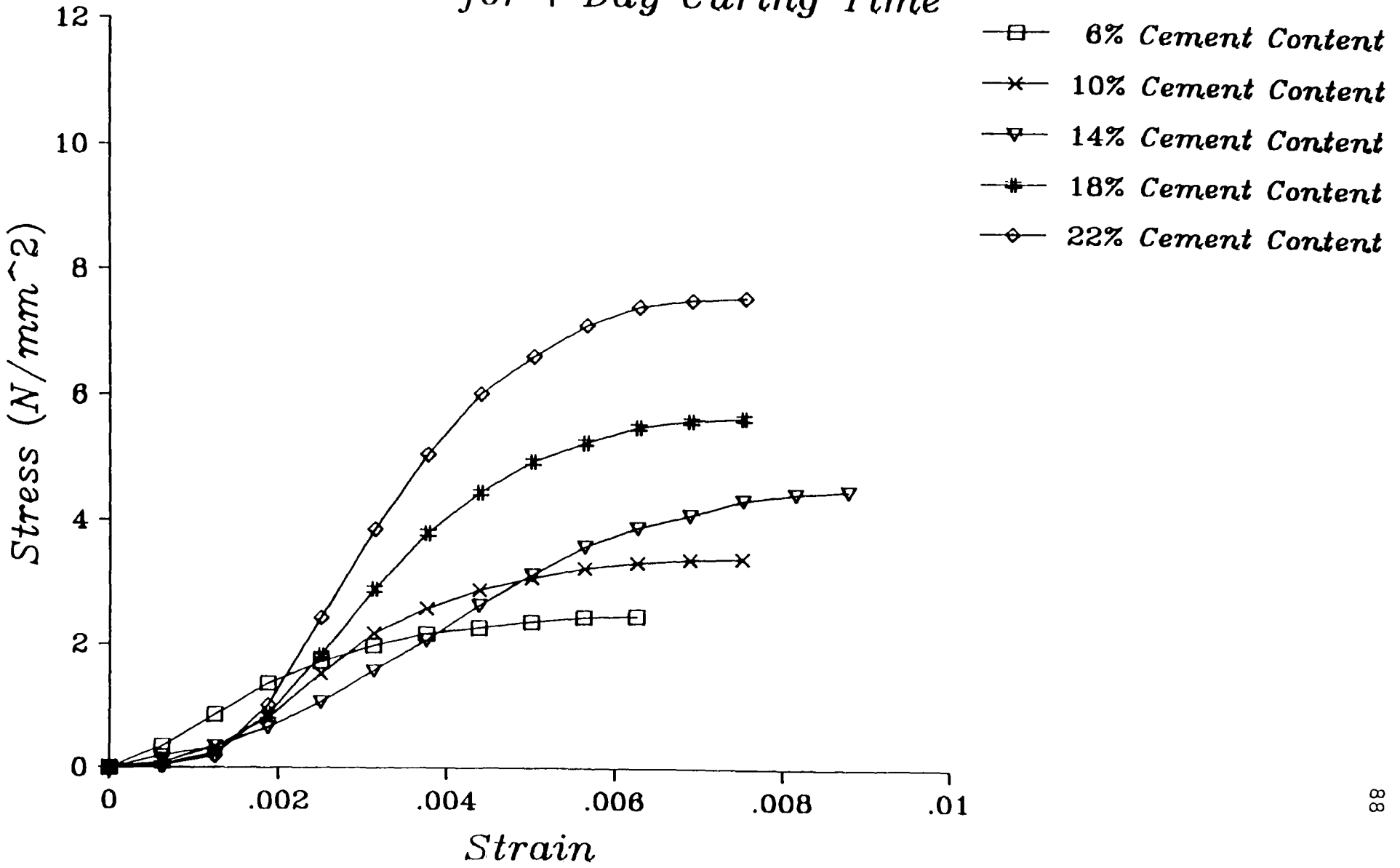

Fig.5.6. Stress–Strain Relationship

for 14 Day Curing Time

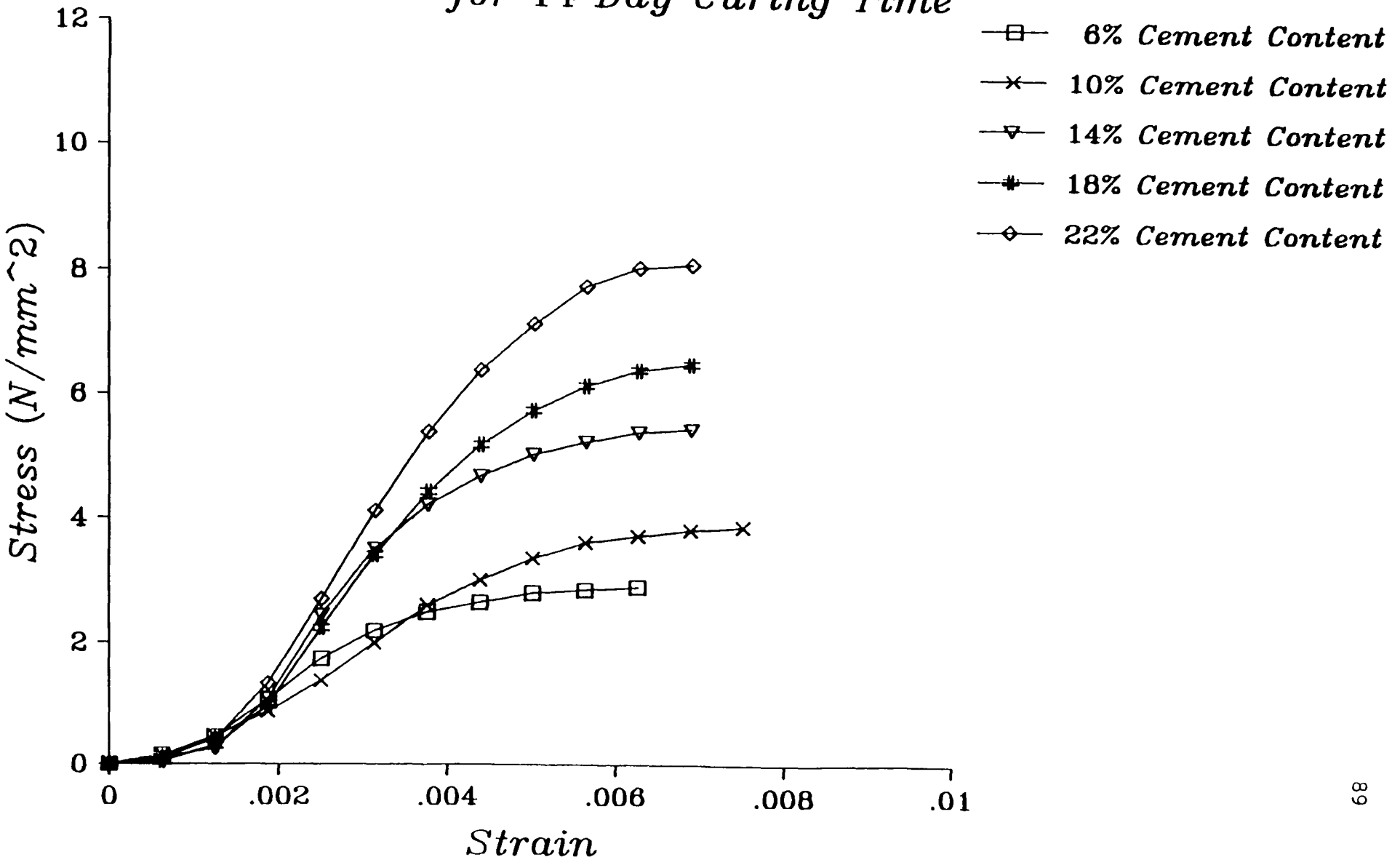

Fig.5.7. Stress–Strain Relationship

for 28 Day Curing Time

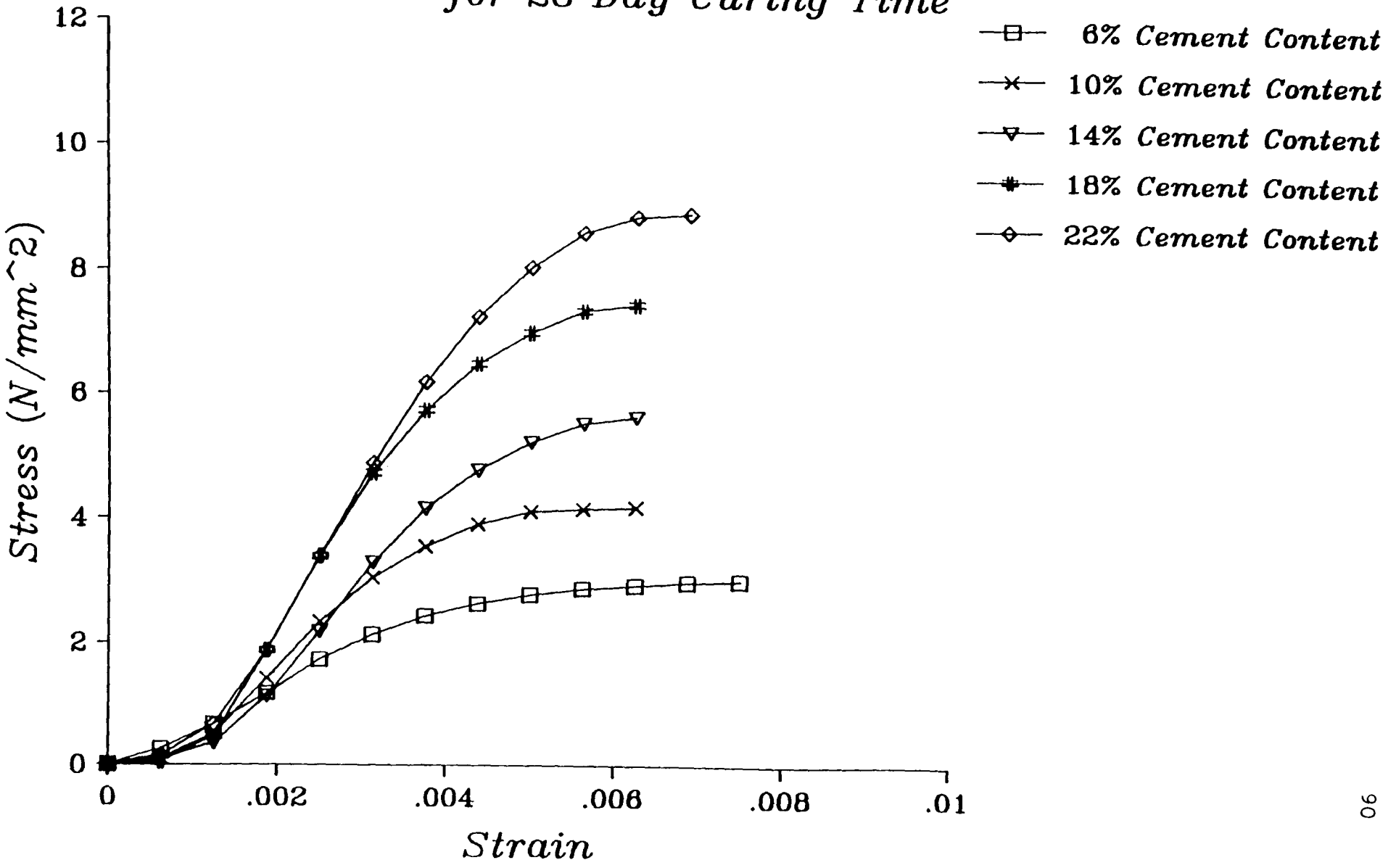

Fig.5.8. Stress–Strain Relationship

for 56 Day Curing Time

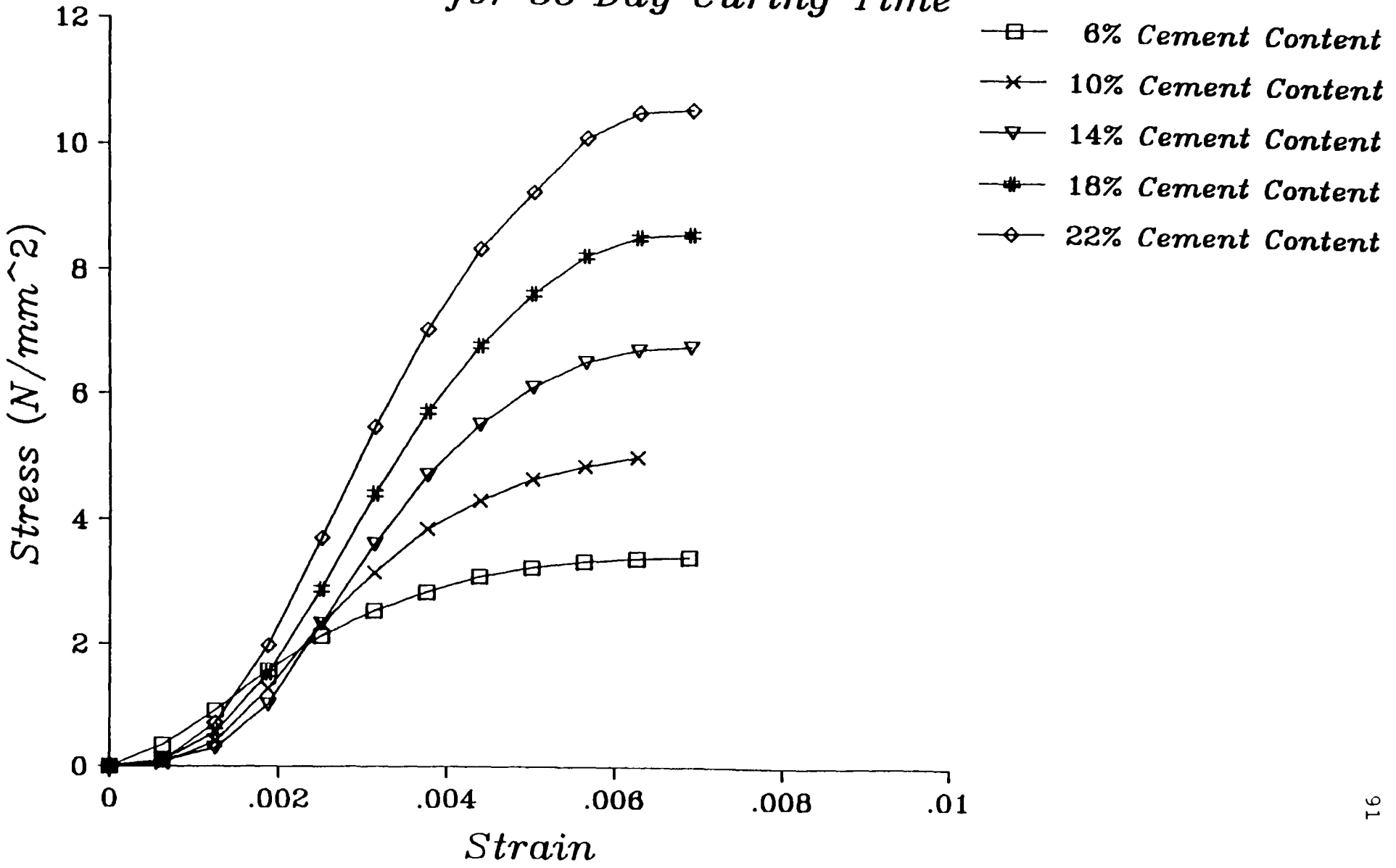

Fig.5.9. Stress–Strain Relationship

for 6% Cement Content

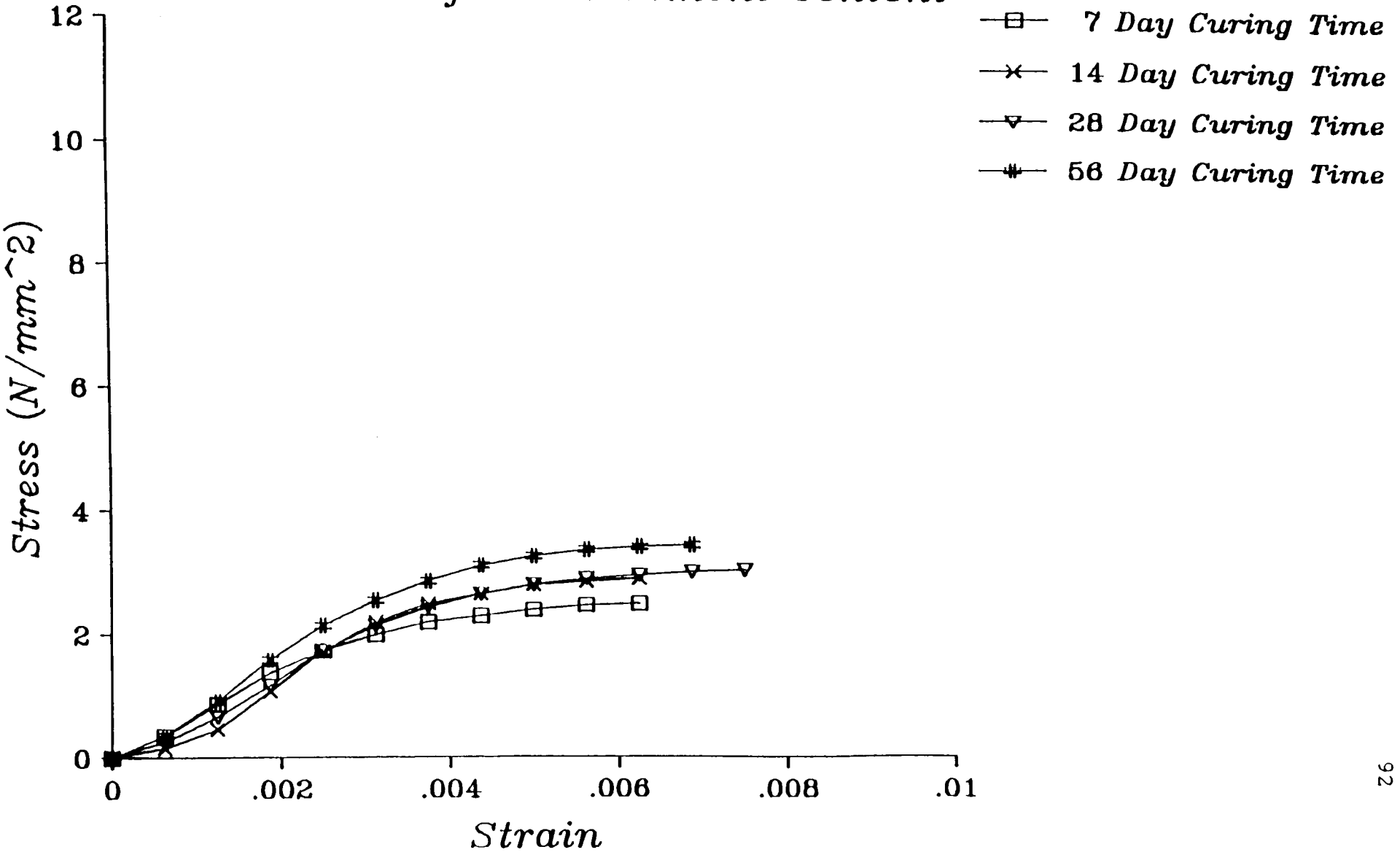

Fig.5.10. Stress–Strain Relationship

for 10% Cement Content

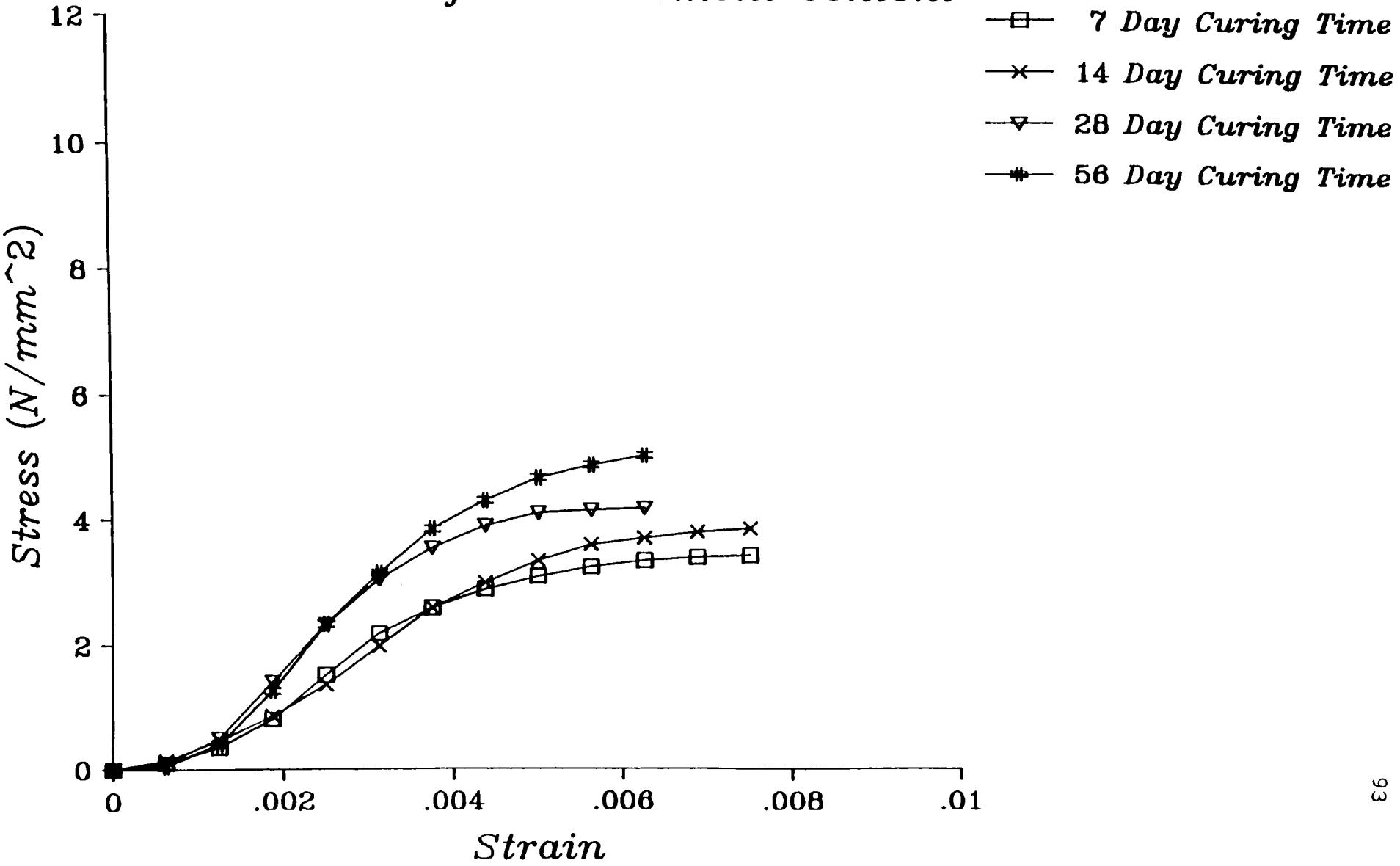

Fig.5.11. Stress–Strain Relationship

for 14% Cement Content

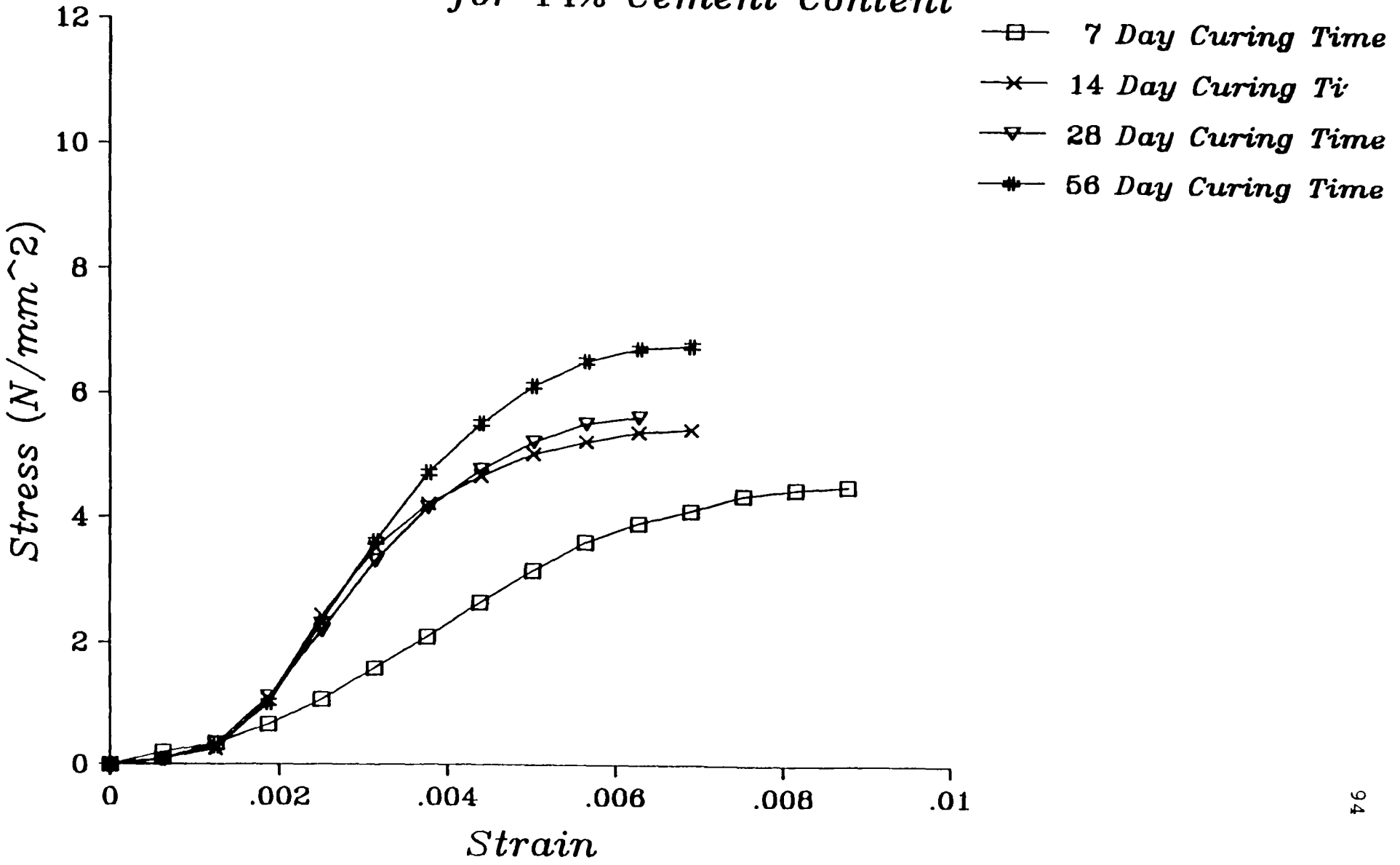

Fig.5.12. Stress–Strain Relationship

for 18% Cement Content

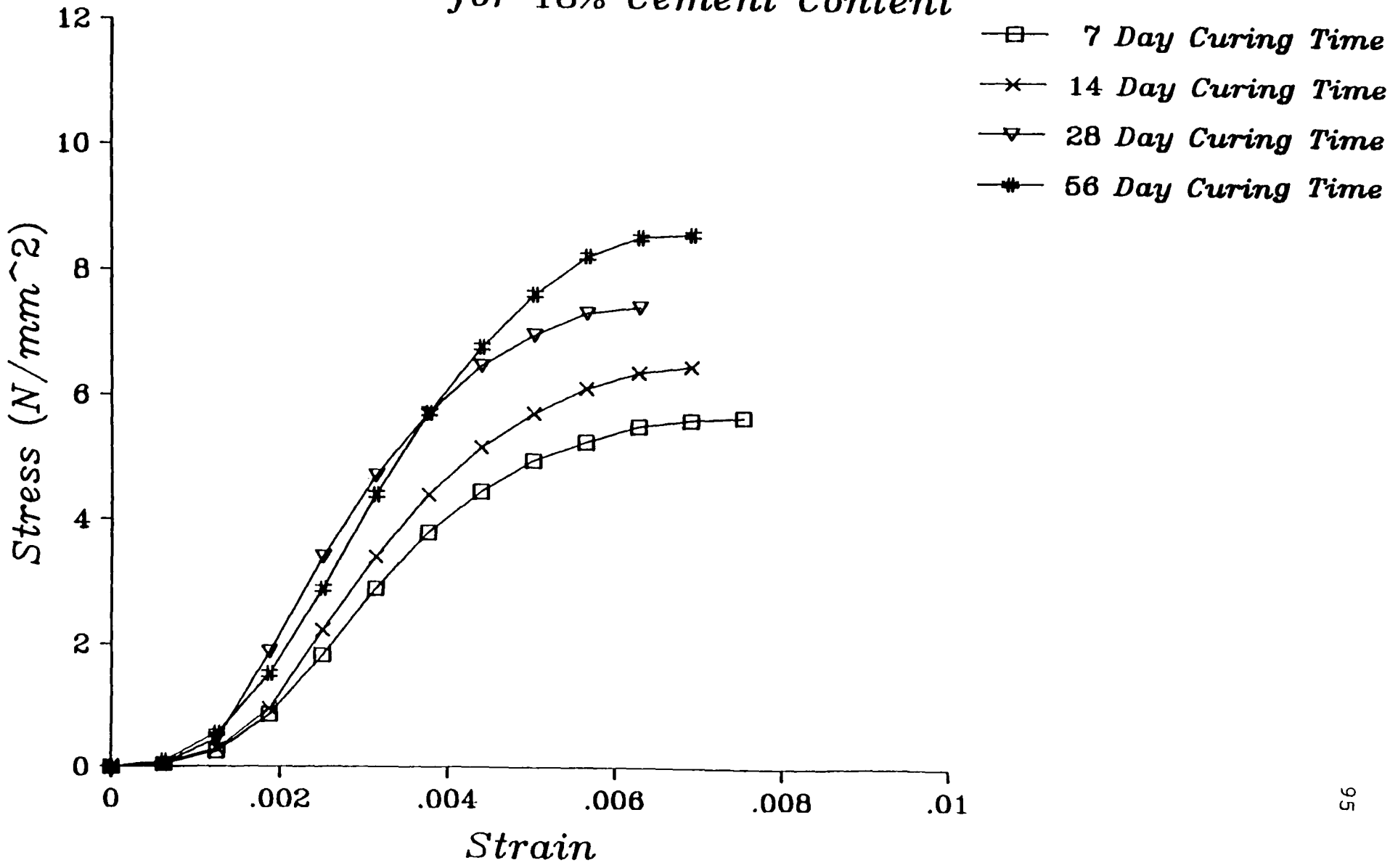

Fig.5.13. Stress–Strain Relationship

for 22% Cement Content

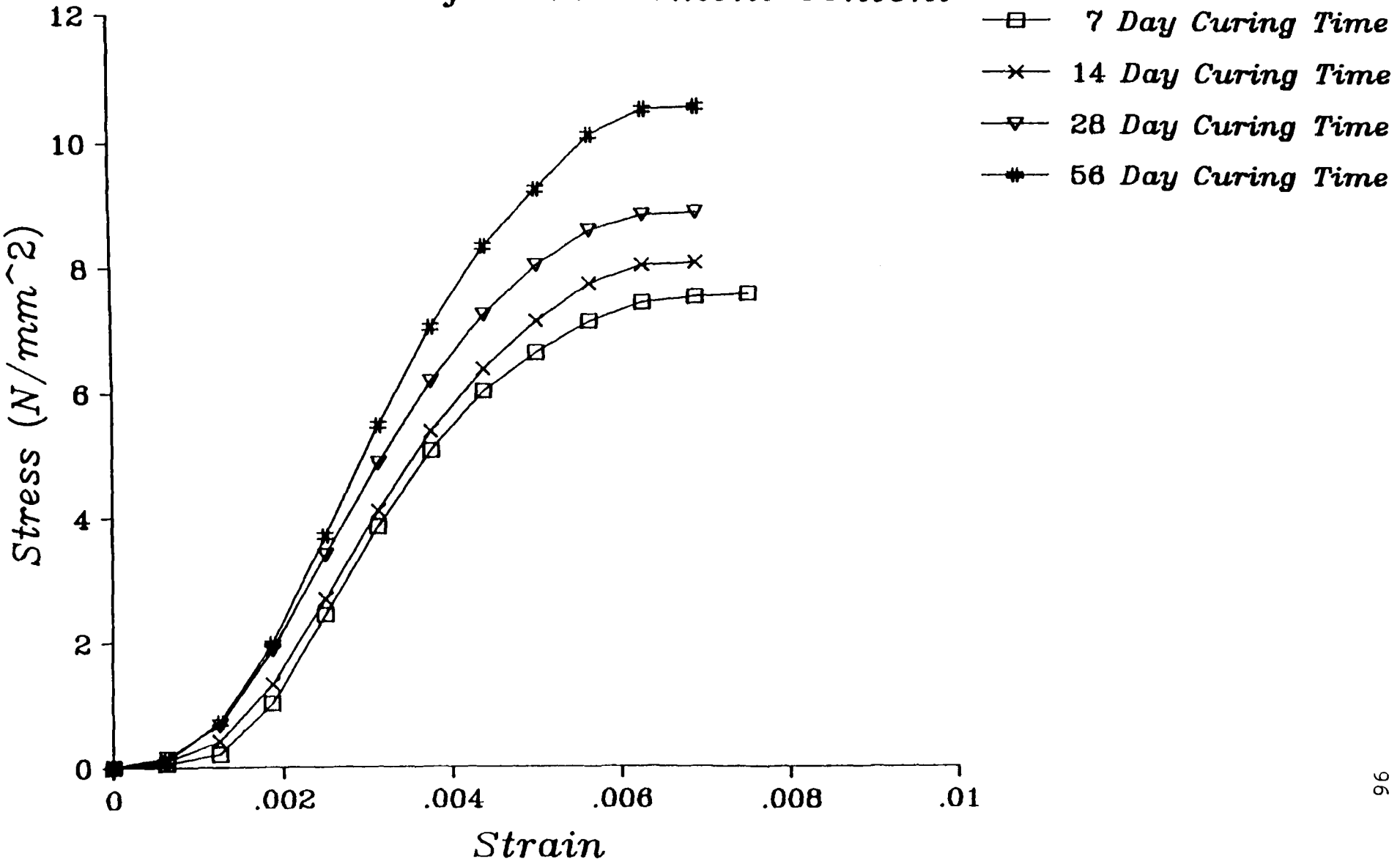

Two important parameters, the stiffness of the material (the Modulus of Elasticity) and the strain at incipient failure have been evaluated from the stress-strain curves. The strain at failure for all the specimens tested was found to be in the range 0.006 to 0.008.

The values of Modulus of Elasticity for the linear portions of the stress-strain curves for various cement contents and curing times are summarised in Table 5.4.

Curing time (days)	Modulus of Elasticity (N/mm²) for cement contents of				
	6%	10%	14%	18%	22%
7	692	800	813	1444	1808
14	700	852	1415	1648	1875
28	712	1220	1418	1939	1981
56	816	1254	1645	1971	2346

Table 5.4. Modulus of Elasticity for various cement contents and curing times

The Modulus of Elasticity increases with increase of cement content and curing time. For example, at 6% cement content and 7 days curing time, the mix has a Modulus of Elasticity of 692 N/mm²; when the curing time reaches 56

days, the mix had a Modulus of Elasticity of 816 N/mm². For a cement content of 22%, the Modulus of Elasticity after 7 days was 1808 N/mm² and after 56 days 2346 N/mm².

The Modulus of Elasticity is plotted against curing time and cement content in Figures 5.14 and 5.15 respectively.

Fig.5.14. Elastic Modulus–Curing Time Relationship for Various Cement Contents

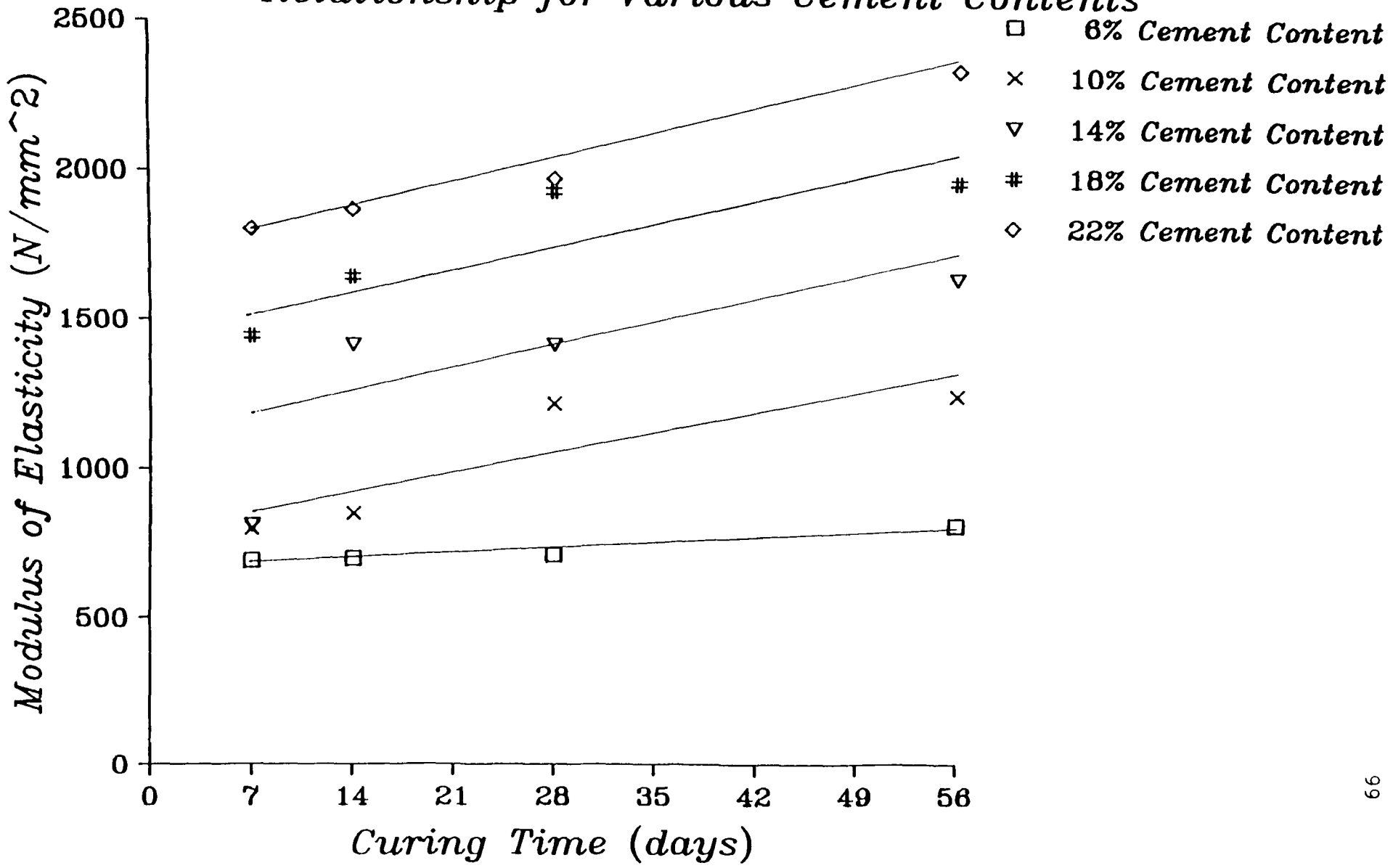

Fig.5.15. Elastic Modulus–Cement Content

Relationship for Various Curing Periods

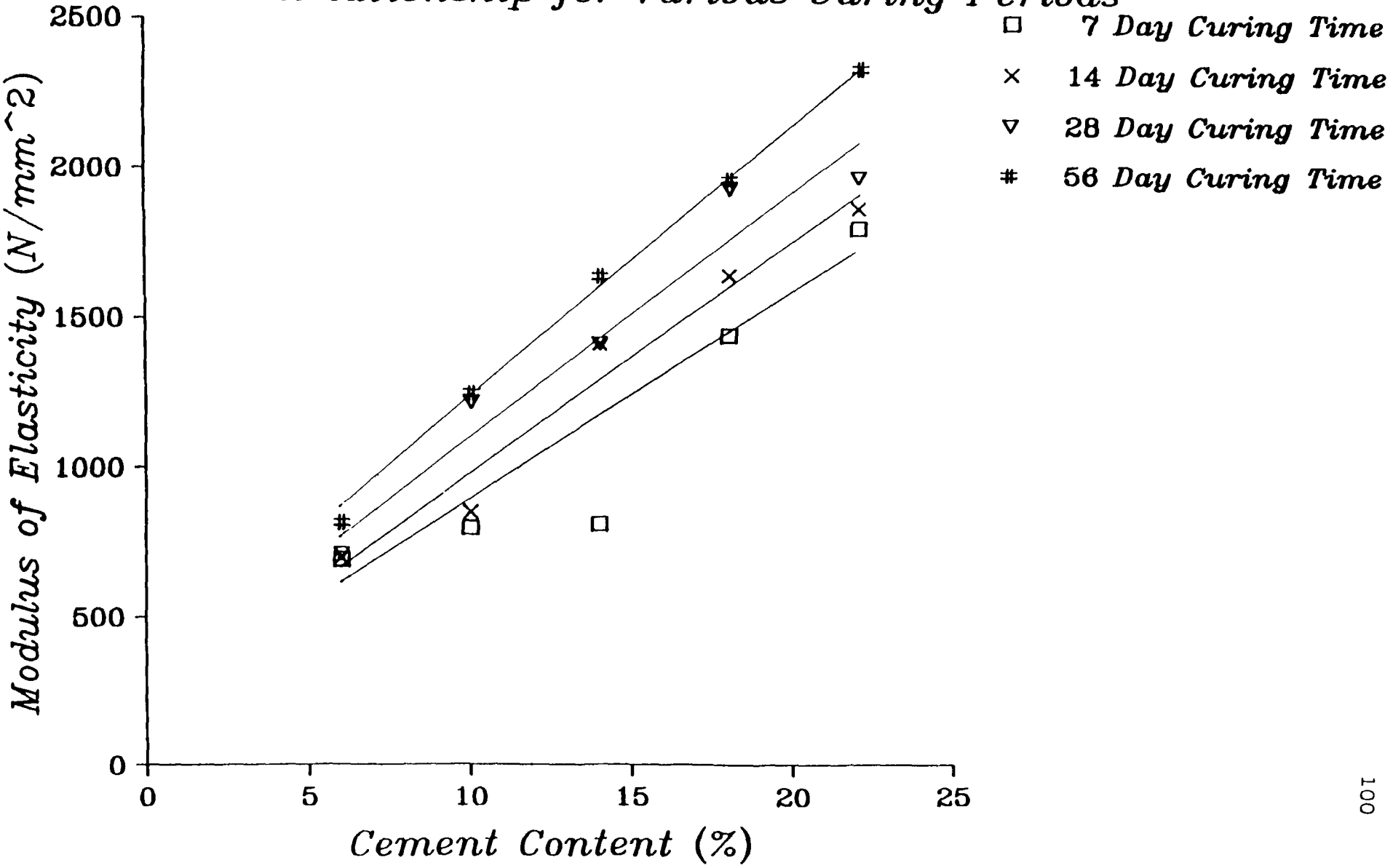

5.3. Unconfined dynamic compression test results

The response of the cement stabilised Red Marl to dynamic loading in compression has been investigated over the range of cement contents and curing times.

A number of specimens were subjected to different stress levels below the UCS, at a frequency of 5Hz. This was carried out in order to develop fatigue relationships for the material.

The results of these dynamic tests are tabulated in Tables 5.5, 5.6 and 5.7. The applied compressive stress-Log_{10} (No. of cycles to failure) relationships for curing times of 7 days, 14 days and 28 days are presented in Figures 5.16, 5.17 and 5.18 respectively and for various cement contents in Figures 5.19, 5.20, 5.21, 5.22, and 5.23.

It can be seen from Figures 5.16, 5.17 and 5.18 that a faster rate of fall off of the compressive stress is needed to cause failure over a given number of cycles at high cement contents compared to low cement contents.

Cement content (%)	Stress (N/mm²)	Stress (%)	Cycles to failure (No.)	Log_{10} cycles to failure
6	2.49	100.00	1	0
	2.29	91.95	3600	3.56
	2.04	81.73	100000	5
10	3.42	100.00	1	0
	3.06	89.37	454	2.66
	2.80	81.92	100000	5
14	4.45	100.00	1	0
	4.25	95.49	197	2.29
	4.00	89.84	391	2.59
	4.04	90.82	1729	3.24
	3.75	84.22	100000	5
18	5.68	100.00	1	0
	5.35	94.14	55	1.74
	5.09	89.65	95	1.98
	4.84	85.17	366	2.56
	4.59	80.69	344	2.54
	4.33	76.21	100000	5
22	7.63	100.00	1	0
	7.13	93.46	19	1.28
	6.88	90.12	80	1.90
	6.62	86.78	52	1.72
	6.37	83.44	558	2.75
	6.11	80.11	1000	3
	5.86	76.77	1539	3.19
	5.60	73.43	100000	5

Table 5.5. Dynamic compression test results for 7-day curing time

Cement content (%)	Stress (N/mm^2)	Stress (%)	Cycles to failure (No.)	Log_{10} cycles to failure
6	2.85	100.00	1	0
	2.80	98.18	82	1.91
	2.56	89.64	821	2.91
	2.31	81.07	100000	5
10	3.80	100.00	1	0
	3.50	92.02	43	1.63
	3.25	85.44	212	2.33
	3.00	78.87	100000	5
14	5.41	100.00	1	0
	5.09	94.07	15	1.18
	4.84	89.37	33	1.52
	4.58	84.67	57	1.76
	4.33	79.96	111	2.05
	4.07	75.26	100000	5
18	6.53	100.00	1	0
	6.11	93.53	47	1.67
	5.86	89.63	142	2.15
	5.60	85.74	188	2.27
	5.35	81.84	35625	4.55
	5.09	77.94	100000	5
22	8.11	100.00	1	0
	7.64	94.17	100	2
	7.13	87.89	157	2.20
	6.62	81.61	1960	3.29
	6.11	75.34	2036	3.31
	5.86	72.20	100000	5

Table 5.6. Dynamic compression test results for 14-day curing time

Cement content (%)	Stress (N/mm^2)	Stress (%)	Cycles to failure (No.)	Log_{10} cycles to failure
6	2.99	100.00	1	0
	2.80	93.73	64	1.81
	2.67	89.47	1100	3.04
	2.67	89.47	1750	3.24
	2.55	85.21	100000	5
10	4.20	100.00	1	0
	4.07	96.99	47	1.67
	3.82	90.93	224	2.35
	3.57	84.87	415	2.62
	3.31	78.80	100000	5
14	5.62	100.00	1	0
	5.09	90.66	33	1.52
	4.84	86.13	2012	3.30
	4.58	81.60	100000	5
18	7.45	100.00	1	0
	7.13	95.69	38	1.58
	6.88	92.28	50	1.70
	6.62	88.86	67	1.83
	6.37	85.44	81	1.91
	6.11	82.02	517	2.71
	5.60	75.19	100000	5
22	8.88	100.00	1	0
	8.15	91.74	138	2.14
	7.64	86.01	563	2.75
	7.13	80.28	23673	4.37
	6.62	74.54	100000	5

Table 5.7. Dynamic compression test results for 28-day curing time

Fig.5.16. Dynamic Compression Tests

for 7 Day Curing Time

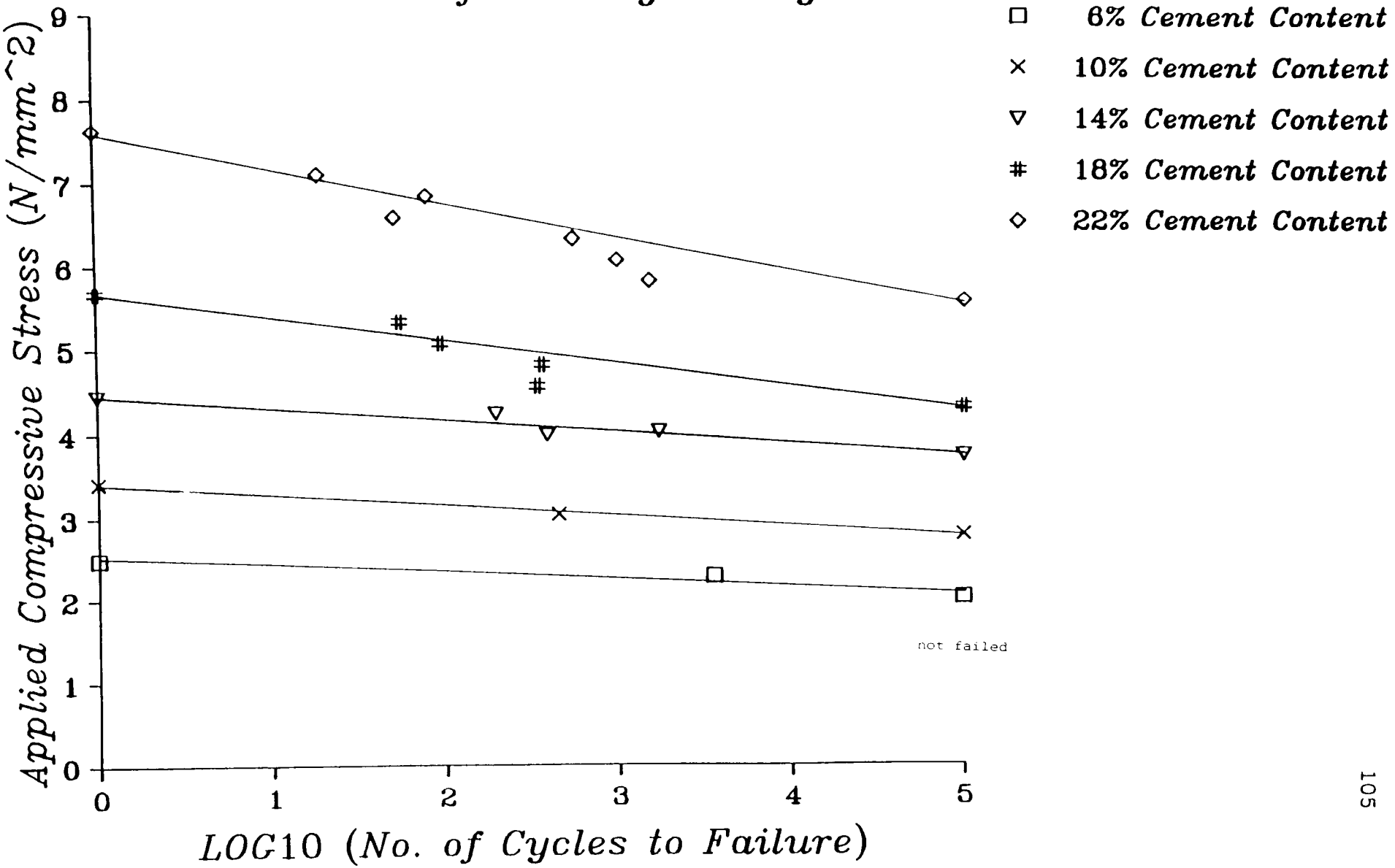

Fig.5.17. Dynamic Compression Tests
for 14 Day Curing Time

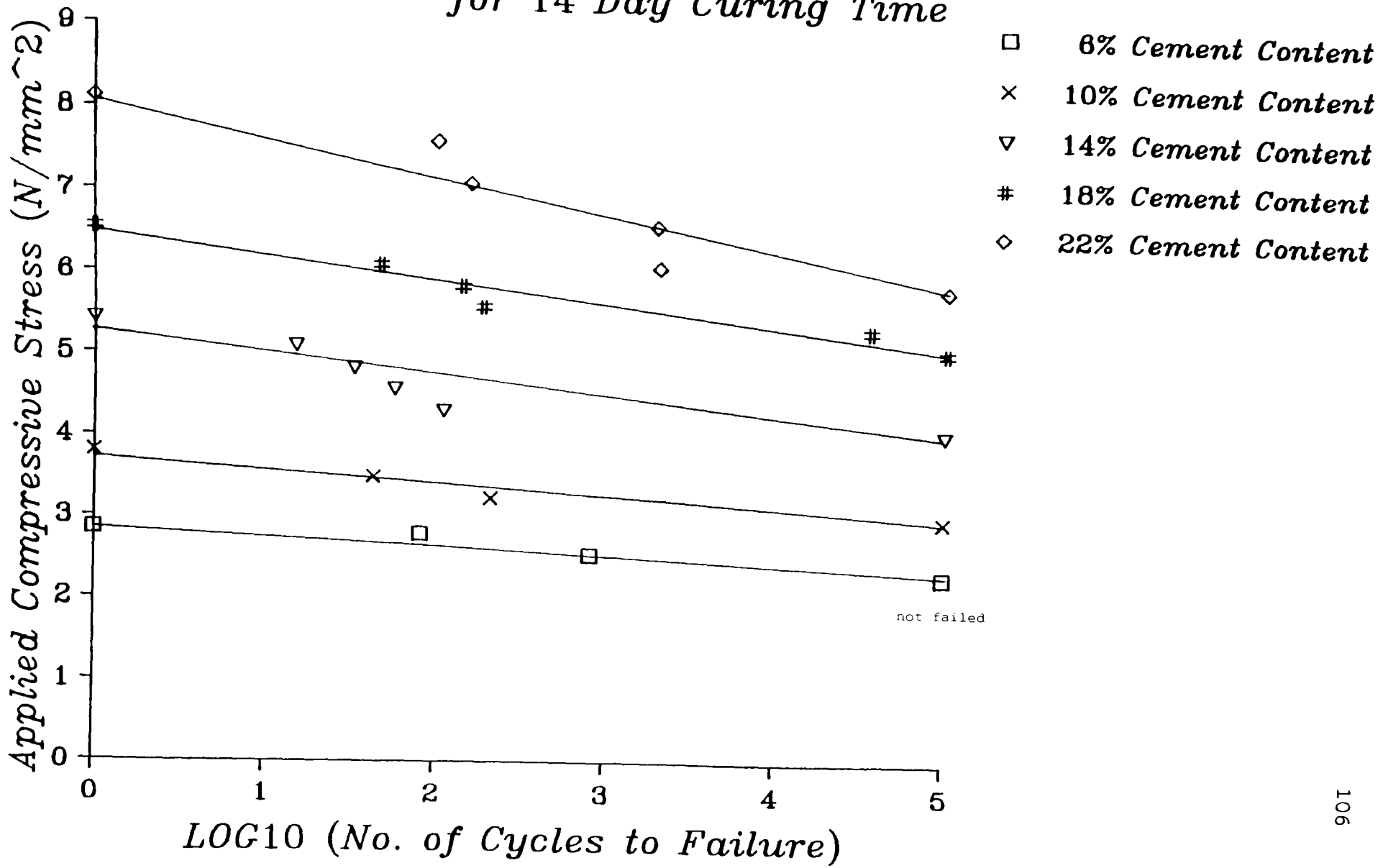

Fig.5.18. Dynamic Compression Tests

for 28 Day Curing Time

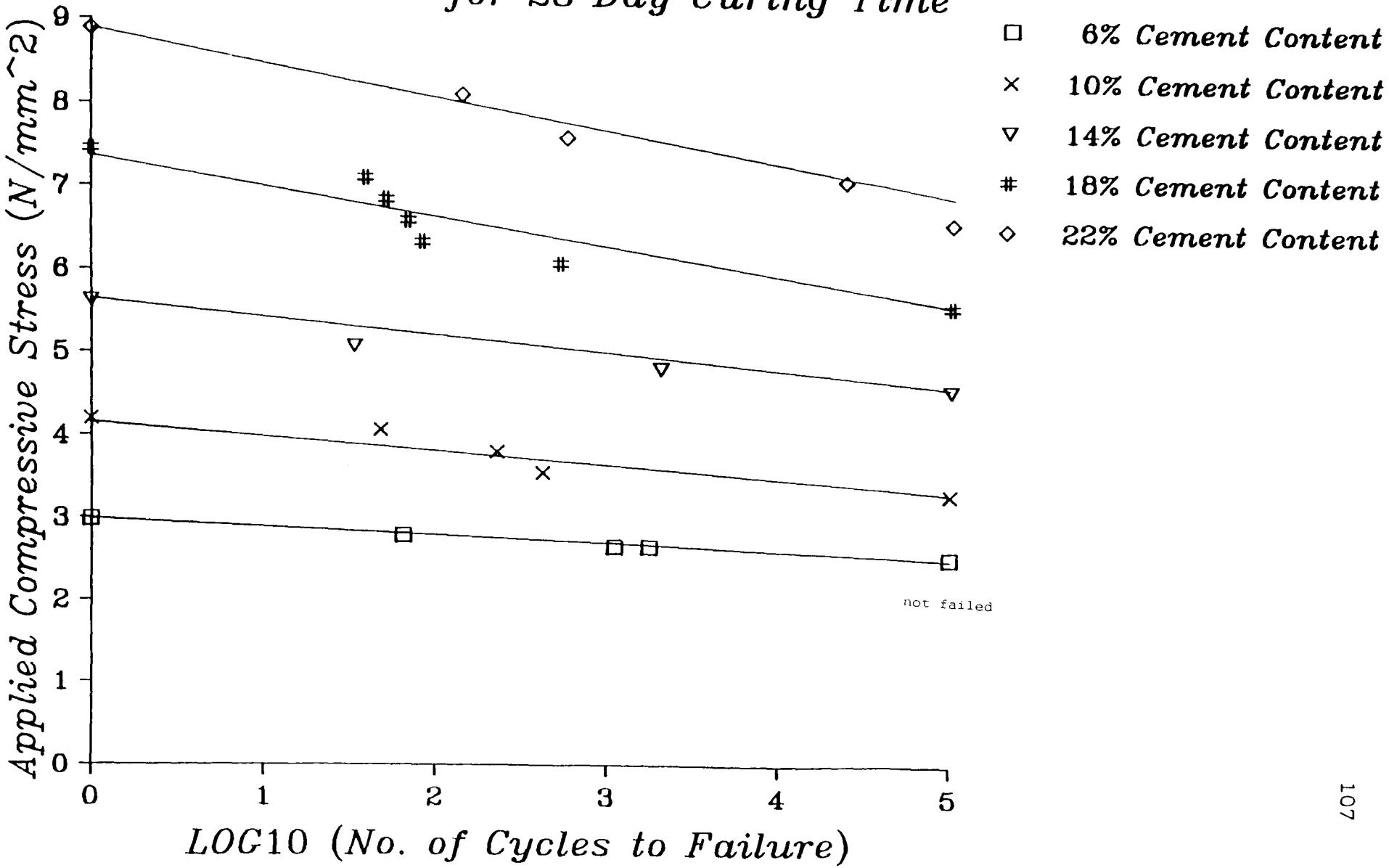

Fig.5.19. Dynamic Compression Tests

for 6% Cement Content

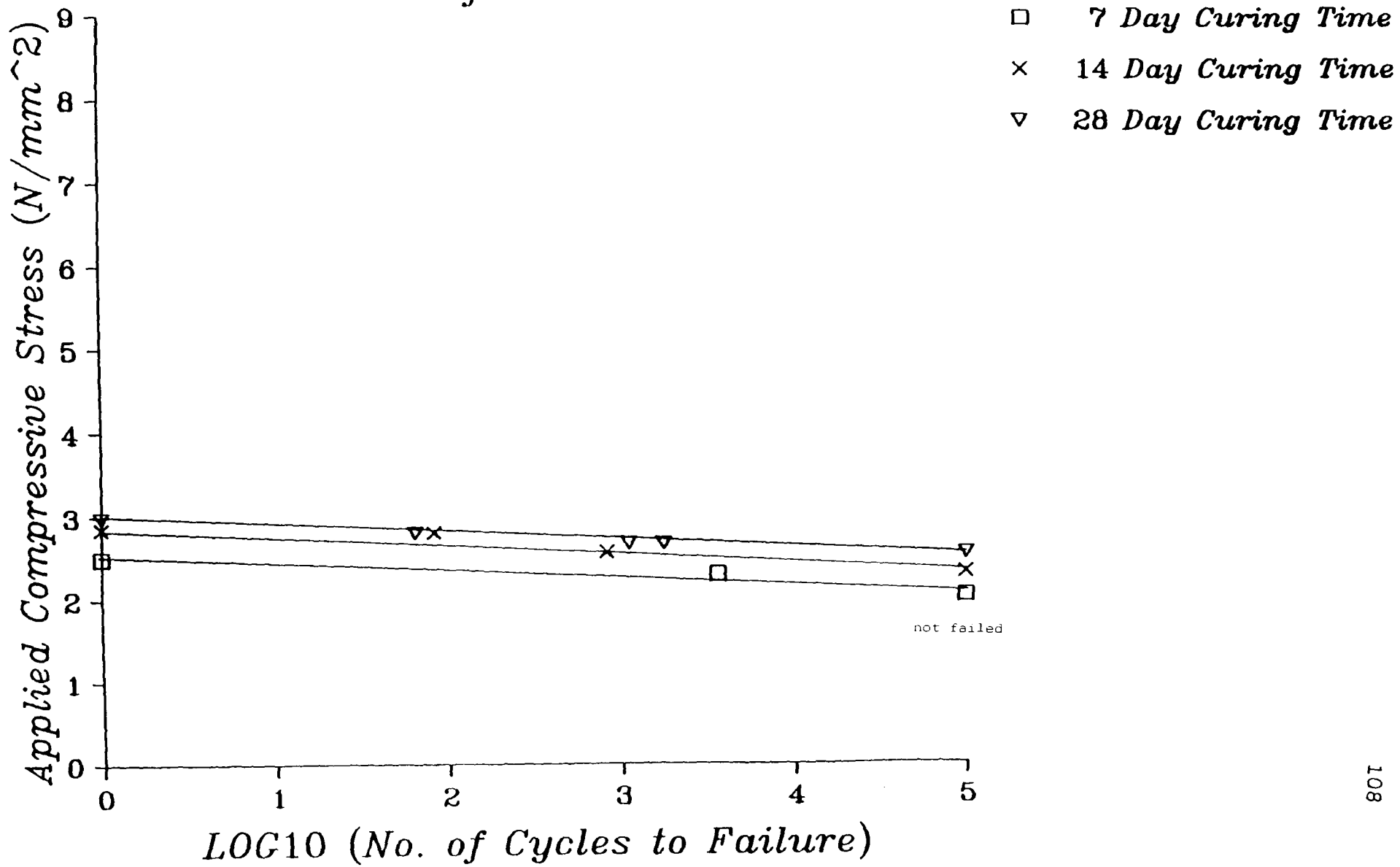

Fig.5.20. Dynamic Compression Tests

for 10% Cement Content

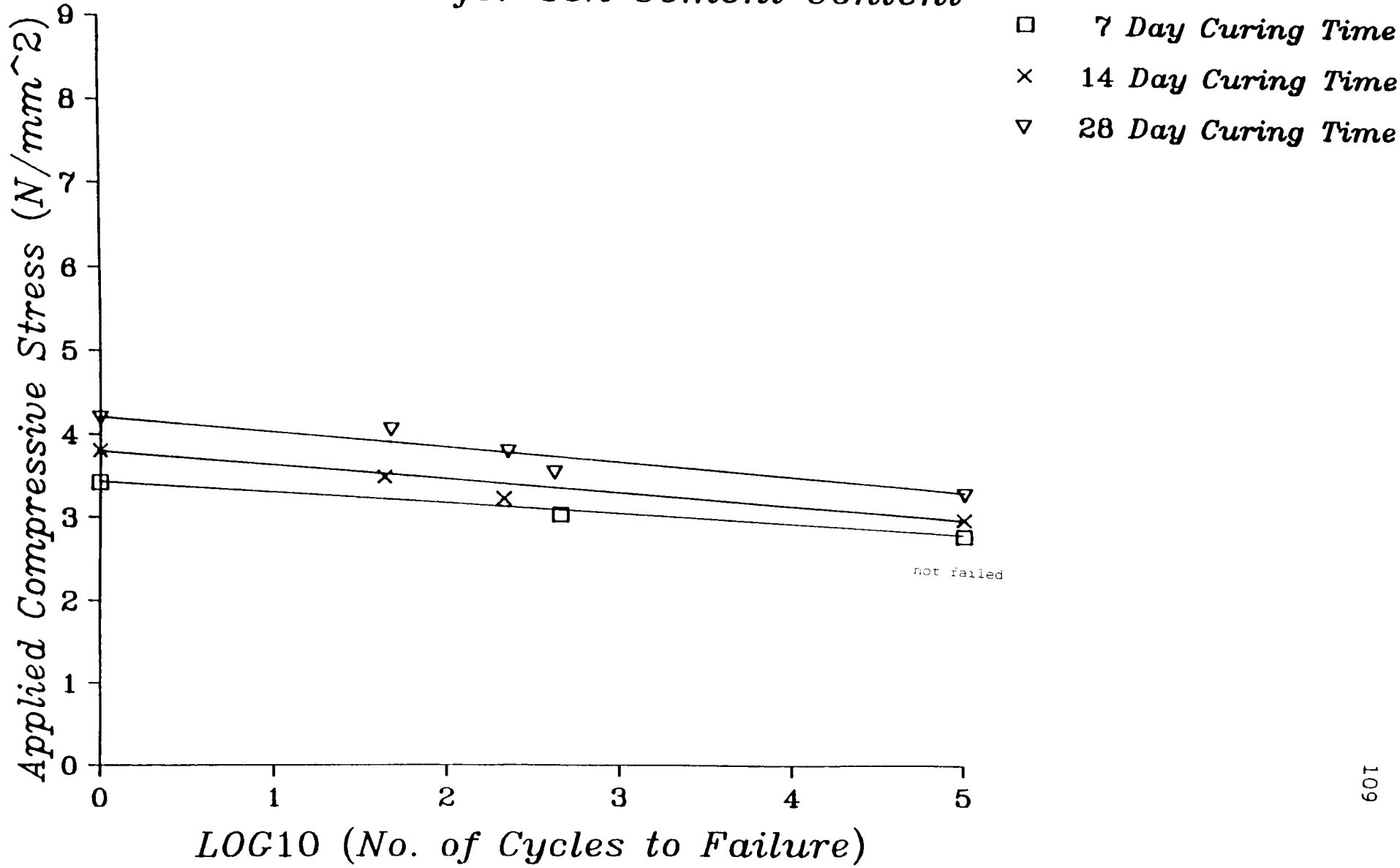

Fig.5.21. Dynamic Compression Tests

for 14% Cement Content

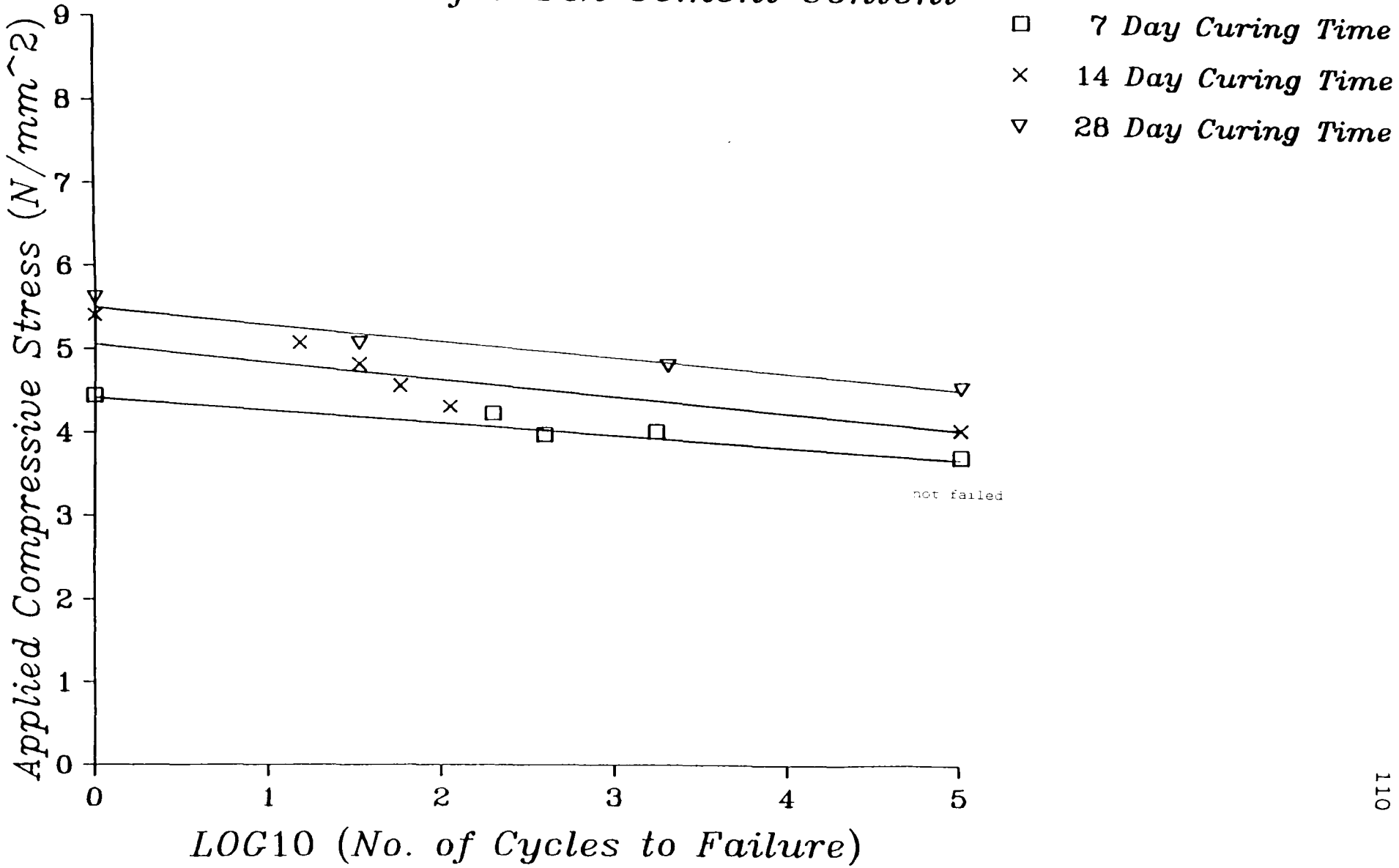

Fig.5.22. Dynamic Compression Tests

for 18% Cement Content

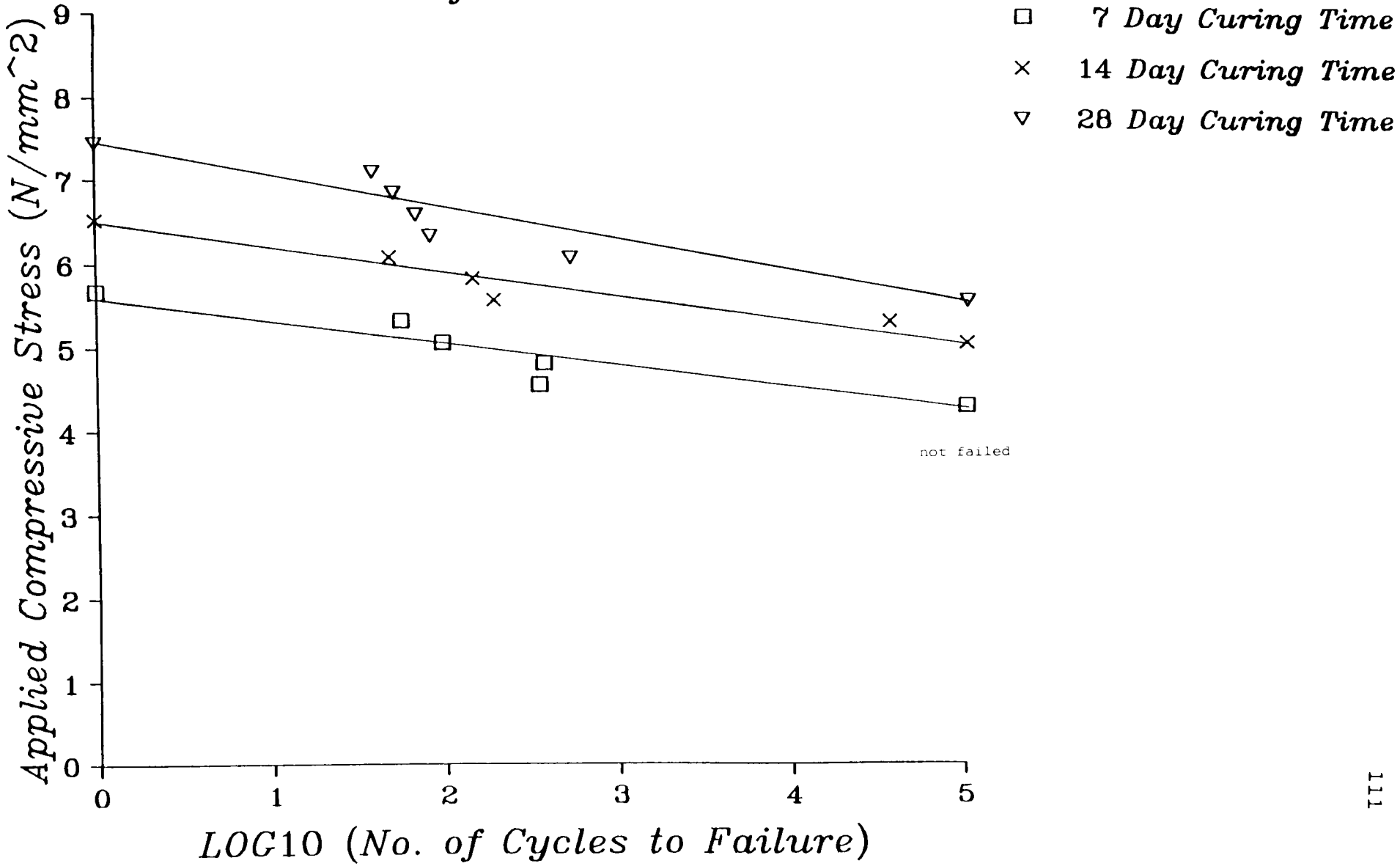

Fig.5.23. Dynamic Compression Tests

for 22% Cement Content

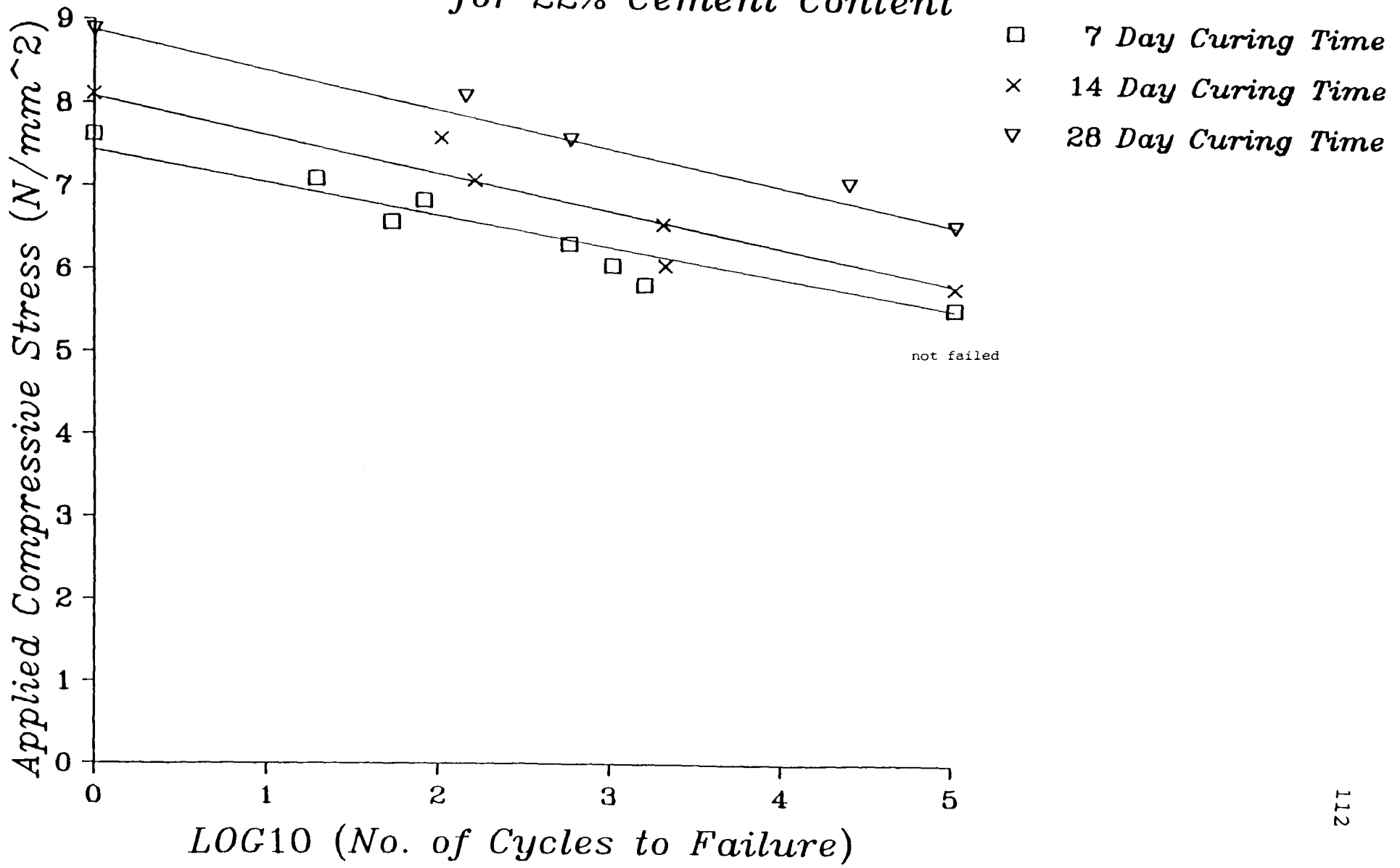

These fatigue failure relationships have been analysed on the VAX main frame computer. Each line is of the form:

$$\sigma c = J + K \log_{10} Nf \quad \ldots\ldots\ldots\ldots\ldots\ldots\ldots\ldots 5.6$$

where,

σc = compressive stress applied

J = an ordinate coefficient of the best polynomial

K = slope coefficient

Nf = number of load cycles to failure

The numerical values of coefficients J and K are tabulated in Tables 5.8 and 5.9 and the sum of errors squared is listed in Table 5.10.

Curing time (days)	coefficient J for cement contents of 6%	10%	14%	18%	22%
7	2.515	3.408	4.470	5.643	7.551
14	2.910	3.747	5.227	6.464	8.216
28	2.971	4.193	5.521	7.410	8.942

Table 5.8. Coefficient J for various cement contents and curing times

Curing time (days)	coefficient K for cement contents of 6%	10%	14%	18%	22%
7	-0.085	-0.124	-0.141	-0.290	-0.436
14	-0.114	-0.161	-0.264	-0.270	-0.495
28	-0.089	-0.194	-0.198	-0.388	-0.441

Table 5.9. Coefficient K for various cement contents and curing times

Curing time (days)	Sum of errors squared for cement conts. of 6%	10%	14%	18%	22%
7	0.009	0.001	0.023	0.167	0.245
14	0.016	0.021	0.025	0.089	0.414
28	0.005	0.141	0.029	0.304	0.061

Table 5.10. Sum of errors squared for various cement contents and curing times

A close examination of results from all dynamic tests in compression has been carried out in order to evaluate the Resilient Modulus, illustrated in Figure 5.24. Resilient Modulus values versus Log_{10} number of cycles to failure are shown in Figures 5.25 and 5.26. These Figures represent test results from two samples having the same cement content and curing time, tested at two different stress levels.

In Figure 5.25 the applied stress was 3.56 N/mm^2, equivalent to 85% of the static UCS. The Resilient Modulus, initially at 2250 N/mm^2, started to decrease at a uniform rate over the first 100 load cycles, and then remained constant for 200 load cycles. During this period microcracks started to develop, and the Resilient Modulus then dropped rapidly to a failure point at about 415 cycles.

In Figure 5.26 the applied stress was 3.31 N/mm^2, equivalent to 79% of the static UCS. The Resilient Modulus, initially at 2400 N/mm^2, started to decrease during the first 100 load cycles, as for Figure 5.25. The Resilient Modulus then remained fairly stable and started to decrease up to about 1000 load cycles. No microcracks were detected and the Resilient Modulus was constant up to 6000 cycles. It then began to increase slowly and remained constant at about 2250 N/mm^2 after 30000 load cycles.

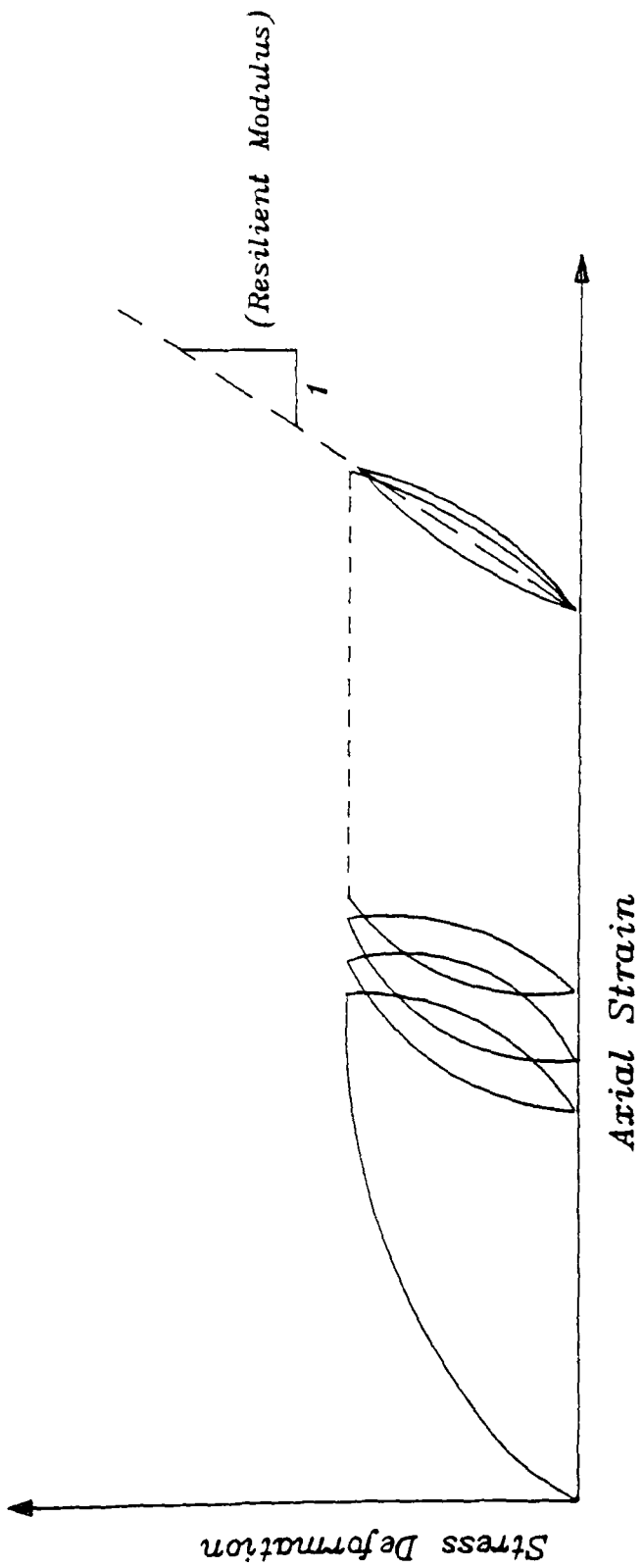

Fig.5.24. Typical stress–strain graph for dynamic compression test

Fig.5.25. Resilient Modulus–Log10(Cycle No)

10%CC 28CT & 3.56N/mm^2 Stress

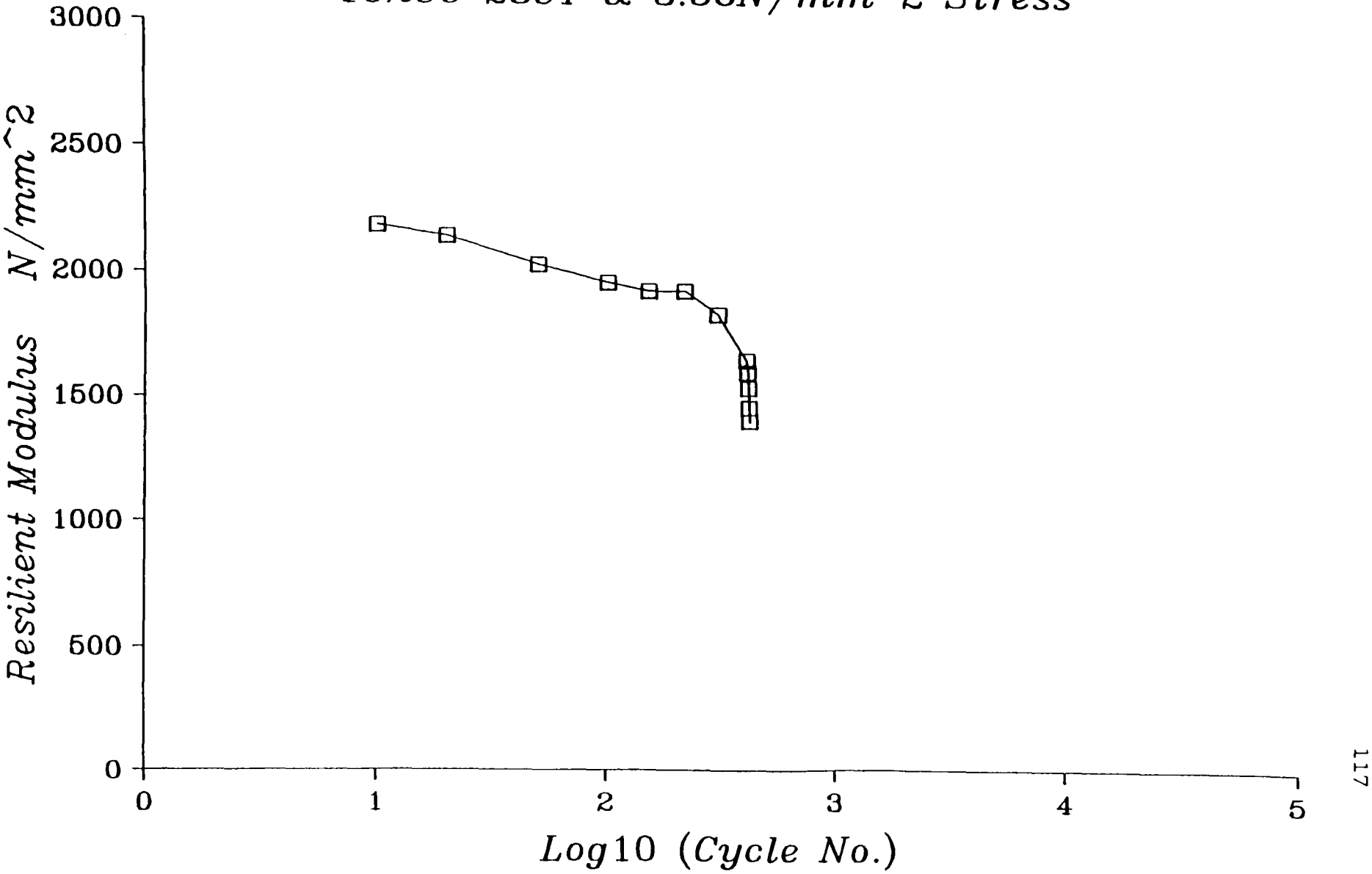

Fig.5.26. Resilient Modulus–Log10(Cycle No)

10%CC 28CT & 3.31 N/mm^2 Stress

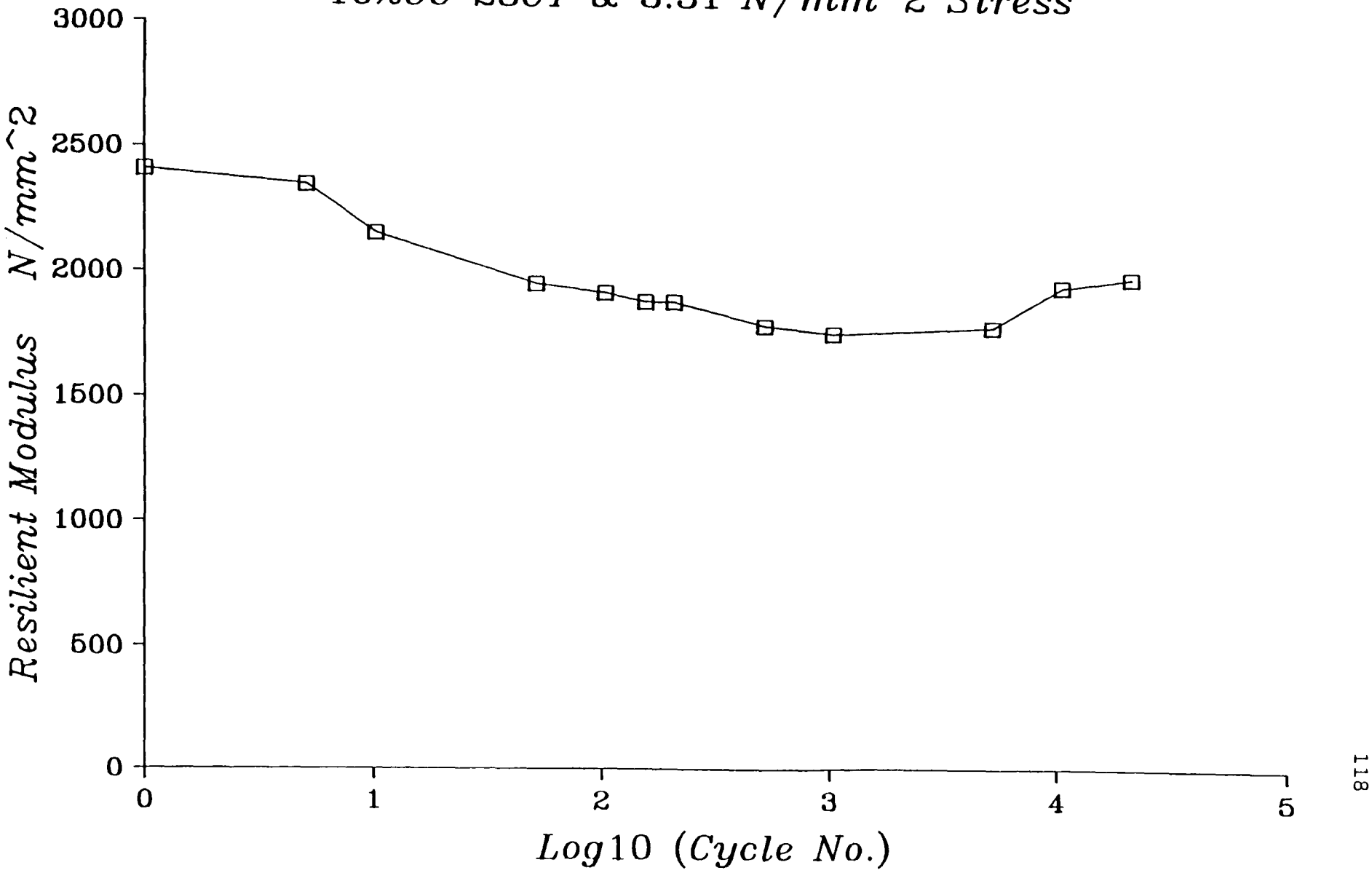

The same pattern was observed in other dynamic compression tests.

The Resilient Modulus concept has been extensively used by researchers in analysing the results for dynamic load tests on soils, granular materials, bituminous materials and cement-treated soils. It can be compared with Young's Elastic Modulus for static loading tests. Comparison of the value of the Resilient Modulus and the Elastic Modulus shows that the Resilient Modulus is generally higher than the Elastic Modulus for the same cement content and curing time. For example in the 14-day curing and 18% cement content test, the Resilient Modulus was found to be 3104 N/mm^2 and the Elastic Modulus 1648 N/mm^2. The Resilient Modulus was almost twice the value of the Elastic Modulus.

5.4. Static and dynamic flexure test results

A comprehensive testing program similar to the static and dynamic compression tests was planned for dynamic flexure tests. A large number of specimens was prepared but only limited results were obtained due to technical problems as explained in Chapter four. The test results for the 6% and 10% cement contents at a 28-day curing time are listed in Table 5.11. Figure 5.27 shows the Dynamic Modulus of Rupture (also known as the bending tensile strength) verses Log_{10} (No. of cycle to failure).

The results show a substantial drop in strength due to fatigue effects in flexure. For example it can be seen that for the 6% cement content and 28-day curing time the static strength reduced from 830N to 470N after 60400 load cycles, a reduction of 43%. It can be seen from Table 5.7 that for the 6% cement content and 28-day curing time under dynamic compression loading, a 14% drop in strength occurred under these conditions. The fatigue failure of the soil-cement in flexure is caused by the development of tension cracks at the underside of the beam specimen.

The Modulus of Rupture (according to ASTM D1632-63) depends on the type of failure of the beam. The Moduli values in Table 5.11 were for fracture occurring within

the middle third of the span length, and were calculated from

$$R = Pl / bd^2 \quad \text{.....5.7}$$

where,

R = Modulus of Rupture (N/mm^2)

P = maximum applied load (N)

l = span length = 228.6mm

b = average width of specimen = 76.2mm

d = average depth of the specimen = 76.2mm

If the fracture occurs no more than 5% of the span length outside the middle third, the Modulus of Rupture can be calculated as

$$R = 3Pa / bd^2 \quad \text{.....5.8}$$

where,

a = distance between the line of fracture and the nearest support, measured along the centre line of the bottom surface of the beam.

If the fracture occurs by more than 5% of the span length outside the middle third, this is generally indicative of influence from the supports or of damage to the soil-cement specimen caused during handling or by non-uniform mixing of materials.

Cement cont. (%)	Load applied (N)	Load (%)	Cycles to failure (No.)	Log_{10} cycles to failure (No.)	Modulus of Rupture (N/mm^2)
6	780	93.98	1	0	0.403
6	790	95.18	1	0	0.408
6	830	100.00	1	0	0.429
6	620	74.70	11	1.041	0.320
6	670	80.72	60	1.778	0.346
6	580	68.67	950	2.978	0.300
6	470	56.63	60400	4.781	0.242
10	1160	100.00	1	0	0.600
10	1150	99.14	1	0	0.594
10	1030	88.79	8	0.903	0.532
10	980	84.48	20	1.301	0.506
10	930	80.17	42	1.623	0.481
10	980	84.48	90	0.954	0.506
10	640	55.17	71000	4.851	0.331

Table 5.11. Dynamic flexure test results for 6% and 10% cement contents at 28-day curing time

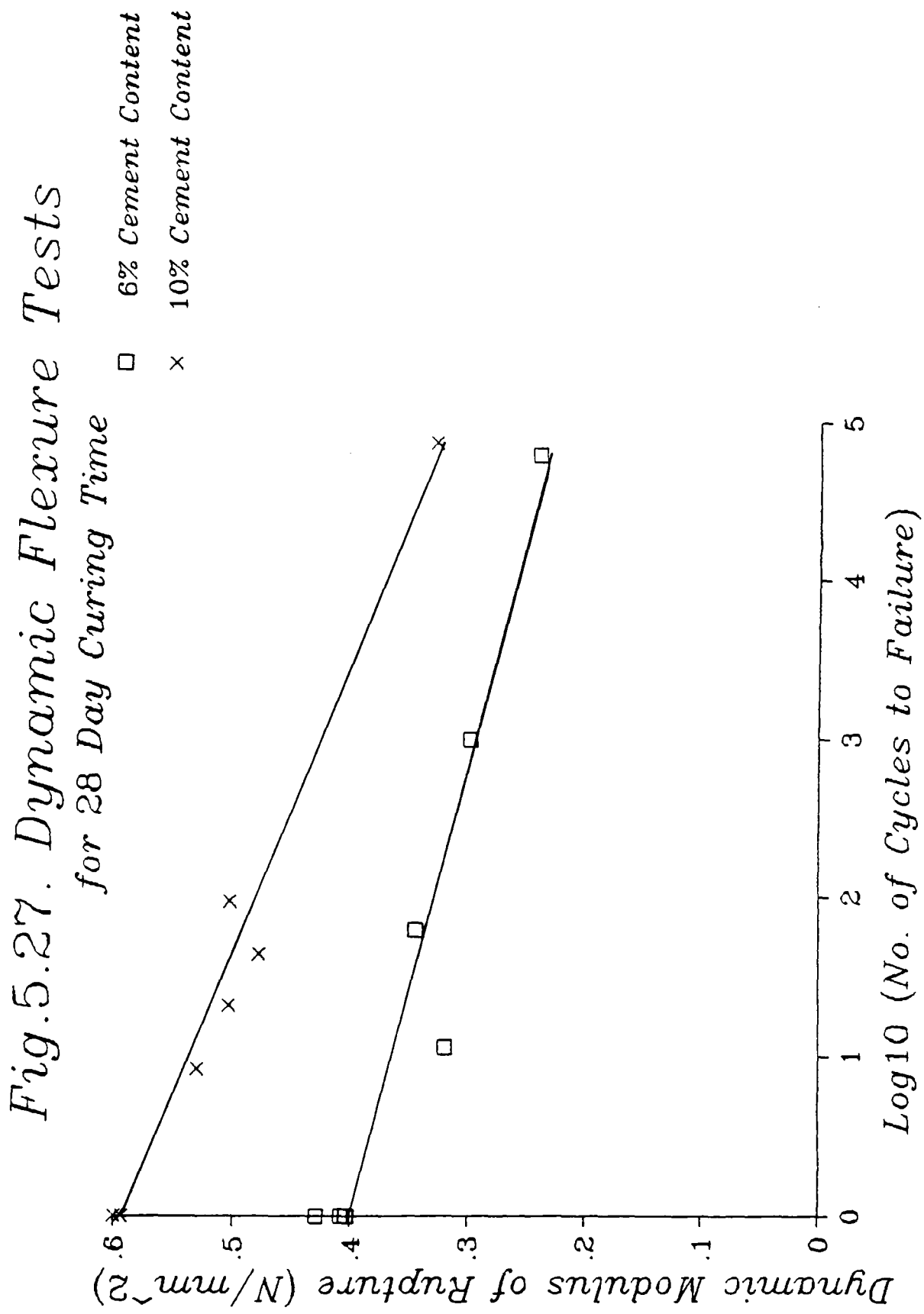
Fig.5.27. Dynamic Flexure Tests
for 28 Day Curing Time
6% Cement Content
10% Cement Content
Dynamic Modulus of Rupture (N/mm^2)
0
.1
.2
.3
.4
.5
.6
0
1
2
3
4
5
Log10 (No. of Cycles to Failure)

5.5. Static and dynamic tension and tension-compression tests

The stresses generated by traffic loading are flexural in nature and flexural fatigue tests are easier to carry out than uni-axial tensile tests. However uni-axial tensile tests are preferred since they provide more reliable information on the fatigue behaviour of the pavement material; they also do not involve uncertainties regarding the extreme fibre tensile stresses induced during flexural fatigue testing.

A large number of trial tests was carried out in uni-axial tension and tension-compression on the MTS-850 testing system, and the test method was well established. However there were problems with the load cell and no reliable results could be chosen for presentation.

CHAPTER 6

Numerical Analysis of a Layered System

6.1. Introduction

Seed et al, (1965, 1967) have indicated that in certain circumstances a Boussinesq distribution may provide a very close approximation of actual stress conditions in a pavement section (in the case of one thick layer of pavement system). However, it has also been demonstrated that when the moduli of the various layers of a pavement structure are considerably different, and provided the stiffer layers can withstand tension, the Boussinesq stress distribution is not adequate. The assumption made in the Boussinesq analysis is based on an infinite strip of homogeneous material but the relationships of stresses and deflections in the real pavement materials and in the subgrade are much more complex. In such cases, a layer-system theory has to be adopted.

Procedures for the prediction of traffic-induced deflections, stresses and strains in pavement systems are based on the principles of continuum mechanics. Barksdale (1972) stated the essential factors that must be considered in predicting the response of layered pavement systems and these are:

a) stress-strain behaviour of the materials

b) initial and boundary conditions of the problem.

Reasonably good prediction of pavement response to load can be obtained provided that carefully selected material properties are used.

6.2. Layered system of linearly elastic materials

For the axi-symmetric load cases, the elastic layered solution was first developed for a two-layer system by Burmister (1943) and then for the three-layer system by Jones (1962). Some solutions for a four-layer system and later adapted for an n-layer system were developed by the Chevron Research Company (Warren and Dieckmann 1963). The computer program dealing with this problem can handle up to 15 layers. An iterative process is used to determine the elastic modulus for each layer as a function of stresses. The solution converges when stresses and deformations in the pavement system are compatible.

6.3. Finite element procedures

The finite element method was first described by Turner et al, (1956), and has since been developed into a very powerful tool for the analysis of all types of continuum

mechanics problems. It is an approximate procedure, which consists of modeling the structure as an assembly of discrete elements, and analysing this assembly by standard methods of structural analysis. Essentially, the technique may be divided into five basic operations:

1) Idealisation of the structure as an assemblage of a finite number of discrete structural elements interconnected at a finite number of nodal points.

2) Development of the element stiffness matrix for individual elements and relating the forces and corresponding displacements within the element.

3) Assemblage of the overall stiffness matrix by adding up the stiffness matrices for the individual elements.

4) Solution of the simultaneous equations for the assembled structure, giving nodal displacements.

5) Calculation of stresses and strains in the structure, by using the nodal displacements and the individual element stiffness matrices.

6.4. The finite element program

The finite element suite used in this study is PAFEC

(Program for Automatic Finite Element Calculations), level 6.1. The program is written in FORTRAN language and is operated on a VAX 11/785 computer. It consists of 10 separate computer programs which, when executed sequentially, give a complete engineering analysis. Each of these programs is known as PHASE of PAFEC. The program is general purpose, solving both plane stress and plane strain problems.

The suite provides a wide range of element types to solve various kinds of structural problems.

The elements are generated automatically provided that types, spacings and material properties are correctly inputed.

Each element, meeting at a node, will in general give different stresses and the continuity is a measure of the overall accuracy of the analysis.

Facilities of the PAFEC Interactive Graphic Suite (PIGS) also include comprehensive data checking, mesh correction and display of intermediate results such as distorted shape, principal stresses or vector contours.

6.5. Numerical modeling of the problem

In developing a numerical model, it is necessary to input data to PAFEC in a modular form. A general description of data preparation procedure can be summarised as follows:

a) Construct a control model which will act as a qualifier for the mesh, or be used as an aid to guide a particular job through the various paths of the program. Types of analysis such as static or dynamic, plane stress or strain analyses, thermal, creep etc., must be selected at this stage.

b) Input nodal coordinates in a standard Cartesian axis set, the origin of which is at the global origin (0,0,0).

c) Input material properties required for each layer or section of the model.

d) Select element types with required capabilities and suitable for the type of analysis.

e) Select restraints, describing the degrees of freedom to be restrained. Each data entry is used to describe the constraints at appropriate nodes using the combination of specific numbers. This enables an analyst to restrain single nodes or whole planes.

f) Input loading vectors and specify the type of loading required (i.e. pressure or point load).

6.6. Finite element analysis

To demonstrate applicability of the Finite Element Method (FEM) of analysis to pavement design, three numerical models were analysed. These models are as follows:

1) Book example model - model 1.
2) Three layer carriageway model - model 2.
3) Four layer carriageway model - model 3.

6.6.1. Book example model - model 1

6.6.1.1. Description of the control model

In this model 1, the flexible pavement was analysed using layer equations and a solution can be found in "Principles of Pavement Design", by Yoder (1975). This example was selected to ascertain the validity of the numerical model used in subsequent studies.

The three-layer pavement section shown in Figure 6.1, having three different Young's modulus values (E1, E2 and E3), layer depths (h1, h2 and h3) and Poisson's ratios

(μ1, μ2 and μ3) was considered. The pressure load (P) was distributed over a circular area, of radius (a).

Due to symmetry only one half of the pavement section was considered. The line of symmetry passes through the centre line of the pressure load.

6.6.1.2. Type of elements used

The structure containing 1576 freedoms with 258 eight-noded isoparametric curvilinear quadrilateral elements was used in the analysis. A 36210 plane stress/strain element which carries loads in its own plane was selected to determine stresses and displacements.

6.6.1.3. Boundary conditions

The line of symmetry which passes through the centre line of the pressure load was represented by a series of rollers allowing for vertical displacement only (see Figure 6.2). The base line was also represented by a series of rollers, in this case allowing for horizontal movement. The right hand plane, assumed 4m from the line of symmetry, was represented by a series of rollers restraining this plane against movement. 4m was considered sufficient for horizontal ground movement at that plane to be insignificant.

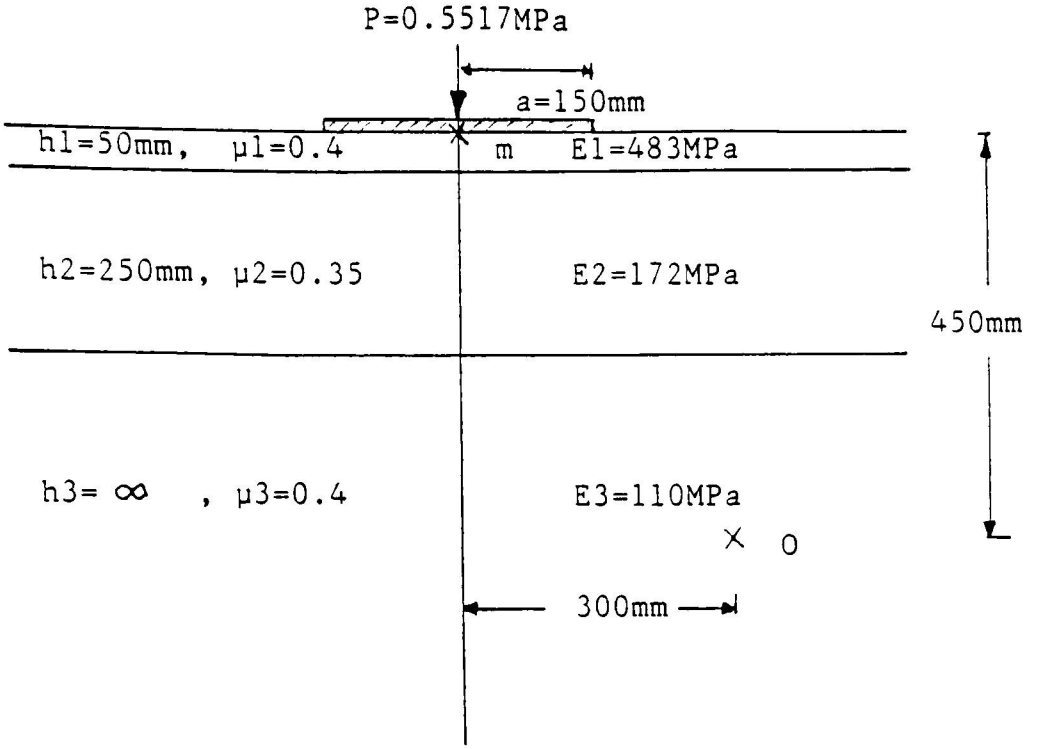

Fig.6.1. Model 1 - Book example pavement section

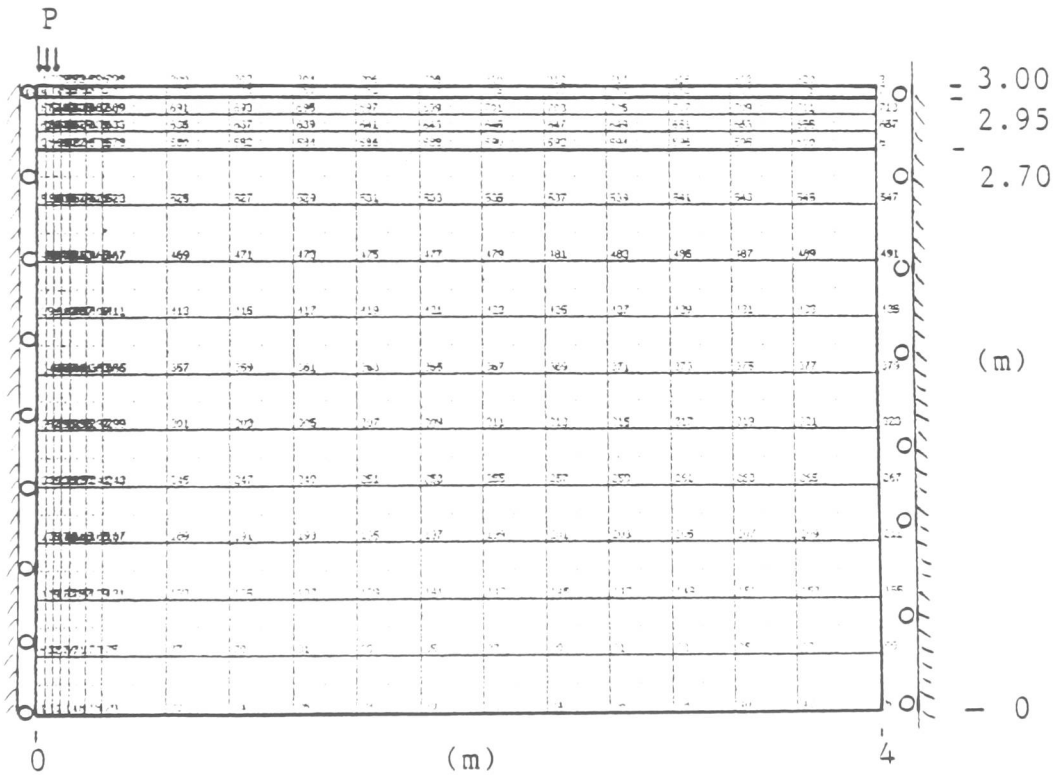

Fig.6.2. Model 1 - Mesh refinement and boundary conditions

6.6.1.4. Loading

A pressure load was applied in the vertical direction as shown in Figure 6.3 (this Figure is an enlarged section plotted using PIGS). The manner in which pressure is applied to an element depends upon the element type being used. For two dimensional plane stress/strain elements, a positive pressure will always act towards the centre of the element i.e. in the direction of the inward normal to the side.

6.6.1.5. Results and discussion

The displacement directly under the pressure load (point m), shown in Figure 6.1 was selected to demonstrate correlation of FEA and mathematical analysis. The book deflection value for this point is 0.525mm and, the numerical value extracted from the output or the graph obtained from PIGS shown in Figure 6.4, was found to be 0.585mm. The difference of 11% is acceptable for engineering applications in mind. Vertical stresses were compared at point (O) with coordinates (0.3, 2.55), as shown in Figure 6.1. An enlarged corner section of the carriageway with the stress contours is shown in Figure 6.5. The book value for vertical stress is 0.036551 MPa and, the numerical value extracted from the graph or the computer output is 0.027690 MPa. The difference of 25% is

Pressure load

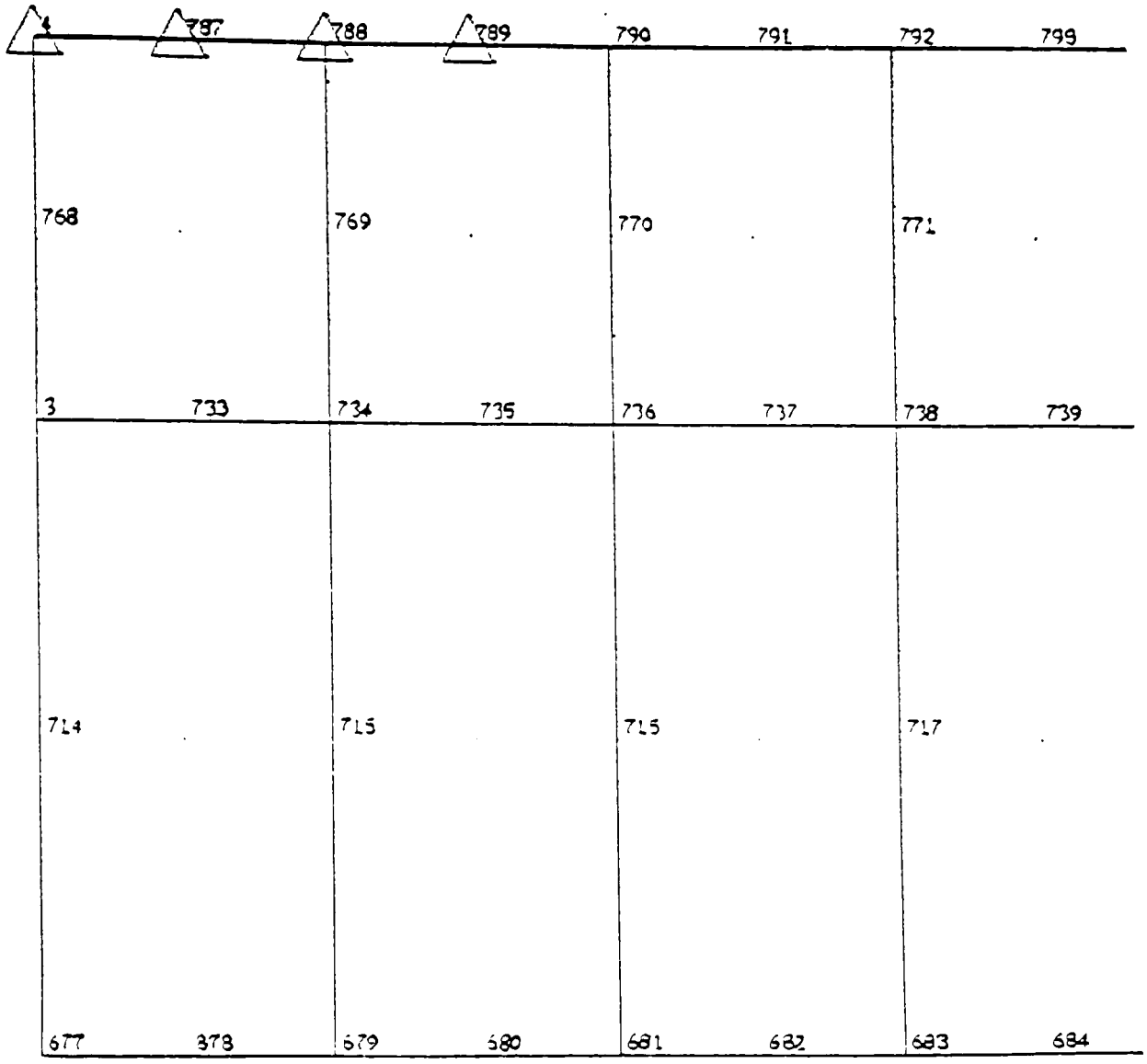

Fig.6.3. Model 1 - Enlarged section showing the pressure load and the number of nodes, plotted using PIGS

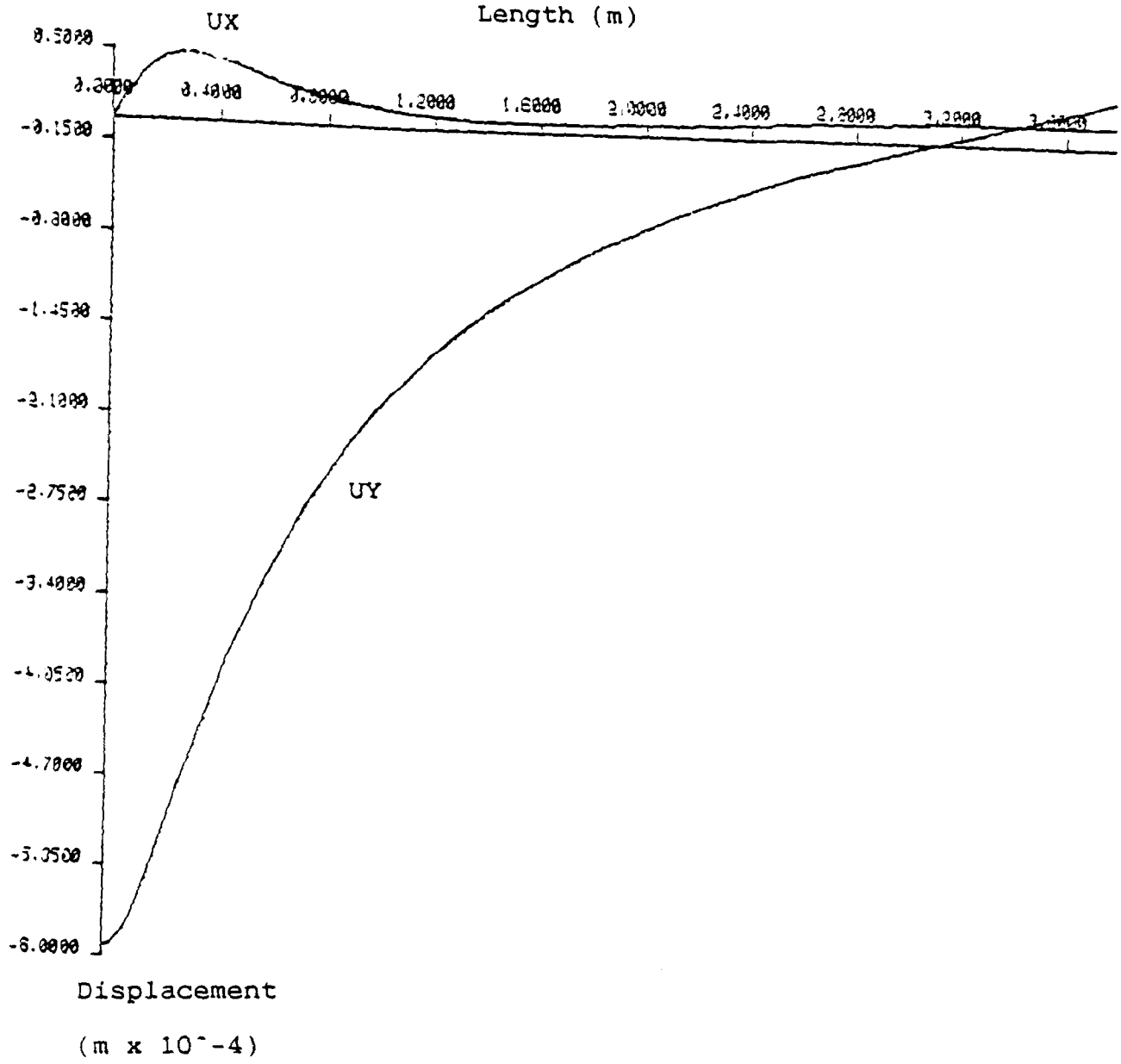

Fig.6.4. Model 1 - Displacement in the vertical UY and the horizontal UX directions

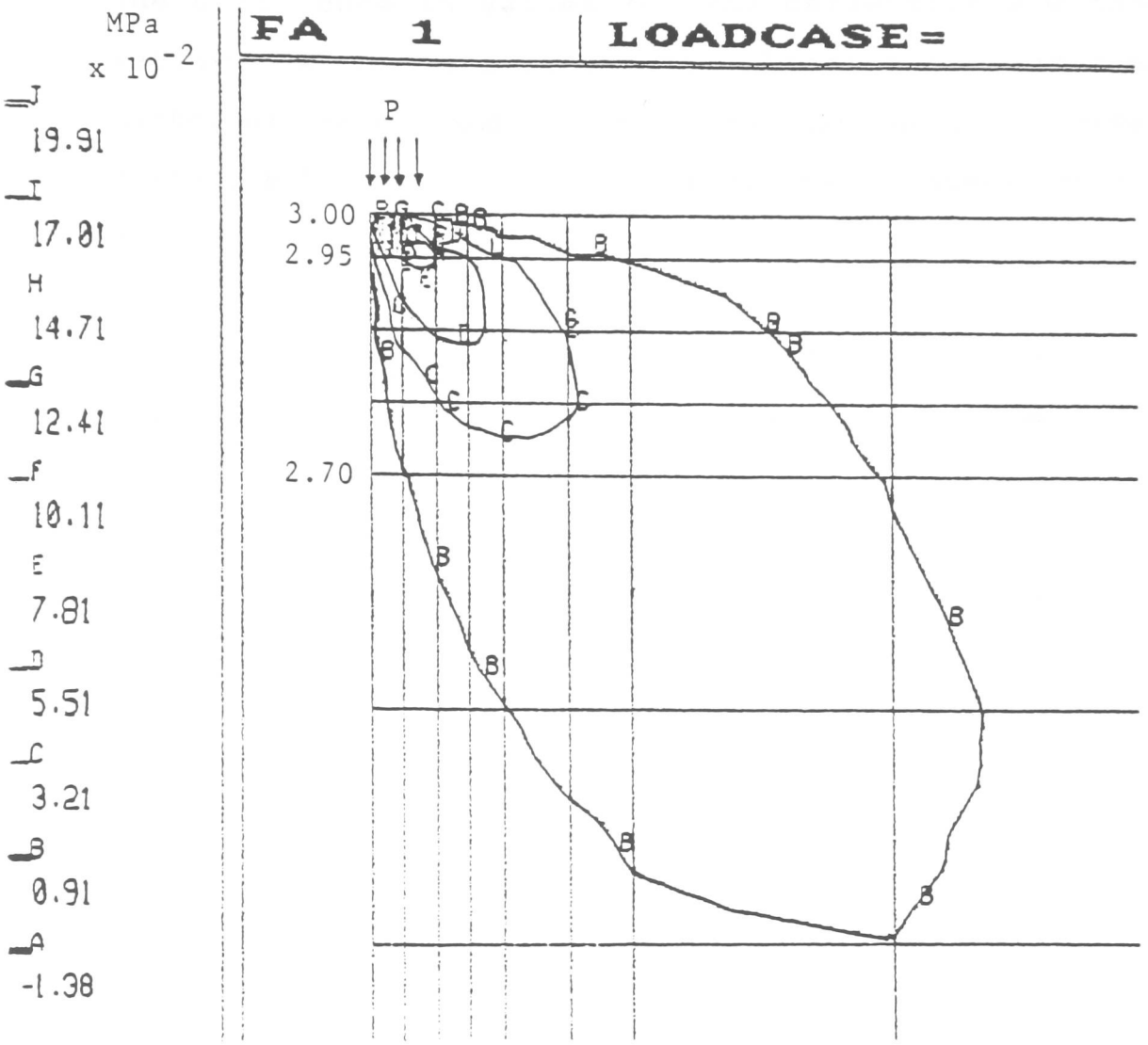

Fig.6.5. Model 1 - Enlarged corner section showing stress contours

acceptable because at this stage only the order of magnitude for stresses was of interest.

The difference in values for the deflection and the vertical stress are acceptable, bearing in mind the number of factors and uncertainties that could influence these results. Some of these factors can be specified as follows:

a) In the absence of other independent solutions, the accuracy of the one-layer analysis used in the book example cannot be clearly quantified.

b) The accuracy of the numerical analysis in general is dependent on the mesh geometry and refinement. Only a coarse mesh was used in this control model.

c) In the book example the pressure is applied through a circular plate. However in the numerical example, uniform pressure of the equivalent intensity was applied over a distance equal to the radius of the circular plate. This was assumed as a sufficient approximation of pressure load without using three dimensional analysis.

Comprehensive investigation of the above points together with a convergence study would be necessary before a numerical model proposed here could be safely used in

pavement design. This would require detailed numerical analysis and it is outside the scope of this research program. However, to demonstrate a feasibility of this approach two more models have been developed showing the versatility of the FE analysis.

6.6.2. Three-layer carriageway model - model 2

6.6.2.1. Description of the model

A general three-layer carriageway section shown in Figure 6.6, with three different Young's modulus values (E1, E2 and E3), layer depths (h1, h2 and h3) and Poisson's ratios (μ1, μ2 and μ3) was considered in this model. The axle load was simulated as a series of uniform pressure loads applied at specified distances.

Due to symmetry only one half of the 7.3m carriageway section was modeled. The line of symmetry passes through the centre line of the carriageway.

6.6.2.2. Type of elements used

A coarse mesh, consisting of 168 eight-noded isoparametric curvilinear quadrilateral elements and 8 six-noded isoparametric triangular elements was used in this

analysis. Both types of elements are plane stress/strain elements which carry loads in their own plane.

6.6.2.3. Boundary conditions

The line of symmetry which passes through the centre line of the carriageway was represented by a series of rollers allowing for vertical displacement only (see Figure 6.6). The right hand plane, assumed 9.65m from the line of symmetry, was represented by a series of rollers restraining this plane against horizontal movement. 9.65m was considered sufficient for ground movement to be insignificant.

6.6.2.4. Loading and materials properties

The pressure load of a commercial vehicle, as shown in Figures 6.6 and 6.7, had a contact pressure of 500 kPa.

The input data for the properties of the materials used in the carriageway section under consideration were selected to simulate the type of material used in this research. The Red Marl subgrade selected has an E value = 35 MPa and a Poisson's ratio of 0.4. The roadbase, considered as a soil-cement layer, has an E Value = 1000 MPa and a Poisson's ratio of 0.2. The 50mm capping layer used has E = 2100 MPa and a Poisson's ratio of 0.4.

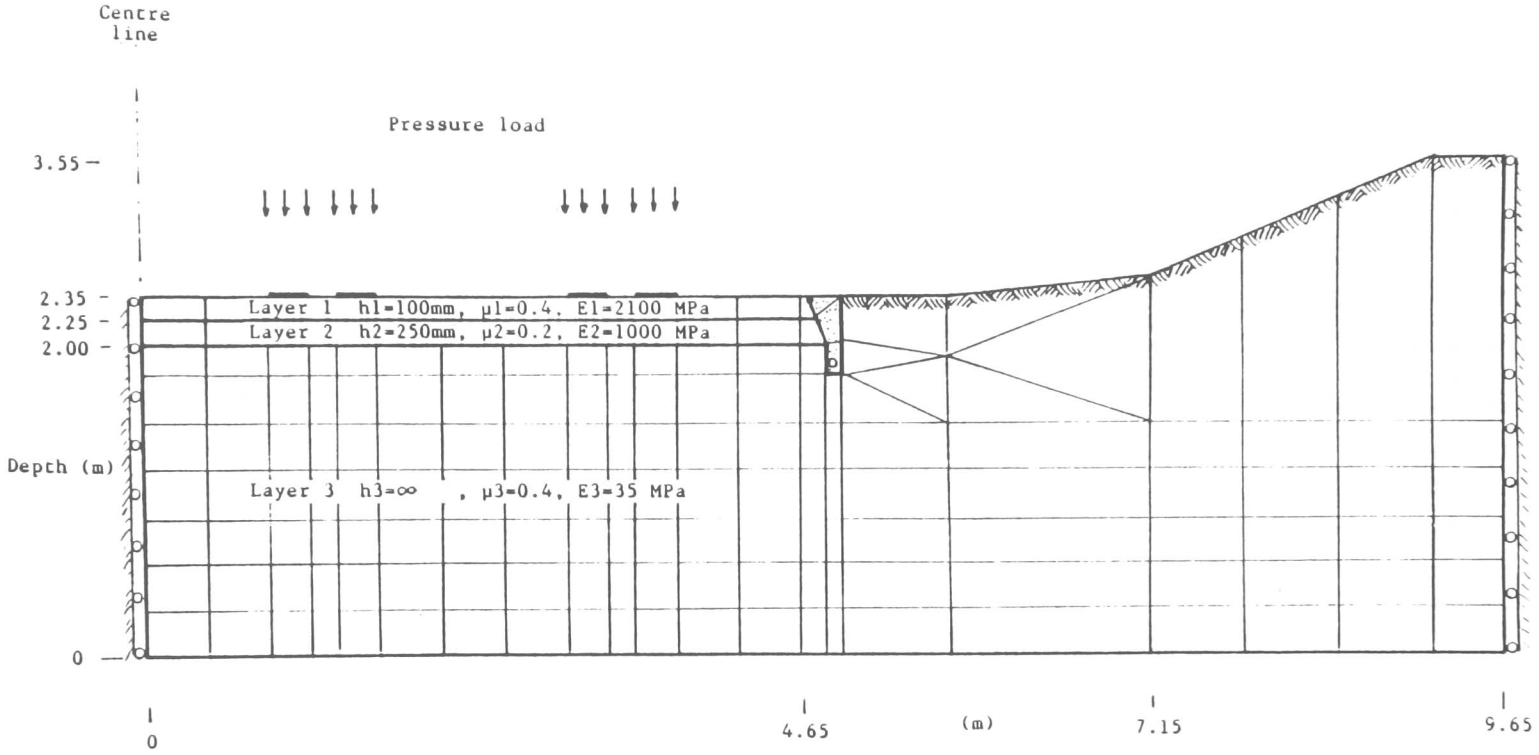

Fig.6.6. Model 2 - Three-layer carriageway section

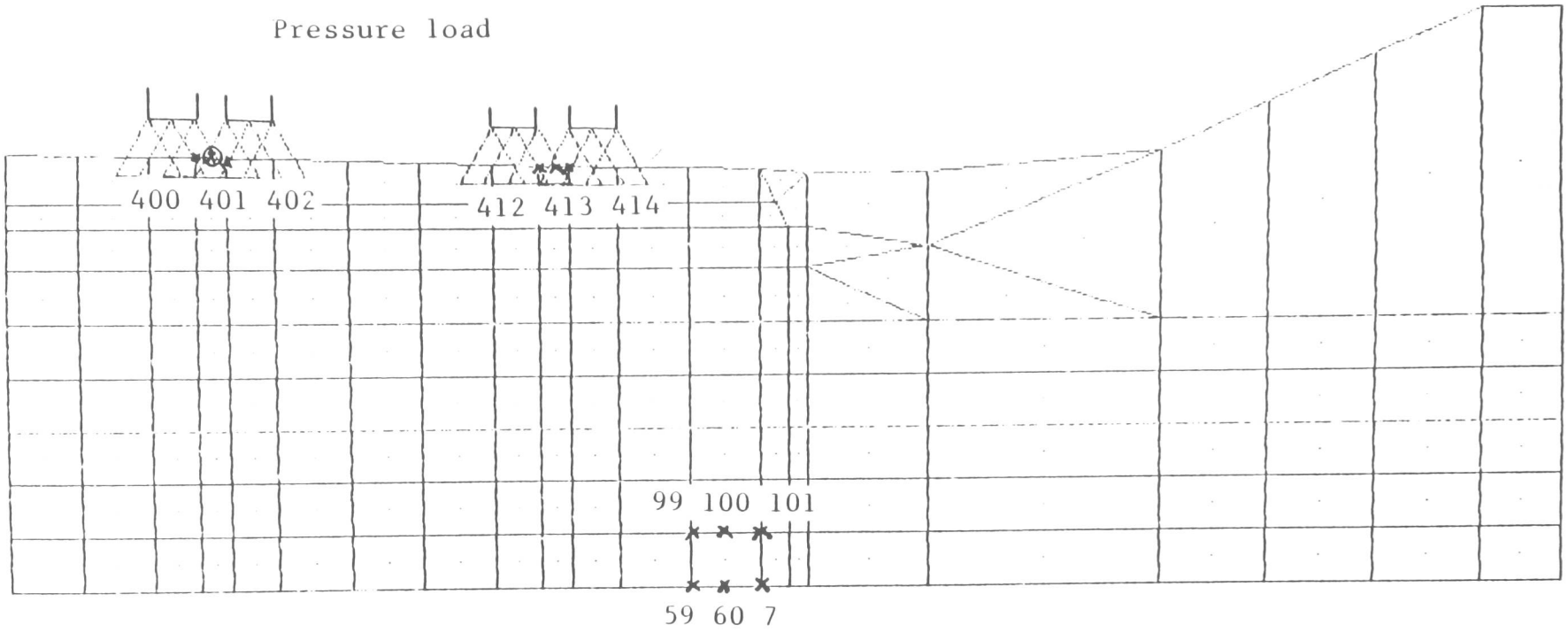

Fig.6.7. Model 2 - PIGS plot showing mesh refinement and number of nodes with maximum displacement

6.6.2.5. Results and discussion

The maximum displacements in the horizontal and vertical directions are selected automatically in Phase 7 of the computer analysis. Results for the 250mm soil-cement roadbase output are presented in Table 6.1 and Figure 6.8 from PIGS. UX represents the horizontal and UY the vertical carriageway surface displacements. From Table 6.1, it can be noted that node number 401 (under the wheel load) has a vertical displacement of 17.9mm.

The analysis indicated that the expected displacements are excessive and therefore that this type of road design would be unsuitable for the given subgrade conditions and traffic load.

A number of computer analyses were carried out using different thicknesses and different Young's modulus values for the soil-cement layer in order to determine the influence of these variables on the variation of displacements and stresses. Properties of other layers remained unchanged. The soil-cement layer thickness was varied from 100 to 250mm and the E value from 600 to 1800 MPa; it was found that the maximum displacements under the wheel load varied by only 0.5mm.

Figure 6.9 is a PIGS plot showing the variation of direct stresses and shear stress through a vertical section at node 401 under the LHS wheel load. This PIGS facility can be used to draw stress variations in any vertical or horizontal planes.

```
PPPPP  AAAAA FFFFF EEEEE CCCCC
P   P  A   A FF    E     C   CC
P   P  A   A FF    E     C
PPPPP  AAAAA FFF   EEE   C
PP     AA  A F     EE    C
PP     AA  A F     EE    C
PP     AA  A F     EE    C
PP     AA  A F     EEEEE CCCCC
```

```
*****************************************
*                                       *
* STATICS  SOLUTION BY BLOCK FRONT      *
*          IN DOUBLE PRECISION          *
*                                       *
*   STRUCTURE CONTAINS  1079 FREEDOMS   *
*                        176 ELEMENTS   *
*     AND THE FRONT SIZE IS    59       *
*                                       *
*****************************************
```

NODE	UX
60	0.0053269
7	0.0053235
74	0.0053145
420	0.0053017
100	0.0052955
101	0.0052869
13	0.0052692
422	0.0052629
421	0.0052591
59	0.0052516

NODE	UY
401	-0.0179508
402	-0.0177750
400	-0.0176408
413	-0.0174616
412	-0.0173640
385	-0.0172907
384	-0.0171554
414	-0.0170615
390	-0.0168956
362	-0.0168758

NODE	RESULTANT
401	0.0180000
402	0.0177964
400	0.0177310
413	0.0175339
412	0.0174943
385	0.0173200
384	0.0172282
414	0.0170934
390	0.0170179
362	0.0169229

Sample of largest displacement at nodes (m)

Table 6.1. Model 2 - PAFEC output showing maximum vertical UY and horizontal UX displacements at element nodes

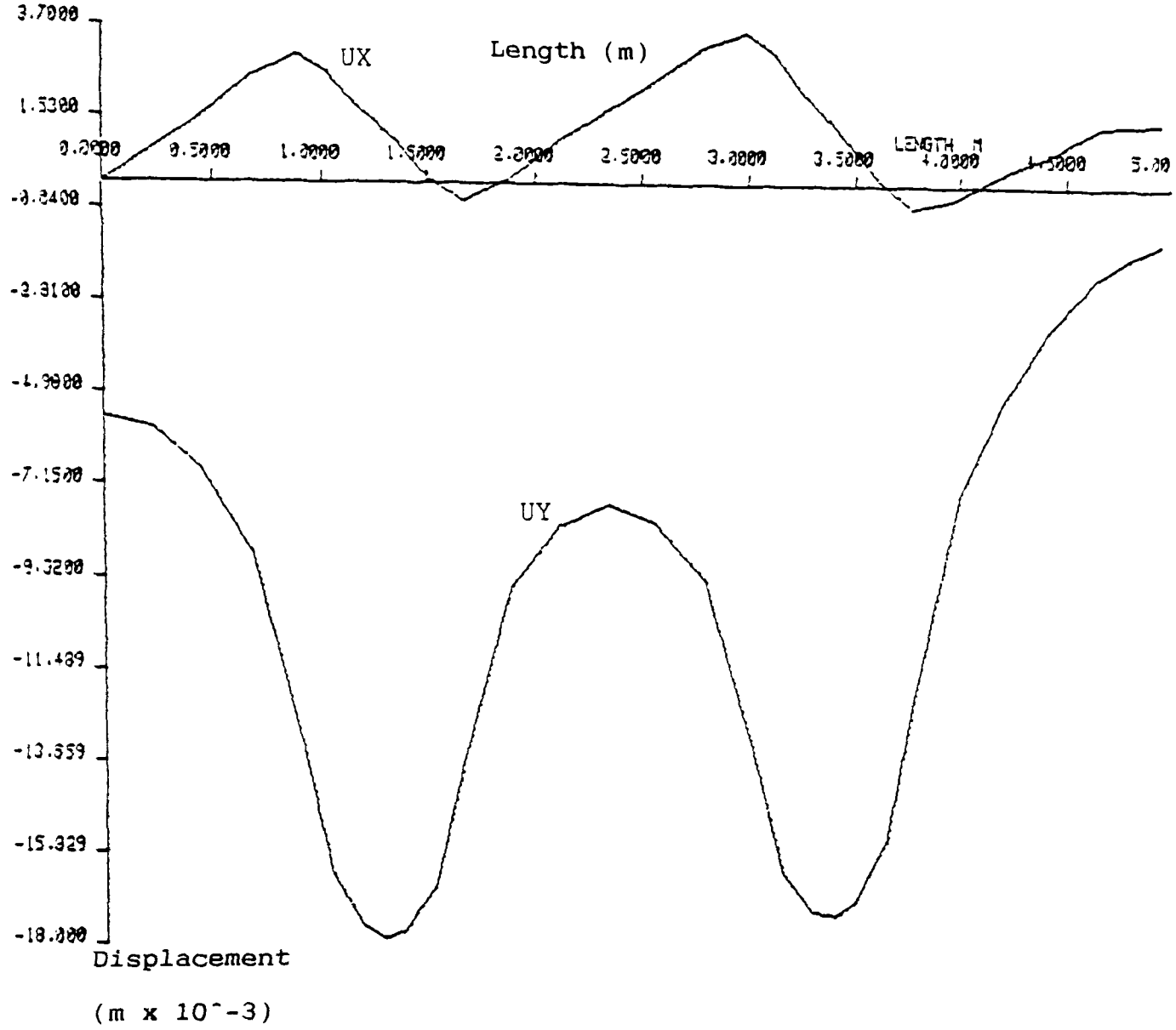

Fig.6.8. Model 2 - PIGS plot showing vertical UY and horizontal UX surface displacements along the carriageway

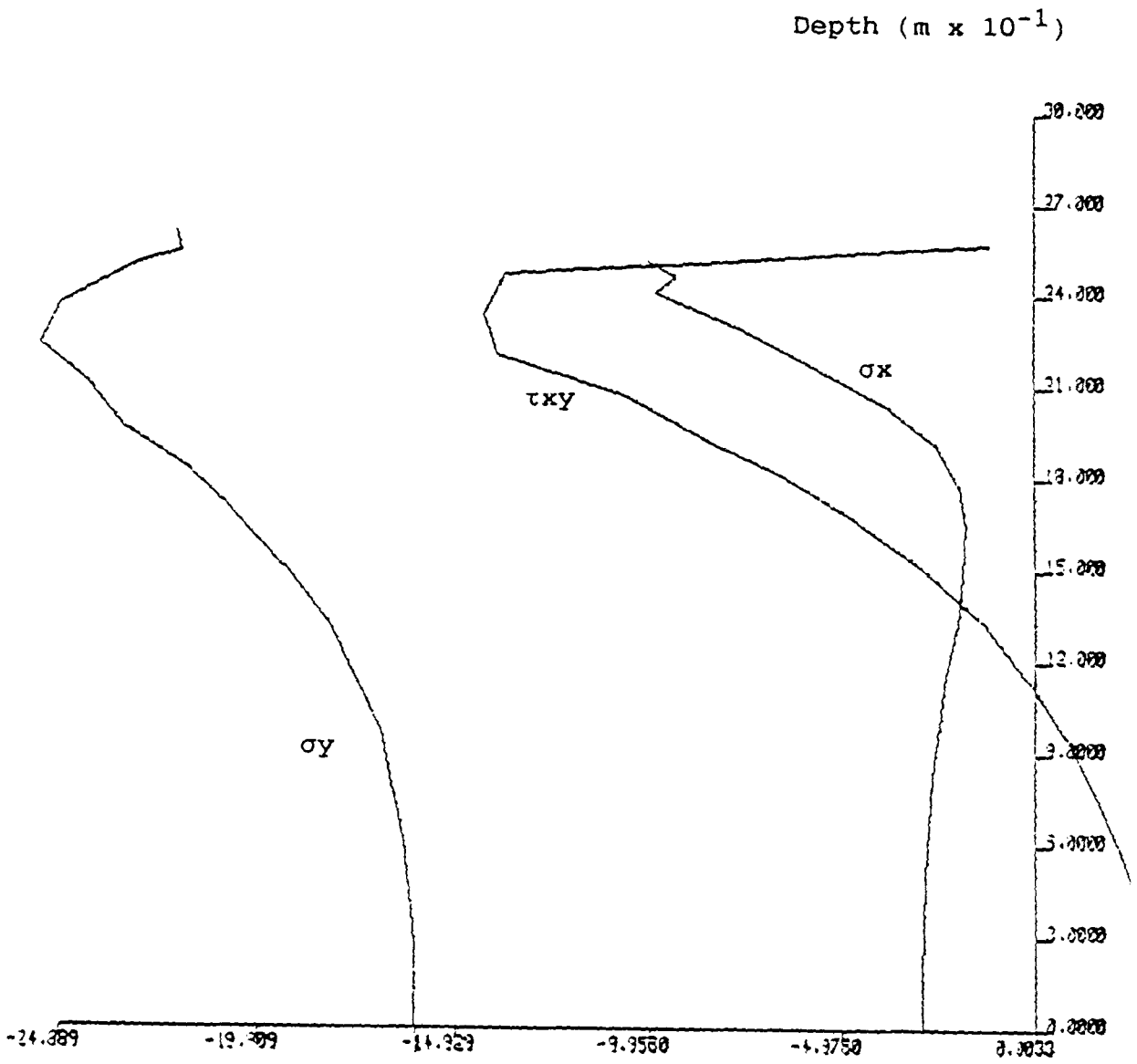

σx = horizontal direct stress

σy = vertical direct stress

τxy = shear stress

Fig.6.9. Model 2 - PIGS plot showing the stresses along the centre line under the LHS wheel load

6.6.3. Four-layer carriageway model - model 3

6.6.3.1. Description of the model

The four-layer carriageway section shown in Figure 6.10, has four different Young's modulus values (E1, E2, E3 and E4), layer depths (h1, h2, h3 and h4) and Poisson's ratios (μ1, μ2, μ3 and μ4). The pressure load was applied through the axle load of a commercial vehicle as before.

Due to symmetry only one half of the 7.3m carriageway section was modeled. The line of symmetry passes through the centre line of the carriageway. A 2.5% surface slope was used in this model for the carriageway section.

The type of elements and boundary conditions were the same as in the previous example, as was the number of elements.

The input data for the properties of the materials used in this carriageway section were selected to simulate the types of material used in this research:

Bituminous wearing layer	E1 = 3600	MPa	μ1 = 0.35
Soil-cement base	E2 = 120	MPa	μ2 = 0.2
Sub-base	E3 = 40	MPa	μ3 = 0.3
Subgrade	E4 = 20	MPa	μ4 = 0.4

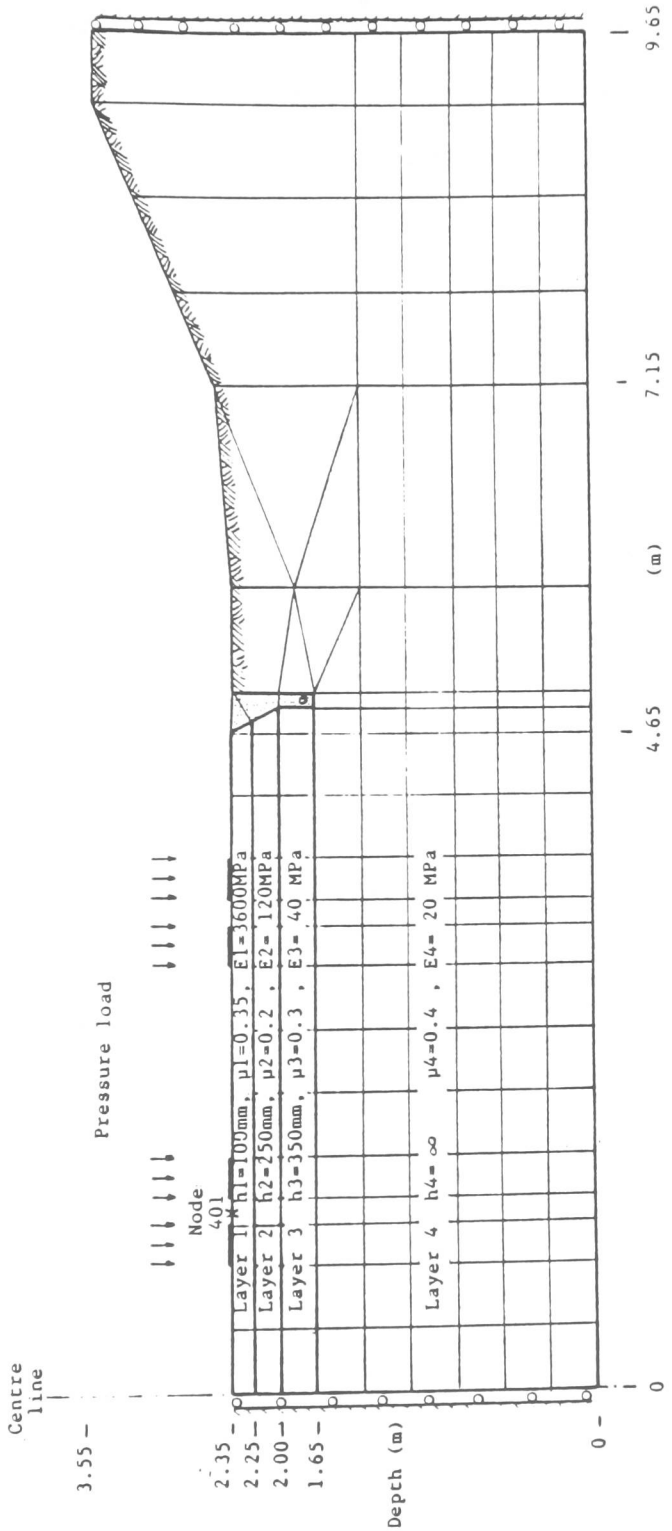

Fig.6.10. Model 3 - Four-layer carriageway section

6.6.3.2. Results and discussion

The largest displacements in the horizontal and vertical directions are selected automatically in Phase 7 of PAFEC and the maximum displacement value of 26mm was noted at node 401 under the wheel load.

The analysis again indicated that large displacements occurred under the wheel loads and that the proposed road design is not satisfactory for the type of subgrade conditions and traffic load.

6.6.4. General conclusion

The three models used in the numerical analysis give a general picture of the pavement behaviour. In models 2 and 3 the maximum vertical displacements are considerably higher than for model 1, but this is directly influenced by the type of subgrade chosen. The Young's modulus values and the maximum displacements are stated below for comparison.

Model No.	E subgrade	maximum vertical displacement
1	110 MPa	0.58mm
2	35 MPa	17.90mm
3	20 MPa	26.00mm

It can be clearly seen that the numerical analysis can be used to assess suitability of the pavement design and the effect of subgrade conditions on the overall behaviour of the road structure. Once a suitable numerical model is determined, a comprehensive stress analysis can be performed by changing variables, thus producing an economic and balanced pavement design.

CHAPTER 7

Summary and Conclusion

Stabilised soil-cement has been used in the sub-base and/or roadbase of flexible pavements for a considerable time. The performance of soil-cement pavements has been investigated. Studies have shown that the structural failure of soil-cement pavements is caused by repeated traffic loads, which result in fatigue failure. This has led to the gradual realisation of the inadequacy of present design methods. Hence, it is essential to design the soil-cement pavement to withstand the dynamic action of traffic loads and have a longer fatigue life.

Pavement failure due to extensive cracking, which was not accompanied by any apparent permanent deformation, led to the recognition that resilient deformation under transient heavy loadings was of major importance. It was assumed that these resilient deformations were essentially elastic in nature. Following this concept, evaluation of resilient deformation under moving load is logical. Consequently, there is a need for a complete study of the dynamic properties of soil-cement material. These properties will be essential input for rigorous numerical analysis of flexible pavement to ensure long life, reduced maintenance costs and economical construction. For this to be achieved

a comprehensive study of the material characteristics under a variety of dynamic loading modes such as compression, flexure and tension would be required.

The main aim of this research was to investigate the behaviour of soil-cement subject to dynamic loading under stresses in compression, flexure, tension and tension-compression. Variables, such as cement content and curing time prior to testing, have been selected to study their effects on the resilience and fatigue characteristics of soil-cement specimens under dynamic loading.

In order to generate consistent data and study the effect of different variables on material characteristics, only one type of homogeneous soil was selected. This was pulverised Red Marl from Abergavenny, South Wales which was mixed with Portland cement stabiliser for the experimental work. The procedure for mixing was consistent for all the specimens prepared. The routine classification tests were carried out according to B.S. 1377:1975. The soil suitability was assessed by the criteria used for stabilised road pavements by the Transport and Road Research Laboratory.

The cylindrical mould used in this investigation is specified in B.S. 1924:1975: Test 10 for the determination

of unconfined compressive strength. Cylindrical specimens were used to investigate the static and dynamic properties of the soil-cement in uniaxial compression, tension and tension-compression tests.

The beam mould used in this investigation is specified in the ASTM D1632-63 standard test method for flexural strength of soil-cement. The static tests were performed according to ASTM 1635-65.

The Instron machine, model 1251 was used for the testing. In all dynamic testing the machine was set up loading sinusoidally from almost zero load to a load level less than that which would cause failure in the static mode. The frequency of 5Hz was chosen to simulate traffic loading. The number of load repetitions was monitored on a cycle counter.

In the development of the tensile loading apparatus, a number of factors had to be considered e.g. eliminating eccentricity in the line of action of the applied tensile loads, which can cause premature failure due to bending, and holding the soil-cement specimen without damaging it because of its relatively low strength and brittleness.

One of the difficulties experienced in this study was the measurement of deformations. The soil-cement materials are

far stiffer and more brittle in character than compacted soils. The amount of measurable deformation under dynamic load corresponds to 0.01% strain axially and 0.001% strain laterally. The techniques of deformation measurement have been investigated, and a transducer system of high accuracy LVDT's developed. The system can meet testing requirements such as reliability, accuracy at high frequency, ease of preparation and assembling.

Fatigue relationships in the form of number of load cycles to failure related to applied stress, based on experimental results, have been developed for use as design input for soil-cement pavement analysis.

The unconfined compressive strength generally increases with increase in cement content and curing time. The rate of increase of UCS with curing time is constant and of higher magnitude at higher cement contents. This results from the improved frictional characteristics of the soil.

Stress-strain output from the static compression tests was analysed in order to generate input parameters for soil-cement pavement analysis.

The response of the cement stabilised Red Marl to dynamic loading in compression has been investigated over a range

of cement contents and curing times. The damage induced by dynamic loading in compression was primarily found in the form of extensions of the tensile microcracks on the surface of the cylindrical specimens.

The Resilient Modulus concept has been extensively used by researchers in analysing results for dynamic load tests on soils, granular materials, bituminous materials and cement-treated soils. It can be compared with Young's Elastic Modulus for static loading tests. Comparison of the values of the Resilient Modulus and the Elastic Modulus shows that the Resilient Modulus is generally higher than the Elastic Modulus for the same cement content and curing time.

The dynamic tension-compression loading regime appears to be the most fatigue-inducing loading mode. In view of these findings particular care has to be exercised at the design stage if structures are expected to be subjected to tension-compression loads.

The stresses generated by traffic loading are flexural in nature. The tensile stress at the bottom of the cement-treated layer is an important factor and should be used as a design criterion. Also, the tensile strength is generally an important engineering property of brittle materials, such as concrete, most rocks and soil cement.

Ironically it remains one of the least well-defined material properties. This results from lack of experimental techniques that are both practical and reliable and rigorous enough from a continuum mechanics viewpoint.

Flexural fatigue tests are easier to carry out than uni-axial tensile tests. However uni-axial tensile tests are preferred since they provide more reliable information on the fatigue behaviour of the pavement material, and do not involve uncertainties regarding the extreme fibre tensile stresses induced during flexural fatigue testing.

Static and dynamic flexure test results show a substantial drop in strength due to fatigue effects in flexure. The fatigue failure of the soil-cement in flexure is caused by the development of tension cracks at the underside of the beam specimen.

The theoretical approach provides a more reliable base for extrapolation beyond the boundaries of empirical approaches. However, the use of elastic theory for pavement design is still limited especially in connection with pavements containing stabilised sections.

The Boussinesq stress distribution analysis is based on an

infinite strip of homogeneous material; however the relationship between stresses and deflections in real pavement materials and in the subgrade are much more complex. In such cases a multi-layer-system theory has to be adopted for pavement design.

Procedures for the prediction of traffic-induced deflections, stresses and strains in pavement systems are based on the principles of continuum mechanics. The finite element method has been developed into a very powerful tool for the analysis of all types of continuum mechanics problems. It is an approximate procedure, which consists of modelling the structure as an assembly of discrete elements, and analysing this assembly by standard methods of structural analysis.

The finite element suite used in this study is PAFEC. The program is written in FORTRAN language and is operated on a VAX 11/785 computer. The PAFEC suite provides a wide range of element types to solve various kinds of structural problems. The elements are generated automatically provided that types, spacings and material properties are correctly input.

Three pavement models involving different loads, different numbers of pavement layers and material properties have been generated on the computer using two dimensional

analysis. This demonstrates the versatility of this package. The numerical analysis can be used to assess suitability of the pavement design and the effect of subgrade conditions on the overall behaviour of the road structure.

Further work is required to develop a feasible mathematical model that could be used to analyse a pavement section. This work would first concentrate on the comparison with reliable examples, frame practice and therefore achieve the type of mesh refinement required. Three dimensional application of pressure loading may be also considered in the analysis. Numerical dynamic analysis could be used to simulate fatigue effect on pavements. This type of analysis would however require more research time and reliable experimental results in order to produce a credible mathematical model.

As a future recommendation the Instron 1251 can be linked to an external computer, through its console, recording all the data output. This will allow longer period dynamic tests to be carried out and an output of a comprehensive set of results.

The static unconfined compressive test results were comprehensive and covered a wide range of cement contents (6, 10, 14, 18 & 22%) and curing times (7, 14, 28 & 56 days). UCS - cement content relationships for various curing times have been established. Stress - strain results were analysed in order to generate input parameters for soil - cement pavement analysis.

The moduli of elasticity (E) for the linear part of the stress - strain curves were established. The E values were found to systematically increase with increase in the cement content and curing time.

From the dynamic compressive test results, fatigue relationships and resilient moduli were established for a wide range soil - cement mixes. This provided a useful input for a more comprehensive numerical analysis for the soil - cement pavement design.

The damage induced by dynamic loading was apparent in the form of extensions to the tensile microcracks on the surface of cylindrical specimens when tested in dynamic compressive, and at the underside of prismatic specimens when tested in flexure.

The resistance to fatigue damage of soil - cement was found to increase with increasing cement content and curing time.

The fatigue failure load of soil - cement specimens caused by the applied dynamic loading was established in compression and in flexure. The fatigue effect in flexure was found to be higher than that in uniaxial compression.

REFERENCES

Abboud, M.M. (1973), "Mechanical Properties of Cement-Treated Soils in Relation to Their Use in Embankment Construction", Univ. of California, Berkeley, PhD Dissertation.

Ahlberg, H.L.& McVinnie, W.W.(1962), "Fatigue Behaviour of a Lime-Flyash-Aggregative Mixture", H.R.B., Bull. No.355.

Atkins, H.N.(1980),"Highway Materials, Soils & Concretes", Reston Pub. Co. Inc., Reston, Virginia.

Attinger, R.O.& Koppel, J.(1983),"A New Method to Measure Lateral Strain in Uniaxial and Triaxial Compression Tests", Rock Mech. 16, No.1, Techn. N., pp.73-78.

Barksdale, R.D. (1972), "Laboratory Evaluation of Rutting in Base Course Materials", Proc. of the 3rd Int. Conf. on the Structural Design of Asphalt Pavements, Univ. of Michigan, pp.161-174.

Bhogal, B.S. (1983), Private communication, The Polytechnic of Wales.

Bofinger, H.E.(1965), "The Fatigue Behaviour of Soil-Cement", Australian Road Res., Vol.2, No.4, pp.12-20.

Bonnot, J. (1972), "Assessing the Properties of Materials for Structural Design of Pavements," Proc. of the 3rd Int. Conf. on the Structural Design of Asphalt Pavements, Vol.1, Univ. of Michigan, Ann Arbor, Mich., pp.200-213.

BS 1377 (1975), "Methods of Test for Soils for Civil Engineering Purposes", British Standard Institution, London.

BS 1924 (1975), "Methods of Test for Stabilized Soils", British Standard Institution, London.

Burmister, D.M. (1943), "The Theory of Stresses and Displacement in Layered Systems and Application to The Design of Airport Runways", Proc., Hwy. Res. Board, pp. 126-144.

Burmister, D.M. (1945), "The General Theory of Stresses and Displacement in Layered Soil Systems", Journ. of Applied Physics, Vol.16, No.5, pp. 296-302.

Corps of Engineers (1956), "Summary Review of Soil Stabilization Processes", Report No. 3, Soil-Cement, Miscellaneous Paper, Waterway Experiment Station, Vicksburg, Mississippi, September.

Croney, D. (1977), "The Design and Performance of Road Pavements", Trans. and Road Res. Lab. HMSO.

Haimson, B.C. (1978), "Effect of Cyclic Loading on Rock, Dynamic Geotechnical Testing", ASTM STP 654, American Society for Testing and Materials, pp.228-245.

Highway Research Board (1955), "The WASHO Road Test, Part 2: Test Data, Analysis, Findings", Special Report No.22.

Highway Research Board (1961), "Soil Stabilization with Portland Cement", Bulletin No.292.

Highway Research Board (1962), "Soil Stabilization with Portland Cement", The AASHO Road Test, Special Report No.61G. & Part 5: Pavement Res., Special Report No.61E.

Howarth, D.F. (1984), "Apparatus to Determine Static and Dynamic Elastic Modulus", Rock Mech. A. Rock Engng., Vol.17, No.4, pp.255-264.

Howarth, D.F. (1985), "Development and Evaluation of Ultrasonic Piezoelectric Transducers for the Determination of Dynamic Young's Modulus of Triaxially Loaded Rock Cores", ASTM Geotech. Test. Journ., Vol.8, No.2, pp.59-65.

Hveem, F.N. (1955), "Pavement Deflections and Fatigue Failures", Design and Testing of Flexible Pavements, Bull. No.114, Hwy. Res. Board, pp.43-87.

Jardine, R.J., Brooks, N.J. & Smith, P.R. (1985), "The Use of Electro-Level Transducers for Strain Measurements in Triaxial Tests on Weak Rock", Int. Journ. Rock Mech. Min. Sci.22, No.5, pp.331-337.

Jones, A. (1962), "Tables of Stresses in Three-Layer Elastic Systems", Highway Research Board Bull. No.342, pp. 176-214.

Kalantary, F. (1986), "Cement Stabilized Red Marl", The Polytechnic of Wales, Internal Report.

Kezdi, A. (1979), "Stabilized Earth Roads", Elsevier Sci. Pub. Co., 1st Edn.

Kolias, S. (1975), "Evaluation of the Strength and Elastic Properties of Cement Stabilized Materials", Ph.D. Thesis, Univ. of Surrey.

Kolias, S. & Williams, R.I.T. (1978), "Uniaxial Tension Tests on Cement-Stabilized Granular Materials", ASTM Geotech. Testing Journ., Vol.1, No.4, pp.190-198.

Lister, N.W. (1972), "Deflection Criteria for Flexible Pavement", TRRL Report LR 375, Transport and Road Research Laboratory, Crowthorne, 1972.

Lotfi, H.& Witczak, M.W. (1985), "Dynamic Characterization of Cement-Treated Base and Subbase Materials", Trans. Res. Rec. No.1031, pp.41-48.

Ministry of Transport (1969), "Specification for Road and Bridge Works", London, H.M.S.O.

Mitchell, J.K. & Freitag, D.R. (1959), "Review and Evaluation of Soil-Cement Pavements", ASCE Proc., Journ. of the Soil Mech. and Foundation Division, December,vol.6, No.sm6, pp.49-73.

Mitchell, J.K. & Monismith, C.L. (1967), "Behaviour of Stabilized Soils Under Repeated Loading", Report 2: Behaviour in Repeated Flexure, Frequency and Duration Effects, Fatigue Failure Analyses, Contract Report 3-145, U.S. Army Corps of Engineers, Waterways Experiment Station, Vicksburg, Mississippi.

Mitchell, J.K., Fossberg, P.E. & Monismith, C.L. (1969), "Behaviour of Stabilized Soils Under Repeated Loading", Report 3: Repeated Compression and Flexure Tests on Cement and Lime Treated Clay, U.S. Army Corps of Engineers, Waterways Experiment Station, Vicksburg, Mississippi.

Mitchell, J.K., Ueng, T.S. & Monismith, C.L. (1972), "Behaviour of Stabilized Soils Under Repeated Loading",

Report 5: Department of Civil Engng., University of California, Berkeley, August.

Mitchell, J.K., Dzwilewski, P. & Monismith, C.L. (1974), "Behaviour of Stabilized Soils Under Repeated Loading", Report 6: A Summary Report with Suggested Structural Design Procedure, U.S. Army Corps of Engineers, Waterways Experiment Station, Vicksburg, Mississippi.

Nussbaum, P.J. & Larsen, T.J. (1965), "Load-Deflection Characteristics of Soil Cement Pavements", Hwy. Res. Rec. No.86, pp.1-14.

Otte, E. (1978), "A Structural Design Procedure for Cement-Treated Layers in Pavements", DSc Thesis, Univ. of Pretoria, Pretoria.

Portland Cement Association, (1971), "Soil-Cement Mixtures Laboratory Handbook", Skokie, Illinois.

Portland Cement Association, (1979), "Soil-Cement Roads Construction Handbook", Skokie, Illinois.

Pretorius, P.C. (1970), "Design Considerations for Pavements Containing Soil-Cement Bases", Ph.D. Dissertation, Univ. of California, Berkeley.

Raad, L. (1976), "Design Criteria for Soil-Cement Bases", PhD Dissertation, University of California, Berkeley.

Raad, L., Monismith, C.L. & Mitchell, J.K. (1977), "Fatigue Behaviour of Cement-Treated Materials", Trans. Res. Rec. No.641, pp.7-11.

Raiss-Saadi, F. (1985), "Cement Stabilized Soil as Sub-Base", The Polytechnic of Wales, Internal Report.

Reid, C.R. (1948), "Report of Committee on Soil-Cement Roads", HRB Bull.14, October.

Sebaaly, P.E. & Mamlouk, M.S., (1988), "Development of Dynamic Fatigue Failure Criterion", Journ. of Trans. Engng., Vol.114, No.4, July , pp. 450-464.

Seed, H.B., Mitry, F.G., Monismith, C.L. & Chan, C.K. (1965), "Factors Influencing the Resilient Deformations of Untreated Aggregate Base in Two-Layer Pavements Subjected to Repeated Loading", Hwy. Res. Rec. No.190, pp.19-57.

Seed, H.B., Mitry, F.G., Monismith, C.L. & Chan, C.K., (1967), "Prediction of Flexible-Pavement Deflection from Laboratory Repeated Load Tests", NCHRP, Rept.35.

Shah, K. (1982), "Cement Stabilized Soil", The Polytechnic of Wales, Internal Report.

Turner, M.J., Clough, R.W., Martin, H.C., & Topp, L.J. (1956), "Stiffness and Deflection Analysis of Complex Structures", Journ. of Aeronautics Sci., September, pp. 805-823.

Verstraeten, J. (1967), "Stress and Displacement in Elastic Layered System", Proc. 2nd Int. Conf. Structural Design of Asphalt Pavements, Univ. of Michigan, pp.277-290.

Warren, H. & Dieckmann, W.L. (1963), "Numerical Computation of Stresses and Strains in a Multiple-layer Asphalt Pavement System", Int. Rept., California Res, Corp., September.

Whiffin, A.C. & Lister, N.W. (1962), "The Application of Elastic Theory to Flexible Pavements", Proc. Int. Conf. on the Structural Design of Asphalt Pavements, Univ. of Michigan, 20-24th August, pp 499-521.

William, W., Crockford, A.M. & Dallas, N. L. (1987), "Tensile Fracture and Fatigue of Cement-Stabilized Soil", Journ. of Trans. Engng., Vol.113, No.5, September, pp. 520-537.

Yoder, E.J. & Witczak, M.W. (1975), "Principles of Pavement Design", 2nd. Edn. New York, Toronto: John Wiley & Sons, Inc.

Zube, E., Gates, C.G., Shirley, E.C., & Munday, H.A. (1969), "Service Performance of Cement-Treated Bases as Used in Composite Pavements", Hwy. Res. Rec. No.291, pp. 57-69.